The Radio Science Bulletin

ISSN 1024-4530

INTERNATIONAL UNION OF RADIO SCIENCE

UNION RADIO-SCIENTIFIQUE INTERNATIONALE

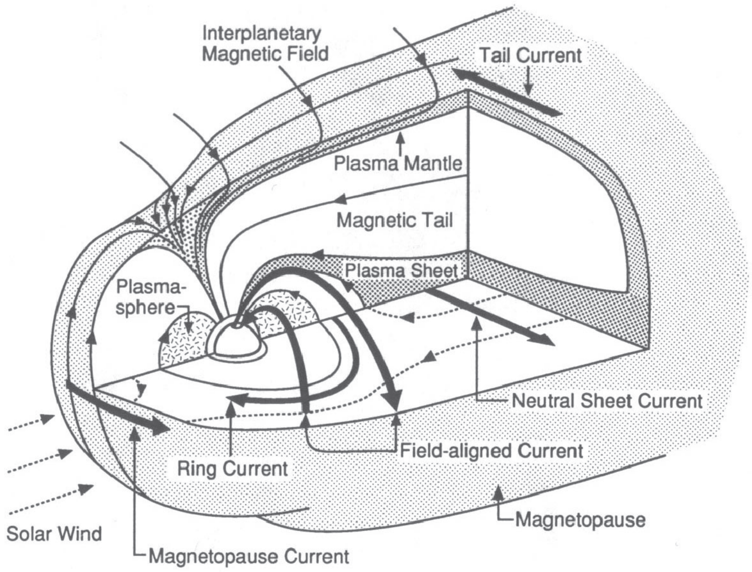

No 308
March 2004

Publié avec l'aide financière de l'ICSU
URSI, c/o Ghent University (INTEC)
St.-Pietersnieuwstraat 41, B-9000 Gent (Belgium)

Contents

Front cover: Figure 1 from "Remote Sensing the Earth's Plasmasphere" (more on pp. 13-29)

For information, please contact :
The URSI Secretariat
c/o Ghent University (INTEC)
Sint-Pietersnieuwstraat 41, B-9000 Gent, Belgium
Tel.: (32) 9-264 33 20, Fax: (32) 9-264 42 88
E-mail: ursi@intec.rug.ac.be
http://www.ursi.org

The International Union of Radio Science (URSI) is a foundation Union (1919) of the International Council of Scientific Unions as direct and immediate successor of the Commission Internationale de Télégraphie Sans Fil which dates from 1913.

Editorial

What's in this Issue

When I was taught Babinet's principle, one of the illustrations used was the idea of making an ELF/VLF antenna using an island. The relatively low-conductivity island in the middle of the relatively high-conductivity ocean would supposedly be equivalent to a slot radiator in an essentially infinite conducting screen. I was also taught that this had been demonstrated experimentally. Well, as is so often the case, the practical properties of real islands in a real ocean mean that while this type of antenna works, it doesn't work exactly as predicted – or, indeed, perhaps as some have thought. The theoretical and experimental history of such antennas is traced by Nikolaos Uzunoglu and Stelios Kouridakis in their paper. They show that the infiltration of the sea water into the land under an island or peninsula has a profound effect on the nature of the radiation of such an antenna. Using the results of the experiments they performed, they demonstrate that the radiation achieved is more consistent with a vertical-loop or horizontal-wire antenna than that of a slot radiator. Their explanation of why this should be is most interesting.

Don Carpenter has provided the invited Commission H *Review of Radio Science* paper in this issue, on remote sensing of the Earth's plasmasphere. We usually think of remote sensing as it is applied to surface features of the Earth. However, as this paper amply demonstrates, there are a variety of remote-sensing techniques that have been very successfully applied to the plasma cloud that surrounds and extends outward from the Earth. In recent years, a tremendous amount has been learned using such techniques about the plasmasphere and how it affects the Earth's near-space environment. This paper provides an excellent and very readable review of both the techniques used and what has been learned by using them. As is often the case, what has been learned has helped to identify important new areas for future research, and the paper also looks at these. In addition to a fascinating look at the variety of methods used for probing the plasmasphere, one of the most interesting aspects of this paper is the understanding it provides of how the plasmasphere interacts with the Earth's magnetosphere and ionosphere – and what we do and do not know about such interactions.

Richard Horne is the Commission H Associate Editor for the *Reviews of Radio Science*, and his efforts are much appreciated.

If remote sensing of the Earth's plasmasphere can be thought of as "looking up," then the remote sensing reviewed in the paper by Paolo Pampaloni and Kamal Sarabandi can be thought of as "looking down" – at the land portion of the Earth's surface. This is the first of the Commission F *Reviews of Radio Science*, and it deals with microwave remote sensing of land properties of the Earth. This is a very comprehensive review. It is organized broadly according to the types of land parameters being determined: land classification, soil moisture, snow, forest properties, and crop vegetation. Both active and passive remote-sensing techniques are described for each category of parameters. This is an area where the radio science involved can have a huge economic impact, can significantly improve the human condition, and can provide information critical to helping to protect the Earth's environment. This paper gives a very interesting overview of this most important field.

Martti Hallikainen is the Commission F Associate Editor for the *Reviews of Radio Science*, and his efforts are also much appreciated. Of course, Phil Wilkinson is the Senior Associate Editor for all of the *Reviews of Radio Science*, and without his efforts we would not have these *Reviews*.

There are several important reports and announcements in this issue. The annual IUCAF (Scientific Committee on Frequency Allocations for Radio Astronomy and Space Science) report is here. There is a report on the ClimDiff 2003 meeting. The "Clim" portion of this refers to what had been the meetings on Climatic Parameters in Radiowave Propagation Prediction. The "Diff" portion refers to diffraction modeling and its applications. This meeting is sponsored by URSI's Commission F and the SCT (Scientific Committee on Telecommunications).

There are items in this issue that have deadlines about which you need to be concerned. The application form for Young Scientists for the next URSI General Assembly appears here. The call for nominations for the 2005 URSI Awards will be available on the URSI Web site (http://www.ursi.org) starting March 1, 2004. An announcement of the new competition for the Commission B International Electromagnetics Prize appears in this issue.

An E-Mail Change

I have recently had some problems with my CompuServe e-mail account. Henceforth, please use the following to address all e-mail to me: r.stone@ieee.org.

This is an "alias," which will permit me to rapidly and easily change the address at which I receive e-mail if future problems arise.

One good way to try out the above e-mail address would be to share what you're doing with our readers. The *Radio Science Bulletin* is always looking for interesting papers that are of broader interest, written to appeal across the areas of more than one of the URSI Commissions.

URSI Commission B International Electromagnetics Prize

URSI Commission B and the URSI Board of Officers have established the URSI Commission B International Electromagnetics Prize. The prize is US$10,000 plus a commemorative plaque and is sponsored by the SUMMA Foundation. It is awarded for an accurate approximate solution of a designated scattering or related problem in electromagnetics and is presented at an appropriate URSI meeting.

General Information

The last 30 years have seen enormous advances in the application of numerical techniques in electromagnetics but there have not been comparable advances in our knowledge of the scattering from simple geometric shapes. It is hoped that the prize will encourage the development of accurate, physically-based approximate analytical expressions for the solution of canonical and similar problems.

The designated annual prize problem is announced on the URSI Web page (http://www.ursi.org) and elsewhere, and solutions are due approximately 16 months after the announcement date. Entries must be in English in the format of a manuscript submitted to the journal *Radio Science* and must not exceed 25 pages in length, including tables, figures and references. Hard copy or electronic submission is acceptable. Entries will be judged by a panel appointed by the Chair of URSI Commission B and the SUMMA Foundation. Factors taken into account in the judging will be the simplicity and elegance of the expressions, their conformity with the known physical properties of the solution, and their accuracy for all values of the parameters involved in the problem. The winner will be announced approximately five months after the submission date. The panel reserves the right to withhold the award if no worthy entry is received.

All scientists are eligible for the prize apart from an officer or Director of the SUMMA Foundation, a member of the panel, or one of their immediate working associates. Multiple authorship is allowed.

2005 Prize Problem (announced February 2004)

The competition problem is the determination of the scattering of a uniform plane wave by a perfectly conducting right circular cone of semi-infinite extent. In terms of spherical coordinates, with the cone axis coincident with the polar (z) axis and the tip of the cone at the origin, the conical surface is specified by $\theta = \theta_c$ with $0 < \theta < \pi/2$. The objective is the determination of the scattering matrix for the exterior problem for either time-harmonic or time-dependent excitation.

There is a sizable body of literature on this problem, but solutions are not known in simple form for all ranges of the problem parameters, nor are accuracy bounds or validity checks known for the available solutions. A solution should be in the form of readily computable, approximate expressions, accompanied by specifications of accuracy and ranges of validity. An acceptable numerical solution must be accompanied by expressions that approximate data. A minimally acceptable solution might be one for which either the incident or scattered wave (but not both) is axial. Contestants are encouraged to submit a solution that is as general as feasible for which the accuracy is specified and for which numerical values can be obtained by simple computations. A solution for which the specified range of validity is limited but for which the accuracy is tightly bounded will be looked upon more favorably than one that holds over a greater range but for which the accuracy is not tightly bounded. Validity and bounds may be based on appeals to, for example, first principles, symmetry, and/or observations drawn from a sufficiently large set of data.

A solution of the cone problem without accuracy bounds, worthy though it may be, is not in accord with the objectives of the competition. Neither is a solution for which much labor is required to obtain numerical values.

Submission

The members of the competition panel are C. E. Baum, C. M. Butler (Chair), K. J. Langenberg, T. B. A. Senior, and S. Ström. Entries in the format described above must be received on or before **15 June 2005** by Professor Chalmers M. Butler at the Electrical and Computer Engineering Department, Clemson University, Clemson, SC 29634-0915, USA; E-mail: cbutler@eng.clemson.edu.

UNION RADIO-SCIENTIFIQUE INTERNATIONALE

INTERNATIONAL UNION OF RADIO SCIENCE

URSI AWARDS FOR YOUNG SCIENTISTS

CONDITIONS

A limited number of awards are available to assist young scientists from both developed and developing countries to attend the General Assembly of URSI.

To qualify for an award the applicant :

1. must be less than 35 years old on September 1 of the year of the URSI General Assembly;

2. should have a paper, of which he or she is the principal author, submitted and accepted for oral or poster presentation at a regular session of the General Assembly;

Applicants should also be interested in promoting contacts between developed and developing countries.

All successful applicants are expected to participate fully in the scientific activities of the General Assembly. They will receive free registration, and financial support for board and lodging at the General Assembly. A basic accommodation is provided by the assembly organizers that permits the Young Scientists from around the world to collaborate and interact. Young scientists may arrange alternative accommodation, but such arrangements are entirely at their own expense. Limited funds will also be available as a contribution to the travel costs of young scientists from developing countries.

Apply before 15 November 2004 to the URSI Secretariat (address below). Please submit ***THREE COPIES*** *of each of the following: (1) a completed application form, (2) a CV and list of publications, (3) an abstract of proposed paper.*

Applications will be assessed by the URSI Young Scientist Committee taking account of the national ranking of the application and the technical evaluation of the abstract by the relevant URSI Commission. Awards will be announced on the URSI web-site in May 2005.

The URSI Secretariat
c/o Ghent University / INTEC
Sint-Pietersnieuwstraat 41
B-9000 GENT
BELGIUM
fax : (32) 9-264.42.88
e-mail : ursi@intec.rug.ac.be

For more information about URSI, the General Assembly and the activities of URSI Commissions, please look at the URSI web site at: http://www.ursi.org

APPLICATION FOR A YOUNG SCIENTISTS AWARD

I wish to apply for an award to attend the XXVIIIth General Assembly of the International Union of Radio Science in New Delhi, India, 23-29 October 2005.

Name : Prof./Dr./Mr./Mrs./Ms. ....

Family Name First Name Middle Initials

Sex : male / female

Date of birth (day / month / year) : .... / .... / .... Nationality : ....

Studying/Employed at : ....

Institution ....

Department ....

Mailing address : Please send all correspondence to my ☐ business / ☐ home address, i.e.

Street ....

City and postal code ....

Province/State .... Country ....

Fax .... E-mail ....

Academic qualifications, with date(s) obtained : ....

....

Title of abstract submitted : ....

....

Type of session preferred: ☐ in an oral session ☐ in a poster session

The subject of the paper is relevant to URSI Commission ……….session (leave blank if uncertain).

Date :............................. Signed ....

For applicants from developing countries only :

I estimate the cheapest return fare to the URSI meeting is EURO ....

For graduate students only - Supervisor's endorsement :

I support the application for an award to enable this young scientist to attend the forthcoming General Assembly of URSI for the following reasons : ....

....

....

....

Supervisor's Name and Title : ....

Address : ....

Date :........................ Signed : ....

Radiation of Very Low and Extremely Low Frequencies (VLF & ELF) by a Natural Antenna Based on an Island or a Peninsula Structure

N. K. Uzunoglu
S. J. Kouridakis

Abstract

The idea of using a geophysical structure, such as an island or a peninsula, to radiate extremely low frequencies (ELF) or very low frequencies (VLF) was proposed approximately 40 years ago. It seems that all efforts to implement this idea remained in a premature experimental phase, while it is known that an ELF system operating at 75 Hz was developed by the United States Navy twenty years ago. In the present paper, a historical review is presented of the previous work on this topic. In order to examine the possibility of constructing such a "natural antenna," the authors developed an experimental system and carried out measurements at the Kynosoura peninsula near Marathon-Greece. They constructed an experimental ELF-VLF antenna in the frequency band of 1-12 kHz. Both the input impedance and electromagnetic field quantities were measured during August-October, 2000, and these are presented. A comparison of the measured results with theory shows that an island or a peninsula can't operate as a slot radiator. However, efficient operation can be achieved using a vertical-loop mode, utilizing an island in which the current return path is achieved through underground media or by a linear wire antenna lying on the island.

1. Introduction

It seems that the possibility of constructing a "natural slot" antenna, operating at very low frequencies, using an island or a peninsula was proposed as early as 1960 by Morgan [1, 2]. In 1961, Gould [3] of the British Admiralty tried to carry out measurements by using an island (or, better, an inland V-shaped lake) in Scotland. The subject matter was studied theoretically by Staras [4] during the same period, who predicted the difficulty in implementing this concept in practice.

The same idea was revisited by Barr [5] in 1980, and Morgan [6] commented on the measurements presented, which were focused on the propagation constant of an insulated conducting line placed on the ground.

The concept of using an island or a peninsula as a low-frequency antenna is based on the physical picture of such a natural structure (Figure 1). The sea, having a high conductivity (1-4 S/m), and a rocky island (or peninsula), having a low conductivity ($\approx 10^{-4}$ S/m) at low frequencies (1 Hz-100 kHz), could be considered to be a slot antenna (an edge slot, in the case of a peninsula). Indeed, this concept sounds correct as a natural picture. The finite conductivity of the sea shouldn't be considered a limiting factor, based on a recent investigation by R. C. Hansen [7], where the satisfactory operation of a slot antenna on a resistive screen with a sufficiently large conductivity was shown. In the case of the sea, the conductivity, being $\sigma \approx 4$ S/m, is sufficiently large to guarantee efficient operation, provided the landmasses have very low conductivity. However, H. Staras [4] has identified the nonzero conductivity of the land medium as being a limiting factor in such "natural" low-frequency antennas, based on a theoretical analysis using an open-waveguide slot-antenna study.

It should be emphasized that if the whole Earth medium in the vicinity of a natural antenna had a conductivity of $\sigma \approx 10^{-4} \sim 10^{-3}$ S/m, this still would not be an obstacle to the antenna's operation in terms of its efficiency. In reality, in a geological structure such as an island or a peninsula, the sea water always penetrates the underground

*Nikolaos K. Uzunoglu and Stelios J. Kouridakis are with the Microwave and Fiber Optics Laboratory, National Technical University of Athens
Athens 15773, Greece.*

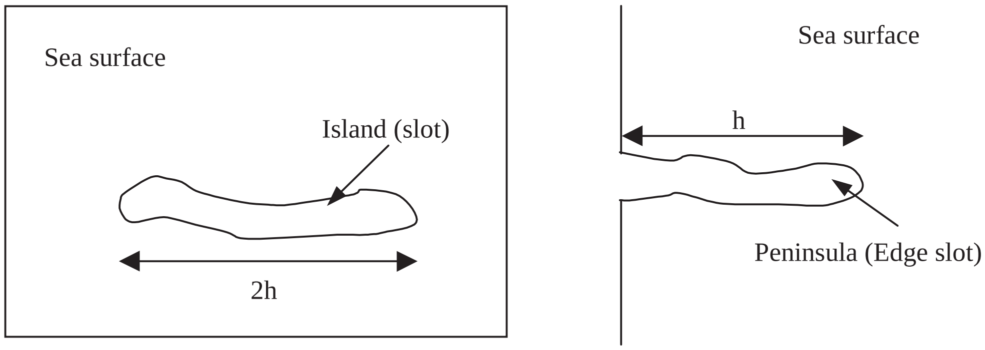

Figure 1: The concept of natural slot antennas

medium to some degree, which effectively short circuits the slot antenna. Indeed, this last statement is the main conclusion of the experimental work that has been carried out by our research group, as presented below. However, this doesn't mean that it is not possible to construct a "natural low-frequency antenna." Indeed, the work presented in this article shows the possibility of constructing an ELF or VLF antenna operating in another mode, such as a vertical-loop antenna or a linear-wire antenna, as will be explained in the following sections.

2. Selection of a Peninsula for Constructing a Natural Slot Antenna

In order to examine the possibility of using a peninsula as an edge-slot antenna, our research group selected the "Kynosoura" peninsula (in ancient Greek, this means a dog's tail), which is located approximately 30 km east of the city of Athens, near the historic Marathon region. A satellite photograph of the peninsula is shown in Figure 2. It has a length of approximately 2500 m, with an average width of 250 m. As a geophysical structure, the peninsula consists mainly of marble, while extremely limited flora exists on its surface only during spring time. Measurements of the ground conductivity at several points on the peninsula showed an average conductivity of $\sigma \approx 10^{-4}$ S/m (during summer months).

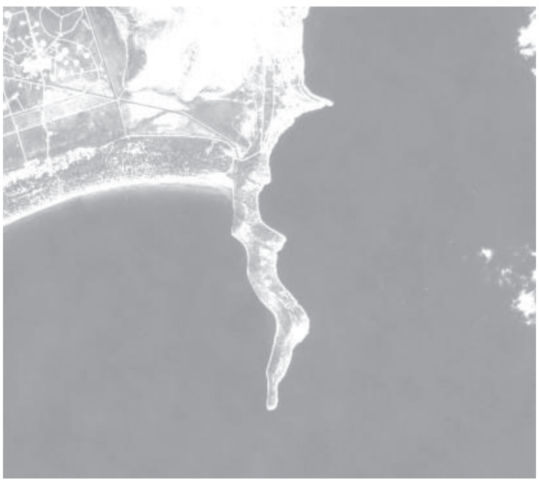

Figure 2: A satellite photograph of Kynosoura peninsula

Based on visual observation, it is possible to argue that the selection of the Kynosoura peninsula fulfills the following edge-slot antenna requirements:

1. The "conductive" surface encircling the Peninsula is sufficiently large to guarantee slot-antenna operation, as required in the radiation of slots [7].

2. The slot medium has a sufficiently low conductivity ($\sigma \approx 10^{-4}$ S/m).

3. The length of the peninsula is $h = 2500$ m. Assuming a very short "edge slot," having a length of at least $\lambda/20$ (λ being the radiation wavelength), one can argue that noticeable radiation could be achieved down to $\lambda = 20h = 50$ km, an approximate radiation frequency of $f \approx 6$ kHz.

The above statements are based on "visual observation," while the effect of seawater penetration underground into the peninsula's structure is not considered. In reality – as verified by measurement of the radiation properties, given in the following sections – the penetration of the seawater throughout the peninsula's base prevents the operation of the natural slot antenna. It seems that previous researchers working in this subject area have missed this point.

3. Construction of Excitation System and Measurement of the Input Impedance

In order to excite the natural slot antenna, an isolated, 16 mm^2 cross-section multi-conductor line, 350 m in length, was laid over the "throat" of the peninsula, directly on the Earth's surface. Two vertically floating copper electrodes,

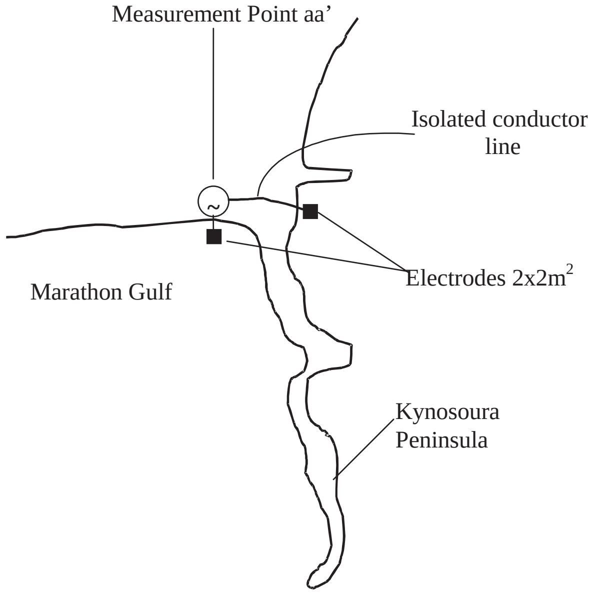

Figure 3: The excitation of a natural slot antenna

each with an area of 4 m^2 (2×2 m^2), were deployed in the sea. The two electrodes were connected to the conductor line as shown in Figure 3. The feeding point was installed on the west side of the peninsula, within Marathon bay (shown on the left in Figure 3). The sea electrode near the feeding point was placed 30 m into the sea, and was connected with a similar line to the power amplifier. The other electrode was placed at a distance of 20 m from the eastern side of the peninsula, which is a cliff. In order to feed low-frequency (3-15 kHz) electromagnetic energy into this natural slot antenna, an audio power amplifier (1 KW) was used.

For matching the antenna's input into the output resistance of the power amplifier (8.0 ohms and 1.0 ohm), two types of matching networks were alternately utilized, as shown in Figure 4. One used double capacitor arrays, which transformed an inductive complex impedance into a higher resistive input impedance (Figure 4a). The was an L-C network, which transformed a high inductive complex impedance into a lower resistive input impedance (Figure 4b). An air coil was built, using a 10 mm^2 single-line conductor; the coil had a diameter of 30 cm, and was 45 cm in length, with many taping points. The capacitor arrays, C_2 and C_4, were arranged with high-voltage polypropylene-type capacitors, having loss factors of $\tan(\delta) = 5\times10^{-4}$ (at 10 kHz). The matching-network efficiency was therefore high, and the power loss on the matching network itself was about 70 W, when the power input to the antenna was 900 W. This was determined by measuring the voltage drops across the passive elements, and by measurement of the quality factor, Q, of the matching network. The matching-network loss was therefore approximately 8%. Indeed, this is an insignificant loss compared to the loss along the 350 m line and in the environment (the sea and land).

The input impedance at the feed point aa' (see Figure 3) was measured by observing the input current (by measurement of the voltage drop along an etalon resistance $R_s = 0.1$ ohm, placed across the feeding line) and the voltage across the capacitor, C (Figure 5) at the resonant frequency. Knowing the current and the value of the capacitor at resonance, the real and imaginary parts of the natural antenna's input impedance were calculated. The distance between the points aa' was always less than 1 m. The measurement results of the input impedance obtained are given in Table 1. Similar numerical results were obtained when the matching networks of Figure 4 were used.

The inductance of the antenna, L_a, can be computed by using the relation $L_a = X_a/\omega$. In the region $f = 5 \sim 14$ kHz, this was found to be approximately $L_a \approx 0.95$ mH.

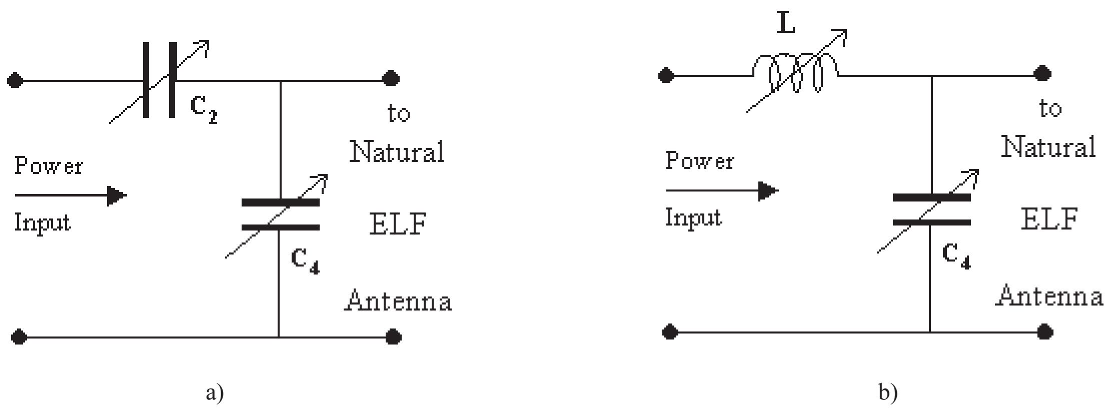

Figure 4: The matching networks used to feed the natural antenna

Frequency (kHz)	Antenna Input Impedance Z_a (Ω) $Z_a = R_a + jX_a$
0 (DC)	0.9
5.24	3 + j31.6
6.87	3.3 + j41.8
7.4	3.5 + j45
8	3.9 + j49
9.7	4.4 + j60
11.4	5.5 + j70
14.4	6.4 + j87

Table 1: The input impedance of the natural antenna

4. Analysis of Impedance Measurements of the Natural Antenna

A review of the measured data concerning the natural antenna's input impedance shows a linear increase of the reactance values, $X_a(\omega)$, and the corresponding inductance coefficient had an approximate value of $L_a \approx 0.95$ mH. As a first approximation, if the natural antenna radiated as a slot element, this would require a decrease in the reactance. Indeed, the slot-antenna impedance, Z_s, is linked to the dipole impedance, Z_d, by the well-known Babinet relation [8]:

$$Z_s = \frac{Z_0^2}{4Z_d}, \qquad (1)$$

where Z_0 is the free-space wave impedance.

As the imaginary part of Z_d is an increasing function of radiation frequency, ω, the slot reactance, Z_s, should show a corresponding decrease, which contradicts the observed data. Therefore, the assumption of the slot-radiation model is not verified. To the contrary, taking into account the loop dimensions, and computing the wire self-inductance using the formula [9]

$$L = 2l\left[2,303\log\left(\frac{4l}{d}\right) - 1\right]\times 10^{-7}, \qquad (2)$$

where $l = 350$ m, $d = 4.5$ mm (the wire diameter), a total inductance value of $L_a \approx 0.82$ mH is obtained.

The measured impedance values show quantitative agreement with the results given by Barr and Ireland in reference [10] for a vertical-loop antenna, for quantities such as the rate of increase of the real part of the impedance and of the reactive part.

5. Measurement of Radiation Fields

In order to observe the radiation of the very low frequency (VLF) waves using the above-described natural antenna, continuous-wave transmission at a frequency of $f = 6.87$ kHz were carried out occasionally during the period of August-October, 2000. The selection of this

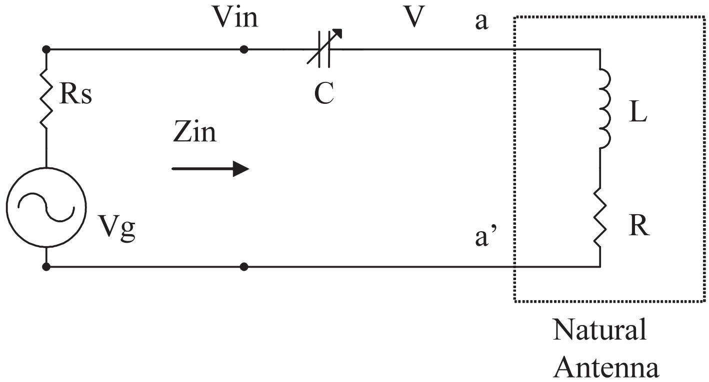

Figure 5: The series-resonant network used to measure the input impedance of the natural antenna

Position Number	Distance, *r*, from Antenna (km)	Measured Magnetic Field Strength, *H*, (nA/m)	Horizontal Wire Antenna Model	Vertical-Loop Antenna Model	Edge-Slot Antenna Model
1	2.5	595	564	295	8000
2	4.5	84	105	30	1400
3	8	27	28	3.7	400
4	15	21	11	0.5	158
5	18	9.6	6	0.35	86

Table 2: The magnetic field, H (maximum level), measured on Attica, compared to the values given by the three models.

specific frequency was arbitrary. However, the frequency of $f = 6.87$ kHz was selected in an effort to radiate at as low as possible a frequency, while keeping the antenna efficiency at a reasonable level. The antenna input was fed with 1 kW of power. Although both *E* (electric) and *H* (magnetic) fields were measured using short-dipole and small-loop antennas, the majority of the measurements were of the *H* field. Field measurements were carried out by using a self-developed bandpass active filter (50 Hz bandwidth), and a spectrum analyzer (HP8560A) that had a 1 Hz resolution bandwidth. The use of a spectrum analyzer highly facilitated the measurements, making it possible to easily distinguish noise and the signal radiated by the natural antenna. Occasionally, and on/off procedure was used to confirm the signal level. The magnetic-field measurement system was calibrated by using a reference magnetic field generated by a known current and a loop-coil antenna of 35 cm diameter in the frequency region of 1-20 kHz. The measured maximum magnetic field (MF) intensities obtained by rotating the receiving loop-coil antenna are given in Table 2, for the geographical positions shown on the map of the Attica peninsula in Figure 6.

Figure 6: A map of the Attica region, with the measurement points shown

6. Analysis of Measured Fields

In order to analyze the measured fields and to estimate the operating mode of the natural antenna, the following three possible radiation models were considered:

1. An edge-slot antenna model, consisting of a half slot length of $h = 2500$ m, and an average width of $w = 250$ m.
2. A vertical-loop antenna model, with a cross section of 7000 m^2 (an equilateral triangle with a base length at the peninsula throat of 350 m and a height of 40 m).
3. A horizontal-wire antenna of approximately 360 m, with a varying height, *h*, above sea level.

In all models, the antenna feeding current was taken to have a value of $I = 16$ A rms, as was measured during the experiments.

The magnetic field strengths for the three antenna models were calculated using formulas given in the book by King, Owens, and Wu [11]. The formulas given in [11, Section 7.10] were used for the horizontal-wire antennas. For the vertical-loop antenna, the results given in [11, Section 2.3] for the horizontal magnetic dipole were used by computing the equivalent magnetic-dipole moment. The case of the edge-slot antenna was computed by using the Babinet duality principle, taking the sea into account as having infinite conductivity (as this is valid for the low frequencies).

The numerical results obtained for the three types of radiators are given in Table 2, along with the measured magnetic fields. A comparison of the measured and theoretically computed results shows that the model of the horizontal-wire antenna provides the best agreement, when the height of the wire above sea level is about 10 m. The physical explanation of the validity of the short horizontal antenna could be attributed to the fact that the return-current path, being diffused at the base of peninsula, contributes insignificantly to the field strength.

Based on the above results, and assuming the validity of the wire-antenna model, the total radiated power was calculated using the Poynting-vector integral. The total power was found to be about 4 mW at a radiation frequency of 6.87 kHz.

In the above analysis, the effects of the ionosphere were neglected, since the measurements were carried out at very short ranges.

7. Conclusions

Based on the analysis of field strengths and the impedance measurements of the natural antenna, the following conclusions can be drawn:

1. The edge-slot model is invalid when associated with a low-conductivity peninsula, and it cannot operate as an efficient radiator. The reason for this is the short-circuiting currents below the peninsula's base. This fact was already predicted theoretically by different arguments (the high dielectric loss of the ground medium) by H. Staras, a long time ago [4].
2. The vertical loop seems to be invalid for the present case, because of the very low antenna height above sea level, and the very small loop cross-sectional area. It seems that the model predicted by Burton, King, and Wu in reference [12] could be valid, if the antenna's diameter and height above sea level is larger than for the present case.
3. The horizontal-wire model seems to predict the observed field measurements, since the current's return path below the peninsula's base is diffused in the ground environment.

8. References

1. M. G. Morgan, "An Island as a Natural Very-Low Frequency Transmitting Antenna," *IRE Transactions of the Professional Group on Antennas and Propagation*, **AP-8**, 1960, pp. 528-530.

2. M. G. Morgan, "In Memoriam: Millett G. Morgan," *Radio Science Bulletin*, No. 300, March 2002, p. 63.

3. R. N. Gould, "Some Preliminary Experimental Tests of a Novel Method of radiating at Very Low Frequencies," *Nature*, No. 42773, April 1961, pp. 332-333.

4. H. Staras, "Analysis of a Natural VLF Slot Antenna," in E. C Jordan (ed.), *Electromagnetic Theory and Antennas*, New York, Pergamon Press, 1963.

5. R. Barr, "A New Interpretation of the VLF Impedance Measurements of Island Slot Antennas," *Radio Science*, **15**, 5, 1980, pp. 959-964.

6. M. G. Morgan, "Comment on 'A New Interpretation of the VLF Impedance Measurements of Island Slot Antennas' by R. Barr," *Radio Science*, **15**, 1980, pp. 965-967.

7. R. C. Hansen, "Slot Antenna in a Resistive Screen," *IEEE Transactions on Antennas and Propagation*, **AP-46**, July 1998, pp. 1028-1031.

8. J. D. Kraus, *Antennas*, New York, McGraw-Hill, 1988, Chapter 13.

9. A. D. Watt, *VLF Radio Engineering*, New York, Pergamon Press, 1967, p. 94.

10. R. Barr and W. Ireland, "Low-Frequency Input Impedance of a Very Large Loop Antenna with a Mountain Core," *IEE Proceedings-H*, **140**, 2, 1993.

11. R. W. P. King, M. Owens, and T. T. Wu, *Lateral Electromagnetic Waves*, New York, Springer-Verlag Inc., 1992.

12. R. W. Burton, R. W. P. King, and T. T. Wu, "The Loop Antenna with a Cylindrical Core: Theory and Experiment," *IEEE Transactions on Antennas and Propagation*, **AP-31**, 2, March 1983.

Remote Sensing the Earth's Plasmasphere

D.L. Carpenter

1. Introduction

The plasmasphere is a doughnut-shaped plasma cloud that surrounds the Earth to an equatorial distance of several R_E (see, for example, [1], and references cited therein). Consisting primarily of cool (~1 eV) H^+ ions and electrons, supplemented by smaller populations of He^+ and O^+, it acts in part as a high-altitude extension of the Earth's regular (<1000 km altitude) ionosphere. As an element of the Earth's space weather system, it is subject to substantial changes during storm-like disturbances in space induced by solar activity. Figure 1 shows the location of the plasmasphere with respect to other features of the Earth's space environment, in cartoon fashion.

As is often the case with experimental work in space, the initial detection and description of the plasmasphere were accomplished without being predicted theoretically. Remarkably, these discoveries occurred through remote sensing from the ground, before the advent of the first high-altitude Earth-orbiting satellites.

In the early 1950s, Owen Storey, a graduate student at Cambridge University, investigated the puzzling phenomenon of whistlers, dispersed audio-range signals from lightning. In a work of profound importance for space physics, Storey [2] showed for the first time that whistler signals followed long paths in space, extending from one hemisphere to the other. He was able to demonstrate that the electron density at ~12,000 km altitude over the Earth's equator was ~400 el/cc, orders of magnitude higher than could be expected based upon contemporary understanding of the Earth's ionosphere and its probable extent above its peak at about 300 km altitude. These results had immediate impact: Within a year, J. Dungey [3], speaking at a 1954 conference on the physics of the ionosphere, speculated that charge exchange between H^+ and O^+ is important in the upper atmosphere, and stated in reference to Storey's work that "the many attractive features of his interpretation make

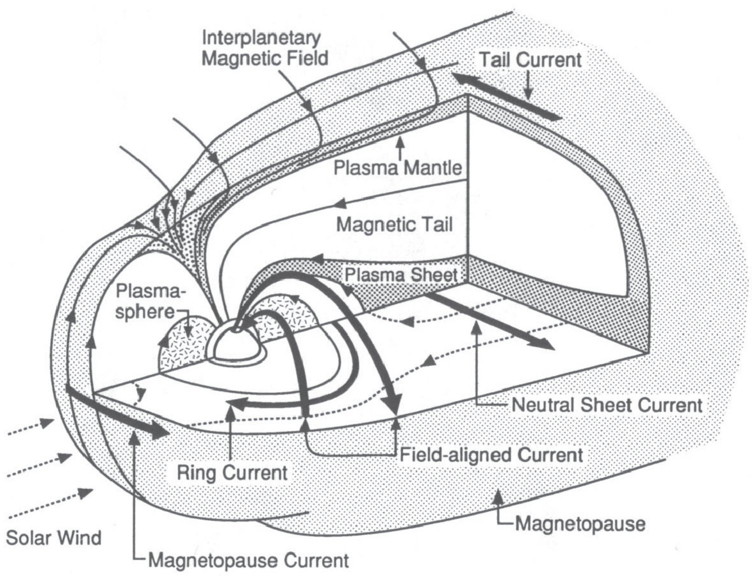

Figure 1. A diagram, from [129], of the space environment of the Earth, showing the location of the plasmasphere within the larger comet-like "magnetosphere," or region dominated by the Earth's magnetic field. Also shown are various important current systems and the interplanetary magnetic field.

D. L. Carpenter is with the Space Telecommunications and Radioscience Laboratory, Stanford University, Stanford, CA 94305-9515 USA;
Tel: +1 (650) 723-3585; Fax: +1 (650) 723-9251;
E-mail: dlc@nova.stanford.edu

Editors Note: This paper is one of the invited *Reviews of Radio Science*, from Commission H.

it [Storey's estimate of electron density at 12,000 km] reasonably certain."

In the early 1960s, thanks to further advances in understanding of their potential as natural probes of the Earth's plasma envelope, whistlers were used to show that the dense plasma region first detected by Storey has a geomagnetic-field-aligned boundary. This boundary was eventually called the plasmapause, the region at which the density level drops by about one order of magnitude [4]. Such a drop, also detected by ion traps aboard the Soviet lunar rockets in 1959 [5], was not expected according to contemporaneous ideas about the behavior of a high-altitude plasma in gravitational equilibrium [1]. Some had argued that plasma in the outer magnetosphere, under the influence of the solar wind, does not undergo bulk motions on trajectories that encircle the Earth [6]. However, there were essentially no predictions that the density in that outer region would be substantially lower than in the inner, approximately co-rotating region (except for reductions attributable to differences in flux-tube volume).

Remote sensing by whistlers thus led to new paradigms: (1) a light ion gas, the protonosphere, floats on the heavier ion gas of the regular, low-altitude ionosphere (see, for example, [7]); (2) an outer magnetospheric circulation pattern, driven by the solar wind, is configured so as to prevent a buildup of ionization along high-latitude field lines. Such a buildup might otherwise occur were there substantially longer periods of plasma interchange with the underlying ionosphere in those field line regions [8-11].

From its initial detection in 1953 to the present day, the plasmasphere has remained an attractive yet challenging target for remote sensing. Huge in size, of the order of 100 times the volume of the Earth, it regularly experiences complex cycles of erosion and replenishment during storm-like space weather events (see, for example, [12]). As an ever-changing plasma-wave propagation environment, it imposes corresponding changes on the conditions under which resonant interactions can occur between various wave modes and the hot, tenuous plasmas of the Earth's radiation belts. Through wave-induced particle scattering, such interactions give rise to particle precipitation into the Earth's upper atmosphere, and thus play a role in the loss of energetic particles injected into the magnetosphere during storm events (see later section). Wave-induced particle precipitation is known to affect the properties of the ionosphere as a wave propagation medium (see below). Such precipitation, varying in intensity and precipitating particle energy from inside to outside the plasmapause [13], may possibly affect the NO chemistry of the ionosphere (see, for example, [14]). Inward displacements of the plasmapause and steepening of its density profile represent conditions in which the potential of a satellite and its detectors can change rapidly, a situation that can complicate particle measurements but which also provides a means of sensing the plasmapause location in situ [15, 16].

Over the years, a variety of remote sensing methods have been developed and applied to the plasmasphere. Among these are: (1) the whistler-mode method of studying plasma-density structure and its variations with time, (2) the whistler-mode method of tracking plasma bulk motions, (3) the study of wave-particle energy and momentum exchange by injection of whistler-mode waves from the ground as well as by means of instruments for detection of wave-induced particle precipitation into the ionosphere. In the last decade, in an ongoing period of revived interest in plasmasphere studies, these methods have been supplemented by: (4) ultra-low-frequency (ULF) wave methods of determining mass density, (5) incoherent scatter and TEC measurements of plasmaspheric effects as they are manifested in the ionosphere, (6) EUV photon imaging of the plasmasphere by satellite measurements of scattered 30.4 nm sunlight from He^+ ions, (7) radio sounding of the plasmasphere along a high-altitude orbit. Without attempting to comprehensively review each topic, we now briefly describe these remote-sensing methods, and note some of the problems to which they have been applied. We also mention a number of the outstanding problems that remain.

2. The Whistler Propagation Method

2.1 Studies of Plasma Density Structure

The whistler method is illustrated schematically in Figure 2. It begins with a lightning discharge, shown in this case as occurring in the Northern Hemisphere. The impulsive very-low-frequency radiation from the lightning spreads in the Earth-ionosphere cavity. A fraction of this radiation penetrates the ionosphere, and at some locations becomes trapped in geomagnetic-field-aligned ducts, propagating therein to the conjugate hemisphere. A portion of the down-coming whistler wave energy is then able to penetrate the highly refracting ionosphere, after which the waves spread in the Earth-ionosphere waveguide and may be detected by ground receivers.

The remote-sensing power of a ducted whistler (see, for example, [17-21]) comes from the fact that its group velocity at any point is approximately proportional to the 1/2 power of the geomagnetic field strength. The observed delay-time-versus-frequency properties of a whistler are thus heavily weighted by the plasma environment along the most remote, near-equatorial, portion of its path, where variations in the plasma parameters per unit distance along the field lines are minimal. As a result, whistlers have been found to provide measures of total electron content within flux tubes of propagation, as well as measures of electron density near the magnetic equator that are relatively insensitive to the functional form of the distribution of plasma along the field lines used in the calculations [22, 23].

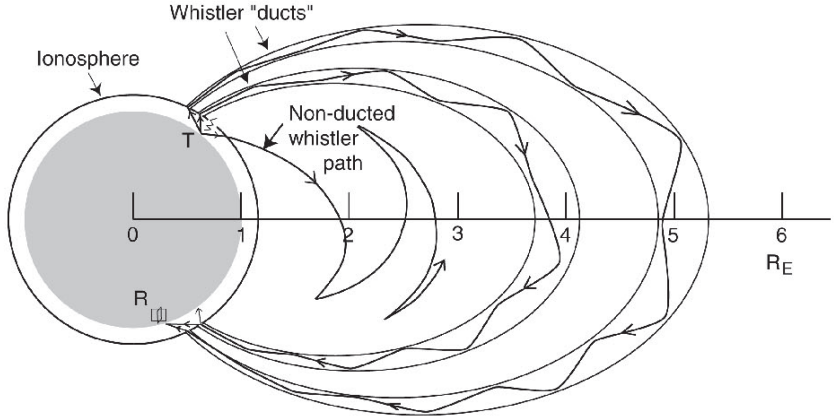

Figure 2. A meridian cross section of the Earth, showing in cartoon fashion the paths by which impulsive very-low-frequency energy from lightning, or signals from a ground transmitter (T), can propagate from hemisphere to hemisphere along discrete geomagnetic-field-aligned paths. The paths are believed to involve field-aligned density enhancements, which trap the waves and allow them to propagate with low loss in a manner analogous to that of waves trapped in optical fibers. A so-called "non-ducted" whistler path is also shown, in which the up-going wave energy, after penetrating the ionosphere, does not become trapped within a duct.

Whistlers regularly exhibit multiple discrete components, and are used to obtain information on equatorial electron density at multiple locations, for example near 4 R_E and 5 R_E geocentric distances in the simplified example of Figure 2.

Whistlers provided much of the early information on the global shape of the plasmasphere, on its equatorial density profile, and on the fact that it undergoes cycles of erosion and recovery during magnetically disturbed periods. In particular, discovery of a bulge-like extension in plasmasphere radius in the dusk sector [24] stimulated early efforts to interpret the shape of the plasmasphere in terms of the interplay between the motion of the plasma imposed by the Earth's rotation and the generally sunward flow in the middle magnetosphere driven by the solar wind as it impinges upon the magnetosphere [9, 10].

As data were accumulated over time and at many locations, it became possible to identify major temporal variations in the density of the plasmasphere, ranging in periods from hours to 11 years [25]. One of the more pronounced and, for many years, least well understood of these is an annual variation, with a maximum in December and a peak amplitude (~2:1) in the vicinity of the 75º W meridian [26]. The inherent difficulty in understanding the interplay between the comparatively rapidly changing ionosphere and the overlying but more slowly varying plasmasphere is illustrated by the fact that mechanisms that could explain the annual variation have been found both in the properties of the ionosphere [26] and in plasmasphere thermal structure [27].

Whistlers also made possible study of the interchange of plasma between the ionosphere and overlying plasmasphere, providing measures of the rate at which upward fluxes from the ionosphere refill depleted overlying regions [28], and clarifying the role of the plasmasphere as a reservoir for the decaying night-time ionosphere [29].

2.2 Tracking Plasma Bulk Motions

In the 1960s, it was realized that the radial, or cross-L, motions of discrete whistler paths could be tracked through measurements of corresponding changes in the

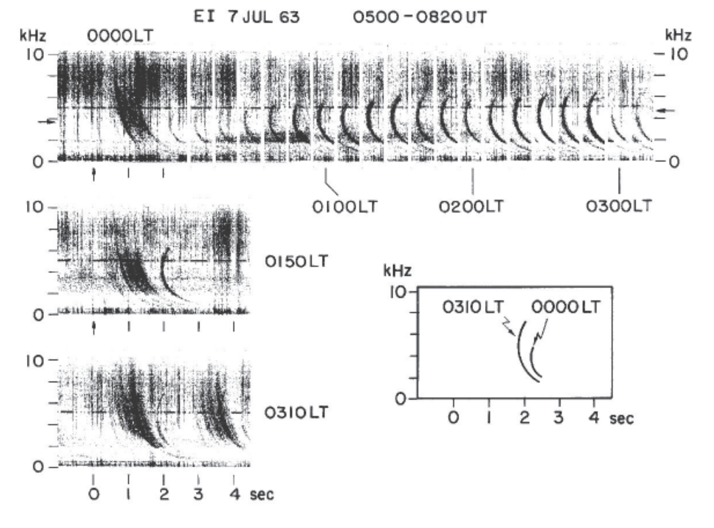

Figure 3. An illustration of the gradual changes in the frequency-time spectra of an individual whistler component as its discrete field-line path underwent bulk motions in a direction transverse to the geomagnetic field (from [24]). The recordings were made at Eights Station, Antarctica, on July 7, 1963.

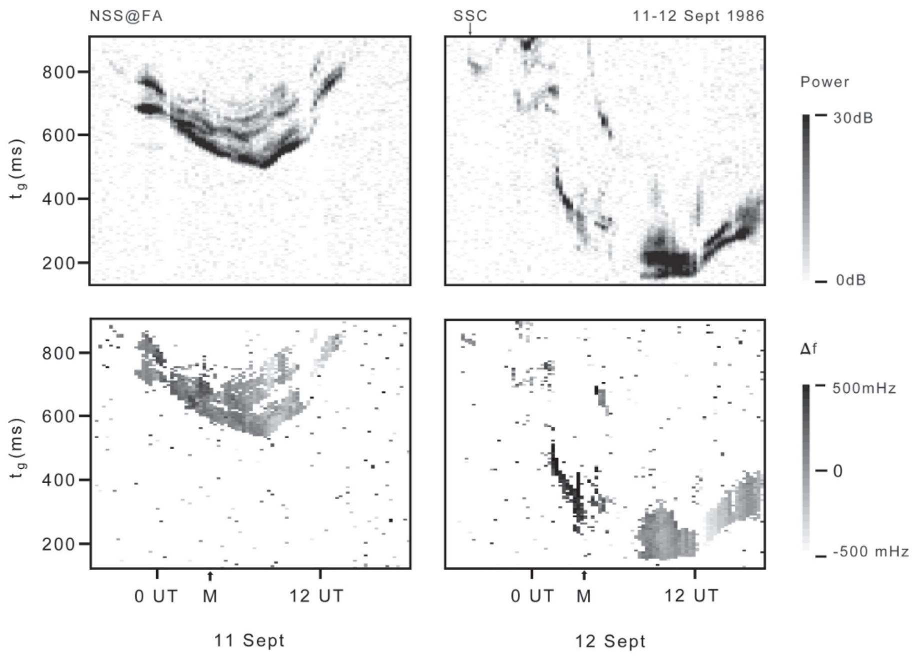

Figure 4. Examples of Doppler receiver data for September 11-12, 1986, showing nighttime changes in the group delay (above) and Doppler shift (below) of signals propagating from the NSS transmitter in the eastern US to a receiver in the Southern Hemisphere at Faraday Station, Antarctica (from [35]). The left panels show quiet-day behavior; the right panels show behavior following a sudden storm commencement (SSC).

travel time and curvature of the associated whistlers [24, 30, 31]. This would allow estimates of the azimuthal, or east-west, component of the large-scale magnetospheric electric field associated with the radial bulk motions. Figure 3 shows an example of gradual changes in the frequency-versus-time spectra of whistlers recorded during a three-hour night-time period [24]. At the left from top to bottom are three whistlers, recorded at 0000 MLT, 0150 MLT, and 0310 MLT, respectively. At the lower right is a tracing of the dispersion curve of one of the whistler components as it appeared at the beginning and at the end of this three-hour period. Along the top panel is a series of spectral segments, showing the traced component at roughly 10 minute intervals; its field-line path was found to have drifted inward through $\sim 0.3 R_E$ during the time displayed.

Extended-time series of whistlers recorded near the 75° W meridian in Antarctica provided the first evidence of enhanced sunward drifts in the outer plasmasphere on the night side of the Earth during substorms [30], an effect that had been predicted by early theoretical work on magnetospheric convection (see, for example, [6]). Eventually it became possible to develop an empirical model of the radial component of substorm-associated drifts [32]. Also studied was a distinctive pattern of quiet-day radial drifts in the plasmasphere, apparently driven by neutral winds of thermal origin that flow in the ionosphere and give rise to the quiet-day SQ current system [33].

Fixed-frequency whistler-mode signals from communication transmitters propagating on magnetospheric paths presented an exceptional remote-sensing opportunity. Through a combination of measurements of group delay and Doppler shift, it became possible during drift events to separately identify and assess the effects of changing path length and of plasma interchange with the underlying ionosphere [34]. Figure 4 shows an example of Doppler receiver data obtained on two successive nights, one calm and the other disturbed by a sudden storm commencement [35, 36]. Local midnight is indicated by an "M" at the bottom. A major part of the quiet-day changes (left) is attributed to interchange fluxes with the ionosphere (decay at night followed by morning-side replenishment). The larger excursions on the second night reflect the occurrence of inward bulk motions of the plasma during episodes of enhanced convection electric fields.

In the 1980s, digital processing was applied to original tape-recorded data of fixed-frequency several-kHz signals from an experimental transmitter at Siple, Antarctica [37]. The signals had propagated along paths near $L = 4$ to a ground station in Canada. From comparisons of the received signal phase with the phase of a stable reference, it was found possible to estimate the drift rate of a signal path with a time resolution of seconds, in comparison to the order of minutes or tens of minutes required through group-delay measurements of whistlers.

2.3. Outstanding Problems in the Area of Passive Whistler Mode Probing

It is a curious fact that although remote sensing of the magnetosphere depends upon propagation guided by field-aligned density structures or ducts [38], very little specific information is available about the structures, including their origin and distributions in space. The situation is illustrated by findings that a single ducted whistler can contain several hyperfine elements [39, 40], and awareness that this could be interpreted either in terms of spatial electron-density fluctuations, or possibly in terms of the excitation of multiple propagation modes within a duct [41]. There is a need to bring theory and observations closer together on this subject, bearing in mind that the literature contains a number of papers about instabilities or electric-field configurations that may give rise to density structure within and beyond the plasmasphere [42, 43, 1]. Through both modeling and experimental work, more needs to be learned about the excitation of ducts by up-going whistler-mode waves, about propagation within ducts, and about the conditions of de-trapping of ducted waves in the topside ionosphere [44].

Whistler-mode probing, both by whistlers and transmitter signals, continues to have great potential for remote sensing of plasma motions, time variations, and density structures. Past work, especially with whistlers, has been limited in scope by the laborious nature of the pattern-recognition methods used. Future work, capable of analyzing large quantities of data and at times based upon controlled wave injection, could fill many gaps in our knowledge, as well as provide routine "space weather" information on key geophysical quantities such as equatorial profile levels and plasmapause radius. One of the challenges in this new work would be to further develop and apply tools for automatic detection and analysis of whistlers, along lines discussed by Hamar and Lichtenberger [45]. Much can be accomplished through applying modern digital signal-processing methods to libraries of tape-recorded data acquired during past measurement campaigns in regions of exceptionally high activity.

Phase measurements of whistler-mode signals can apparently be used to detect the equatorial component of ULF field-line perturbations. Paschal et al. [46], using several-kHz signals from the experimental Jupiter transmitter at Siple, Antarctica (L ~ 4.3), showed how this method could be used to detect ULF activity along a particular L shell, the L value being determined from dispersion measurements on multi-frequency components of the signals. The possibilities of this method, which would not be restricted to the dayside of the Earth, have yet to be explored.

3. Remote Sensing of Hot Plasma Effects

3.1 Whistler-Mode Wave-Injection Experiments

Early studies showed that whistler-mode signals that emerge from the magnetosphere and are incident on ground antennas can carry both an imprint of the cold component of the magnetospheric plasma through which they have propagated, as well as evidence of interactions with the hot electrons of the Earth's radiation belts [47-51]. The cold dense plasma provides a slow-wave structure that controls the velocity-versus-frequency characteristics of the waves. The radiation-belt electrons can exchange energy and/or momentum with the waves through cyclotron or Landau resonance interactions along the geomagnetic field line paths, and hence influence the amplitude spectra of the waves (see, for example, [52]).

It was found that both whistlers and fixed-frequency whistler-mode signals from transmitters can trigger emissions at new frequencies [49, 53]. The transmitter

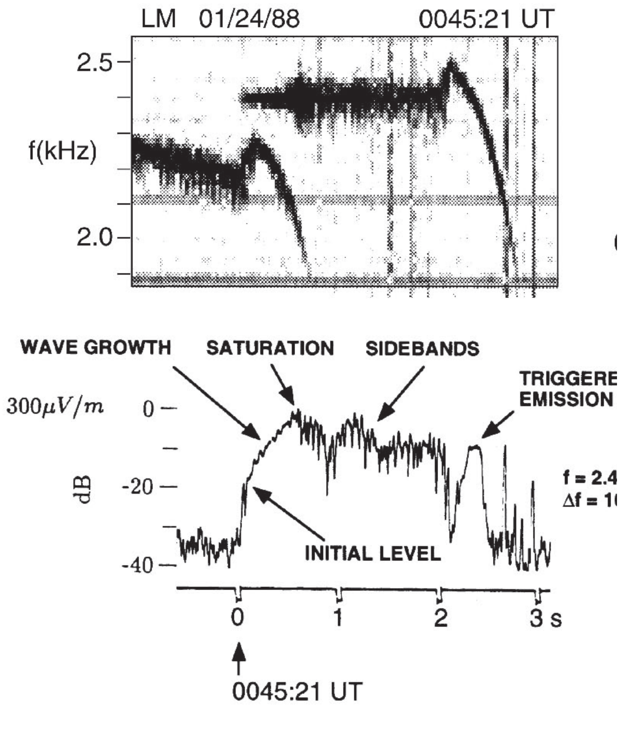

Figure 5. A frequency-time spectrogram and associated amplitude record illustrating the occurrence of the Coherent Wave Instability (adapted from [58]). The recording was made at Lake Mistissini, Canada, on January 24, 1988, during reception of signals propagating through the magnetosphere from Siple Station, Antarctica.

signals were of particular interest; they showed evidence of pulse-length-dependent emission triggering, indicative of fast temporal growth of the triggering signal [50]. Such findings became the impetus for controlled whistler-mode wave-injection experiments initiated in the late 1960s and early 1970s. A number of such experiments were successfully conducted on a campaign basis between Alaska and New Zealand, using a transportable VLF source and a balloon-borne antenna [54]. The most extensive work was carried out on a regular basis from 1973 to 1988 between Siple Station, Antarctica, and conjugate stations in Quebec, Canada [55]. In this case, it had been speculated that extensive signal processing would be needed for detection of magnetospherically propagating signals near $L = 4$ from such a weak source, radiating at most a few kilowatts from a 21-km or 42-km-long horizontal dipole over a 2-km-thick Antarctic ice sheet. Instead, signals were regularly received at levels tens of dB above the background noise, showing evidence of temporal wave growth of the order of 30 dB, and growth rates in the range 20 to 250 dB/sec [56].

Over time, the major elements in what became known as the coherent wave instability (CWI) were studied under various conditions of transmitter frequency and pulse length [57]. Figure 5, from [58], shows a spectrogram of two Siple signals received in Canada: a descending-frequency ramp (first part not shown) and a two-second fixed-frequency pulse transmitted at 2400 Hz. Below is an amplitude record of the two-second pulse; it includes evidence of CWI elements such as exponential growth, saturation, sidebands, and triggering of emissions. Models of a feedback process involving an interaction region at or near the geomagnetic equator, an injected wave, and counter-streaming electrons were developed to explain what appeared to be a fundamental aspect of wave-particle interactions in near-Earth space [59, 60].

3.2 Outstanding Problems in Wave-Injection Experiments

One of many fundamental questions raised by the wave-injection experiments concerns the level of the input signal to the hypothesized high-altitude interaction region required to initiate fast temporal growth. In some theoretical treatments of the interaction problem, the input signal is assumed to be at a level sufficient to trap cyclotron-resonant electrons in the magnetic potential well of the wave (e.g., [61, 62]). In other interpretations – for which experimental evidence has been offered [63] – the input signal can be at any level above a threshold imposed by the background noise in the medium [60, 64].

3.3 Remote Sensing of Wave-Induced Particle Scattering

Scattering of radiation-belt electrons by whistler-mode waves has been a topic of interest in space physics for over 40 years [65-69]. One of the most sensitive tools for studying wave-induced precipitation of energetic electrons is the measurement of phase and amplitude perturbations on sub-ionospherically propagating VLF transmitter signals. Such perturbations, associated with secondary ionization created in the night-time ionosphere at ~80 km altitude by precipitating energetic (> 40 keV) electrons, were found to be correlated on a one-to-one basis with the propagation along the related field lines of lightning-generated whistlers (the "Trimpi Effect") [70-72]. Studies of the ionospheric perturbations and their geophysical implications were, for some time, focused on the scattering action of ducted whistlers received on the ground [73-75]. However, such studies have recently broadened to consider effects of the more general non-ducted type of whistler [76], the ray path of which may execute many crossings of the magnetospheric equator and does not usually reach the ground, as illustrated in Figure 2. Thanks to the deployment of arrays of receiving stations, it has become possible to separately identify the ionospheric perturbations induced by ducted and non-ducted waves [76, 77].

Other ground-based tools for remote study of the mechanisms of wave-induced particle scattering include X-ray detectors (see, for example, [78, 79]) and photometers [80], which have been used to investigate the effects of quasi-periodic, burst-like precipitation near the ionospheric projection of the plasmapause.

3.4 Outstanding Problems in Particle Scattering

The sub-ionosphere VLF signal work aims at understanding the contribution of both non-ducted and ducted lightning whistler waves as well as transmitter waves to losses of particles from the radiation belts. Interest continues in improved modeling of the VLF signal propagation in the presence of ionospheric perturbations, with the objective of using the observed data to infer both the ambient ionospheric profile and the size of the density perturbation [81, 82]. A longstanding question, first raised many years ago, concerns a reported widespread perturbation of the night-time lower ionosphere at plasmasphere latitudes, not apparently associated with transient whistler events, but occurring during periods of substorm activity [83, 84]. Important questions remain on the nature and geophysical significance of the strong interactions that occur between naturally occurring whistler-mode waves and energetic particles at or near the plasmasphere boundary.

4. Ultra-Low-Frequency Studies of Plasmasphere Mass Density

4.1 Experimental Method

It has long been realized that ULF pulsations detected on the ground carry information about the specific

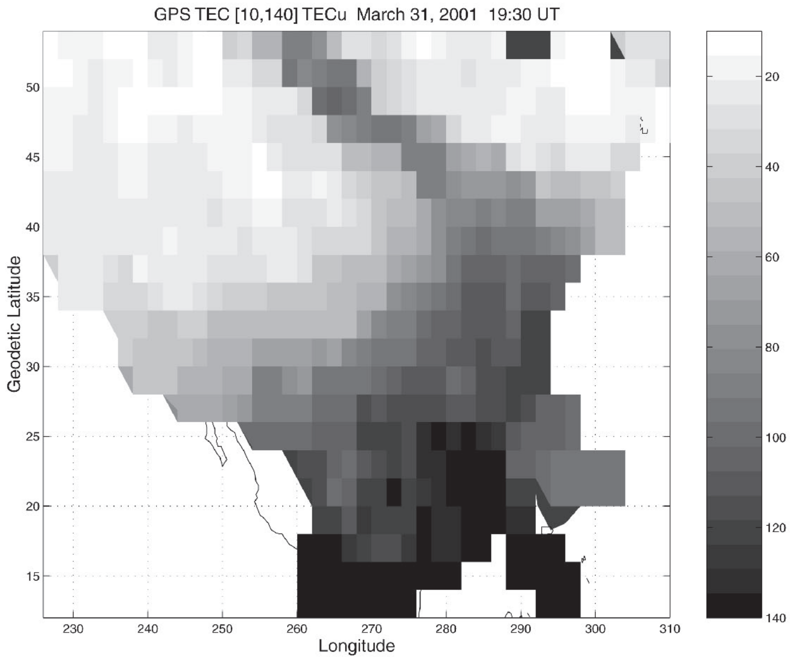

Figure 6. A map over North America of the total electron content (TEC), an integral measure of the plasma density between ground points and GPS satellites. The data were acquired on March 31, 2001, at 1930 UT, during a period of strong geomagnetic storm activity. The darker regions include an extension upward and toward the left that is interpreted as evidence of a plume of dense ionization drawn out into the afternoon sector during an erosion event in the overlying plasmasphere (from [102]).

magnetospheric regions through which the waves propagate. The idea that field-line resonance can be used to estimate the mass density at high altitudes was advanced more than three decades ago [85, 86]. The use of ULF-inferred density to study plasmaspheric properties was initiated by Webb et al. [87] and by Lanzerotti et al. [88]. In early studies, the determination of resonant frequencies suffered from contamination of the wave spectrum by the driving-wave energy. This observational difficulty was first resolved by Baransky et al. [89] with their "gradient method," using a pair of stations separated by roughly 100-200 km in latitude. This method continues in use to the present day; one seeks information on field-line resonance (FLR) frequency as a function of observing-station latitude (see, for example, [90, 91]). The phase and amplitude of the various observed ULF frequency components are determined, and through auto- and cross-correlation techniques involving spaced stations, particular ULF frequencies are identified as the eigenfrequencies associated with particular magnetic shells or L values. The value of the eigenfrequency for a particular L shell is then used to estimate the mass density along that field line at high altitudes, and from a latitudinal array of stations, a multi-point profile for the plasmasphere may be obtained, analogous to an electron-density profile obtained from a multi-component whistler. The gradient method can successfully identify eigenfrequency signatures in both the plasmasphere and the outer magnetosphere, for L values from as low as 1.5 [92] to as high as 11 [93].

Temporal changes in the profile depend upon factors such as plasmasphere erosion and refilling that affect total plasma density, and also upon changes in ion composition, which are expected to depend upon a number of factors involved in the transport of mass and energy through the magnetosphere. The ULF method is most effectively applied under daytime conditions, and continues to be developed as a geophysical tool (see, for example, [94]).

4.2 Outstanding Problems in Mass Density Measurements

Key questions that remain concern the relative abundance of heavy ions in the plasmasphere, as well as the question of plasma losses through interchange with the underlying ionosphere during magnetic storms. Study of these questions will clearly involve coordination with other experiments, as exemplified by recent comparisons among ground-based measurements of plasmasphere mass and electron density, and IMAGE satellite maps of plasmasphere He^+ content [95], supported by local measurements of electron density along IMAGE orbits.

5. Incoherent Scatter and TEC Measurements

5.1 Detection of Plasmaspheric Effects

Understanding the behavior of the ionosphere in the presence of the overlying plasmasphere has presented a major challenge to researchers over the years, in part because of the different time scales on which the two regions act in response to "space weather." For example, the disturbance processes that establish a new plasmapause boundary may leave a clear imprint on the underlying ionosphere in the form of SAR arcs (stable auroral red arcs) [96, 97], light-ion troughs [98], and electron-temperature enhancements [99], but these coincidences are not the rule during the later phases of a disturbance/recovery cycle (see, for example, [1, 100]). However, incoherent-scatter radar data have for some time revealed plumes of enhanced ionization at ionospheric heights with plasma flow direction generally sunward [101]. Recent evidence, including measurements of total electron content (TEC) along lines of sight through the ionosphere and plasmasphere to spacecraft such as the GPS constellation, indicates that these low-altitude features are ionospheric projections of sunward-extending plumes that develop in the afternoon-dusk sector of the overlying magnetosphere as part of the plasmasphere erosion process [102]. The projections have been called SEDs, or Storm Enhanced Density(s).

The relationship between low- and high-altitude plasmas has come to light with clarity, thanks to the recent development of large-area TEC maps with a time resolution of ~15 minutes [103]. These maps have been combined with radar measurements of plasma-flow velocities in and near the SED structures, making it possible to confirm that the plumes, at least during the early phases of a disturbance, act to drain dense plasma from the main plasmasphere [102]. Figure 6 shows an example of plume effects as they have appeared on a TEC map covering a region in the Eastern US and Canada.

5.2 Outstanding Problems

It is far from clear just how faithfully ionospheric structures and motions reflect corresponding aspects of the overlying region (see, for example, [104]). Studies are needed that compare the distribution and movements of cool plasmas in the outer dayside magnetosphere with the behavior of the ionosphere. As the structure of the plasmasphere is more completely mapped on a global basis, corresponding effects in the ionosphere must be sought. One outstanding question concerns the substantially reduced density levels found within the plasmasphere in the aftermath of a period of erosion. Such losses would appear to occur via plasma interchange with the ionosphere, but corresponding ionospheric effects have yet to be clearly identified [105].

6. EUV Photon Imaging of the Plasmasphere

6.1 Observations by the EUV Instrument on the IMAGE Satellite

Arguably the most significant advance in remote sensing of the plasmasphere since the early applications of lightning whistlers is the development of wide-field cameras that map the dense plasma near the Earth by recording

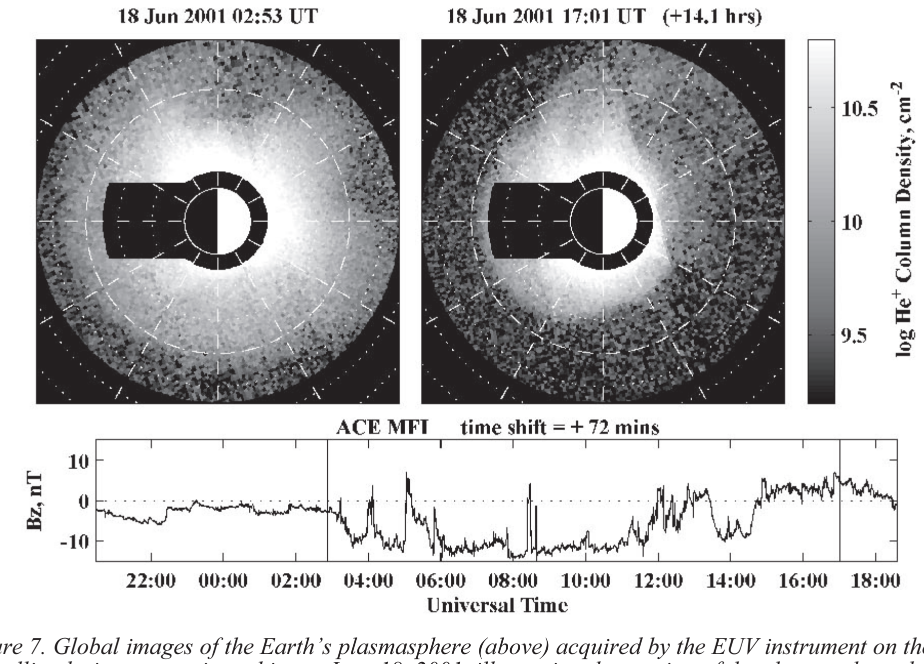

Figure 7. Global images of the Earth's plasmasphere (above) acquired by the EUV instrument on the IMAGE satellite during successive orbits on June 18, 2001, illustrating the erosion of the plasmasphere during an interval when the interplanetary Bz magnetic field component was strongly negative. The vertical lines on the magnetometer record (below) indicate the times of the EUV records, one preceding the erosion event and the other in its aftermath. The ACE magnetometer record, acquired upstream of the Earth, was shifted by 72 minutes to account for a propagation delay from spacecraft to Earth. In the EUV records, the nightside region and a region close to the Earth have been masked so as to emphasize the main body of the plasmasphere. The slanting change in brightness on the sunward side of the Earth in the right-hand panel is an artifact of the differences in view between the EUV cameras (figure courtesy of M. Spasojeviæ).

resonantly scattered 30.4 nm sunlight from the He^+ component of the plasmasphere [106]. Previously known in certain respects in a composite sense, the bulk of the entire plasmasphere suddenly leaped into view. Figure 7, upper panels, shows two 30.4 nm images of the plasmasphere acquired 14 hours apart on successive orbits by the EUV instrument on the IMAGE satellite, launched in March 21, 2000. The view is from near $8 R_E$ geocentric distance over the northern polar region. Local noon is to the right; a nightside shadow region and a high-density region near the Earth have been masked so as to emphasize the main body of the plasmasphere. Below is a magnetometer record from the ACE satellite, showing an interval of strongly negative Bz, a southward turning of the solar-wind magnetic field. Vertical lines show the times of the EUV observations above, shifted by a propagation delay from the magnetometer observation point in the solar wind to the Earth.

Continuing work with the EUV instrument has led to the ability to map the He+ content integrated along the camera lines of sight into the magnetic equatorial plane. It has also led to the ability to verify the many circumstances in which the apparent outer "edge" of the He^+ envelope corresponds to the actual plasmasphere boundary, as determined from the RPI (Radio Plasma Imager) instrument on IMAGE [107], when IMAGE crosses that boundary earlier or later on the same orbit [108].

The images in Figure 7 show, in dramatic fashion, the diminution in plasmasphere size that can occur as the result of an interval of enhanced coupling of solar-wind energy to the magnetosphere. The image at the left, representing quiet conditions, shows a plasmasphere extending well beyond $4 R_E$ (dashed circle) at most local times. The image at the right shows a well-defined outer limit to the He^+ brightness across the night side. This apparent plasmapause boundary curves inward inside $3 R_E$ in the dawn sector, and appears to remain near that radius across the dayside. (The slanting brightness variation running from 10 LT into the afternoon sector is an artifact of the differences in the fields of view of the three cameras involved.)

The regular availability of plasmasphere images acquired at intervals of 10 minutes over orbital segments of several hours has led to important advances in understanding of plasmasphere dynamics during the various phases of magnetic storms [12, 109, 110]. Spasojeviæ et al. [12] have used the EUV data to obtain equatorial cross sections of the plasmasphere during magnetic-storm events as the plasmasphere radius on the nightside is sharply reduced and the apparent steepness or scale width of the plasmapause is reduced, as well. The inward displacement of the boundary was found to be most pronounced in the post-midnight sector, a result consistent with earlier findings from whistlers. However, the global scale of the view has made it possible to observe previously unknown features, such as the tendency for any preexisting irregularities in nightside plasmasphere radius to disappear as the plasmapause forms a smooth curve (on spatial scales of a few tenths of an R_E). The EUV data also show a feature only hinted at in earlier work, namely, a sunward surge of plasma on the dayside during the erosion activity on the nightside.

A distinctive feature of the right-hand record in Figure 7 is a plume extending outward from the main body of the plasmasphere, in this case at 18 MLT. Evidence of such features extending outward in the afternoon-dusk sector has previously been obtained from the in-situ perspectives of satellites [111-113], and from ground-based whistlers [114-116]. Such features were predicted in some of the earliest attempts to model the dynamic behavior of the plasmasphere during an erosion event [117]. However, this has been the first opportunity to investigate plume development in real time on a global scale.

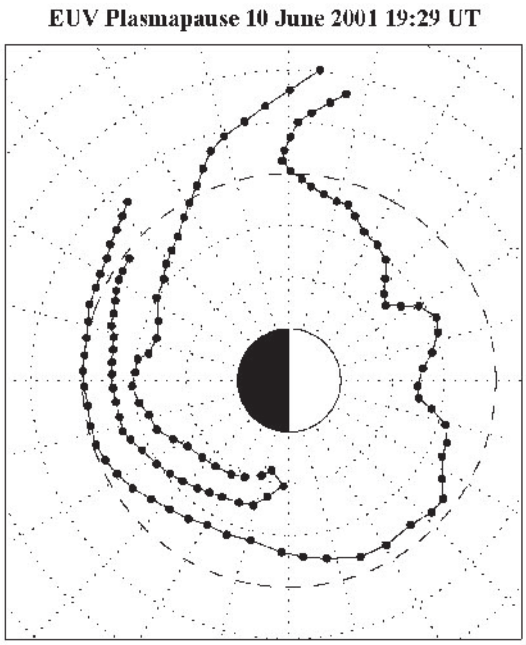

Figure 8. The magnetic equatorial configuration of the plasmasphere during a period of deep quieting following plasmasphere erosion activity on June 10, 2001 (from [12]). A low-density channel appears on the nightside between the main body of the plasmasphere and an outlying feature that earlier appeared as a density plume extending sunward from the dusk sector. Another more recently formed plume appears in the dusk sector. The plasmasphere outline was scaled from an EUV global image.

Figure 8, from [12], shows a remarkable example of the development of plasmasphere structure in the recovery phase of a storm, as a previously sunward-extending plume begins to wrap around the plasmasphere under the combined influence of the Earth's co-rotational dynamo and the reduced but ongoing convection activity that is often present at such times. As the result of the nonuniform rotation of the plume with the Earth, a cavity develops between the main plasmasphere and the plume, extending across the night-side of the Earth, while near dusk a new plume develops, apparently as a consequence of the ongoing weak substorm activity.

6.2 Outstanding Problems in EUV Imaging

Photon imaging of the plasmasphere is just beginning, and allows for pursuit of many important questions. To what extent does the plasmasphere rotate with the Earth, and to what extent can one model the flow of plasma by simply combining the equipotentials established by the solar-wind dynamo with an assumed distribution from co-rotation? How much plasma is lost to the magnetopause during a storm or substorm, and how much is lost due to storm-time interchanges with the ionosphere? How granular is the plasmasphere? On what scales can the granulation be measured? How does the plasmasphere interact with the hot plasmas of the plasma sheet during storm/recovery cycles? What can be learned from auroral data on IMAGE about the relations between precipitation into the ionosphere and plume-like extensions of the plasmasphere?

7. Radio Sounding of the Plasmasphere at High Altitudes

7.1 Sounding by the Radio Plasma Instrument on the IMAGE Satellite

Radio sounding has been highly successful in remote sensing of the Earth's ionosphere, both from the ground and from the topside ionosphere. The ISIS series of satellites, among others, created a rich body of knowledge and experience, which is currently being extended through operation of a sounder at high altitude, the Radio Plasma Imager (RPI) on the IMAGE satellite [107]. Since April, 2000, RPI has been operating in a polar orbit with apogee at $\sim 8 R_E$ and perigee ~1200 km altitude [118].

The general range-versus-frequency forms of RPI echoes returning from various locations in the plasmasphere tend to agree with pre-launch predictions [119, 120]. However, they have unexpectedly exhibited range spreading of the kind observed during topside sounding in the auroral zones [121], with indications of both coherent scattering from irregularities near the spacecraft and a variety of other interactions with density structures that appear to be field aligned [120]. In contrast, those RPI echoes that do exhibit discrete forms are of an unexpected kind, one that follows geomagnetic-field aligned paths, often into both the local and the conjugate hemispheres [118]. The discrete returning signals allow for direct study of the plasma distribution along the field lines, a subject of great interest because of the dynamic nature of that distribution [122].

Figure 9a shows a plasmagram, analogous to an ionogram but with virtual range in Earth radii plotted upward versus sounder frequency. The traces on the plasmagram are echoes propagating for the most part in the right-hand extraordinary mode (R-X), along field-line paths near $L = 3$ within the plasmasphere. Figure 9b shows a simplified diagram of the location of IMAGE in the southern hemisphere at $-24°$ and $L \sim 3$. Two field-aligned propagation paths are indicated, path A into the local hemisphere and path B into the northern, conjugate, hemisphere. In Figure 9b, the echo from path A begins at zero range at f_X, the X-mode cutoff frequency of ~240 kHz, while the echo from path B begins at an undefined long range at the same frequency. Also seen above in Figure 9a is an echo that represents the sum of delays along paths A and B (see the caption of Figure 9 for more details).

From plasmagrams of the kind illustrated, it is possible to construct the field-line density distribution from the data through established as well as newly developed inversion techniques [123]. Figure 10 shows the profiles obtained from a series of field-line echoes in coordinates of density versus magnetic latitude, obtained along a single IMAGE orbit as the satellite moved through the plasmasphere [123].

The remote-sensing experience of the plasmasphere by radio sounding, using both the direct and field-aligned echoes, indicates a region regularly permeated by small-scale irregularities [120, 124]. RPI has therefore extended to high altitudes evidence of types of sounder interactions with plasma structures already familiar from near-equatorial low-altitude work, as well as auroral zone studies.

The richness of the O- and X-mode sounding data from RPI is being augmented through study of echoes obtained both in the whistler mode and the Z mode [125, 126]. In both cases, there is substantial activity during low-altitude soundings, below about 5000 km altitude, allowing for study of density in regions that are not easily reached by the free-space mode echoes being observed from higher-altitude IMAGE locations.

7.2 Outstanding Problems in Radio Sounding of the Plasmasphere

What is the origin and distribution of the irregularities that are observed both inside and outside the plasmasphere?

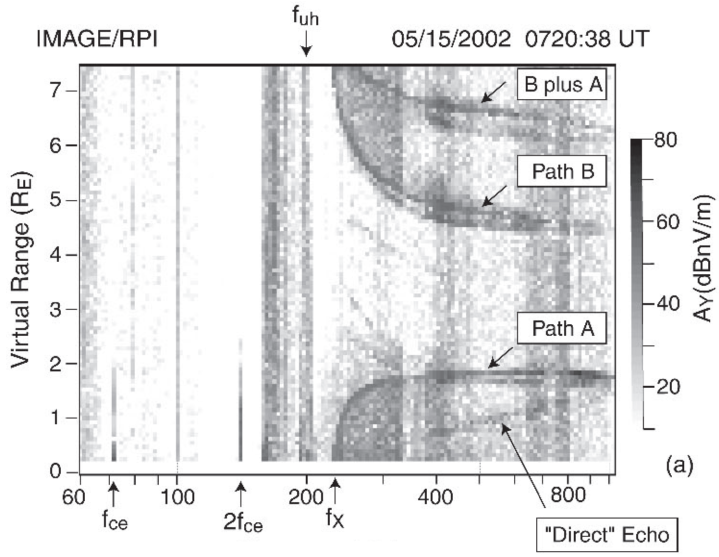

Figure 9. (a) A RPI Plasmagram from May 15, 2002, showing in coordinates of virtual range (range assuming speed of light propagation) versus sounding frequency examples of X-mode echoes that propagated along geomagnetic-field-line paths both into the local (Southern) hemisphere (Path A) and into the conjugate hemisphere (Path B).

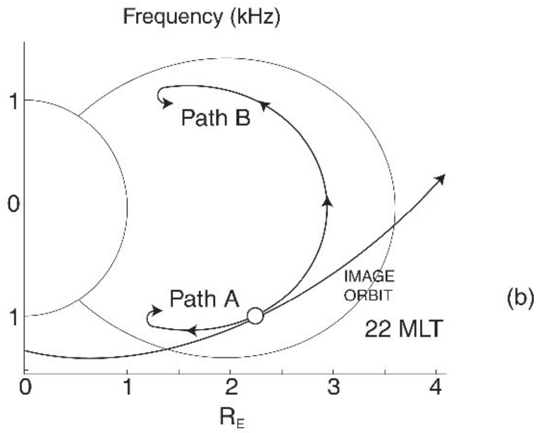

Figure 9. (b) A diagram of the IMAGE location in the plasmasphere and the directions along field lines of Path A and Path B. The ranges of the echo marked B plus A represent a combination of the ranges for Path A and Path B, implying that after initial reflection, propagation continued back and forth along the same discrete field-line path. At this time, IMAGE was moving just inside a geomagnetic-field-aligned cavity in the plasmasphere, where electron density was a factor of approximately three less than in the adjacent (outer) region. The echoes with ranges slightly shorter than those of the stronger traces in (a) are also believed to have propagated along essentially field-line paths, possibly in a whispering gallery mode at the outer edge of the density cavity. At bottom is a "direct" X-mode echo, relatively weak in comparison to the field-line echo, but with form expected for propagation deeper into the plasmasphere in a direction generally transverse to the field lines [119, 120].

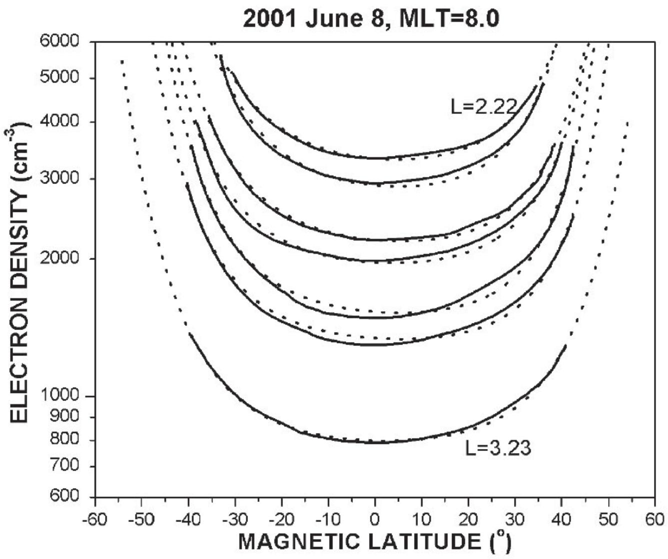

Figure 10. Profiles in coordinates of electron density versus magnetic latitude, obtained by inversion of echoes detected on a series of RPI soundings along a single IMAGE orbit through the plasmasphere on June 8, 2001 (from [123]).

What can be learned about the physics governing the field-line plasma distributions in the polar regions and within the plasmasphere (see, for example, [127])? There are many longstanding issues involving the Z and whistler modes, and about coupling between modes, that can be studied using RPI (see, for example, [128]). There is much to learn about the operation of a sounder, for example, about the behavior of a long-wire electric antenna in the plasma. That problem has always been considered a difficult one (see, for example, [130]), and it has complicated the efforts to do direction finding with the three-axis RPI antenna system. It was previously thought that the special class of sounder echoes found to be returning to RPI from the geomagnetic-field-line direction would provide a clear basis for multiple-antenna calibration and, hence, for achieving a general direction-finding capability. However, the observed field-line echoes have not provided the consistently unambiguous directional information that was anticipated. This is believed to be attributable to the tendency of the returning signal to be a superposition of waves arriving with a random distribution of wave normals within a cone around the magnetic-field direction [Bodo Reinisch, personal communication].

8. A Suggested New Term: Plasmasphere Boundary Layer (PBL)

Much attention within the space-physics community is paid to boundary layers, such as the Low-Latitude Boundary Layer (LLBL) at the magnetopause, and the Plasma-Sheet Boundary Layer (PSBL) at the edge of the plasma sheet in the Earth's magnetic tail. Such layers tend to develop at interfaces between plasmas that have distinctly different properties when considered as fluids, or on the basis of kinetic descriptions (see, for example [131, 132]). Curiously, the plasmapause region is almost never described as a boundary layer, in spite of: (1) the fact that it has been associated with locations where the cool dense plasmasphere may overlap with, or otherwise be in close proximity to, the hot plasmas of the plasma sheet and ring current [133, 134]; (2) widespread belief in a shielding effect, whereby nightside juxtapositions of hot and cold plasmas give rise to currents flowing along geomagnetic field lines and associated electric fields that dynamically "shield" the interior of the main plasmasphere from a higher-latitude flow pattern (see, for example, [133-135]). Part of the problem may be that many introductory discussions of plasmasphere dynamics, in particular those in textbooks, tend to describe the erosion and recovery of the plasmasphere in simple MHD terms: a newly developed plasmapause emerges as a topological consequence of the existence of two plasma-flow regimes perpendicular to **B**, one induced by the rotating Earth and the other by the solar wind as it impinges upon the magnetosphere (see, for example, [136, 137]). Such discussions regularly treat plasmasphere dynamics in terms of a "Last Closed Equipotential" (LCE) of the combined cross-**B** flow regimes. This is a pedagogically attractive device that tends to deflect attention from important questions about specific physical processes that may, in concert with the dynamo sources underlying the main flow, contribute to plasmasphere erosion; interchange instabilities; turbulence and the formation of irregularities; heating of the plasmapause region; energetic particle precipitation; fast, latitudinally narrow westward flows during substorms; etc. In reaction to this situation, and as a step toward more balanced and penetrating introductions to the physics of the plasmasphere, it would seem appropriate to add the concept of a Plasmasphere Boundary Layer (PBL) to our lexicon. It is noteworthy that as long ago as 1974, M. Rycroft and J. Lemaire acted as conveners of a symposium on the physics of the plasmapause at the second European Geophysical Society meeting [139], and that in 1983, J. Green and J. Horwitz organized a conference at the NASA Marshall Space Flight Center on physical processes in the plasmapause region [140].

9. Concluding Remarks

Interest in the plasmasphere has recently surged, with the development of new or more refined remote sensing tools and with an associated increase in awareness of the region's geophysical importance. Increasing attention is now being paid to the broad subject of interactions between the cool plasmasphere and hot plasmas injected during storms and substorms. Important questions are being asked about the fate of plasma eroded from the plasmasphere and convected sunward. Many areas have yet to receive the attention they deserve: for example, we still do not know exactly how a new plasmapause is formed, nor do we know much about the role of instabilities in creating or modifying the properties of that boundary region. Furthermore, we have only rudimentary knowledge of the coupling of the plasmasphere to the nonuniform underlying ionosphere. In short, there is much to do, and remote sensing will surely play an important role in this future work.

10. Acknowledgment

This review is dedicated to the memory of Yela Bogitch, who always symbolized for me the best that is URSI. I wish to acknowledge important contributions to the preparation of the review by A. J. Smith, M. A. Clilverd, P. Chi, J. C. Foster, X. Huang, M. Spasojeviæ, J. Lemaire, and B. Reinisch. Their comments and those of other colleagues are deeply appreciated. Part of the preparation of this review was supported by subcontract No. 03-08482 to Stanford University from the University of Massachusetts Lowell.

11. References

1. J. F. Lemaire and K. I. Gringauz, *The Earth's Plasmasphere*, Cambridge, Cambridge University Press, 1998.

2. L. R. O. Storey, “An Investigation of Whistling Atmospherics,” *Philosophical Transactions of the Royal Society (London) A*, **246**, 1953, pp. 113-141.

3. J. Dungey, “Electrodynamics of the Outer Atmosphere,” in *The Physics of the Ionosphere*, report of the Physical Society Conference held at the Cavendish Laboratory, Cambridge, September 1954, The Physical Society, London, 1955, pp. 229-236.

4. D. L. Carpenter, “Whistler Evidence of a ‘Knee’ in the Magnetospheric Ionization Density Profile, *Journal of Geophysical Research*, **68**, 1963, pp. 1675-1682.

5. K. I. Gringauz, V. G. Kurt, V. I. Moroz, and I. S. Shklovsky, “Results of Observations of Charged Particles up to R = 100,000 km with the Aid of Charged Particle Traps on Soviet Cosmic Rockets,” *Astronomicheskii Zhurnal*, **37**, 1960, pp. 716-735.

6. W. I. Axford and C. O. Hines, “A Unifying Theory of High-latitude Geophysical Phenomena and Geomagnetic Storms,” *Canadian Journal of Physics*, **39**, 1961, pp. 1433-1464.

7. W. B. Hanson and I. B. Ortenburger, “The Coupling Between the Protonosphere and the Normal F Region,” *Journal of Geophysical Research*, **66**, 1961, pp. 1425-1435.

8. D. L. Carpenter, “The Magnetosphere During Magnetic Storms; a Whistler Analysis,” PhD thesis, Stanford University, 1962, pp. 44-47.

9. A. Nishida, “Formation of Plasmapause, or Magnetospheric Plasma Knee, by the Combined Action of Magnetospheric Convection and Plasma Escape from the Tail,” *Journal of Geophysical Research*, **71**, 1966, pp. 5669-5679.

10. N. M. Brice, “Bulk Motion of the Magnetosphere,” *Journal of Geophysical Research*, **72**, 1967, pp. 5193-5211.

11. J. W. Dungey, “The Theory of the Quiet Magnetosphere,” in J. W. King and W. S. Newman (eds.), *Proceedings of the 1966 Symposium on Solar-Terrestrial Physics, Belgrade*, London, Academic Press Inc., 1967, pp. 91-106.

12. M. Spasojeviæ et al., J. Goldstein, D. L. Carpenter, U. S. Inan, B. R. Sandel, M. B. Moldwin, and B. W. Reinisch, “The Global Response of the Plasmasphere to a Geomagnetic Disturbance,” *Journal of Geophysical Research*, **108**, (A9), 1340, doi:10.1029/2003JA009987, 2003.

13. W. L. Imhof, H. D. Voss, J. Mobilia, M. Walt, U. S. Inan, and D. L. Carpenter, “Characteristics of Short-Duration Electron Precipitation Bursts and Their Relationship With VLF Wave Activity,” *Journal of Geophysical Research*, **94**, 1989, pp. 10079-10093.

14. L. B. Callis, R. E. Boughner, D. N. Baker, R. A. Mewaldt, J. B. Blake, R. S. Selesnick, J. R. Cummings, M. Natarajan, G. M. Mason, and J. E. Mazur, “Precipitating Electrons: Evidence for Effects on Mesospheric Odd Nitrogen,” *Geophysical Review Letters*, **23**, 1996, pp. 1901-1904.

15. N. C. Maynard and J. M. Grebowsky, “The Plasmapause Revisited,” *Journal of Geophysical Research*, **82**, 1977, pp. 1591-1600.

16. H. Laakso, “Variation of the Spacecraft Potential in the Magnetosphere,” *Journal of Atmospheric and Solar-Terrestrial Physics*, **64**, 2002, pp. 1735-1744.

17. R. L. Smith, “Properties of the Outer Ionosphere Deduced from Nose Whistlers,” *Journal of Geophysical Research*, **66**, 1961, pp. 3709-3716.

18. M. J. Rycroft, “Magnetospheric Plasma Flow and Electric Fields Derived from Whistler Observations,” in D. E. Page (ed.), *Correlated Interplanetary and Magnetospheric Observations*, Dordrecht, Holland, D. Reidel Publishing Company, 1974, pp. 317-335.

19. Y. Corcuff, “Probing the Plasmapause by Whistlers,” *Annales de Géophysique*, **31**, 1975, pp. 53-67.

20. Gy. Tarcsai, “Routine Whistler Analysis by Means of Accurate Curve Fitting,” *Journal of Atmospheric and Terrestrial Physics*, **37**, 1975, pp. 1447-1457.

21. S. S. Sazhin, M. Hayakawa, and K. Bullough, “Whistler Diagnostics of Magnetospheric Parameters: A Review,” *Annales Geophysicae*, **10**, 1992, pp. 293-308.

22. J. J. Angerami and D. L. Carpenter, “Whistler Studies of the Plasmapause in the Magnetosphere, 2. Electron Density and Total Tube Content Near the Knee in Magnetospheric Ionization,” *Journal of Geophysical Research*, **71**, 1966, pp. 711-725.

23. J. E. Geisler and S. A. Bowhill, “The Relation Between the Dispersion of a Whistler and the Electron Temperature in the Protonosphere,” *Journal of Atmospheric and Terrestrial Physics*, **27**, 1965, pp. 122-125.

24. D. L. Carpenter, “Whistler Studies of the Plasmapause in the Magnetosphere, 1, Temporal Variations in the Position of the Knee and Some Evidence on Plasma Motions Near the Knee,” *Journal of Geophysical Research*, **71**, 1966, pp. 693-709.

25. C. G. Park, D. L. Carpenter, and D. B. Wiggin, “Electron Density in the Plasmasphere: Whistler Data on Solar Cycle, Annual, and Diurnal Variations,” *Journal of Geophysical Research*, **83**, 1978, pp. 3137-3144.

26. M. A. Clilverd, A. J. Smith, and N. R. Thomson, “The Annual Variation in Quiet Time Plasmaspheric Electron Density, Determined from Whistler Mode Group Delays,” *Planetary and Space Science*, **39**, 1991, pp. 1059-1067.

27. P. G. Richards, T. Chang, and R. H. Comfort, “On the Causes of the Annual Variation in the Plasmaspheric Electron Density,” *Journal of Atmospheric and Solar-Terrestrial Physics*, **62**, 2000, pp. 935-946.

28. C. G. Park, “A Morphological Study of Substorm-Associated Disturbances in the Ionosphere,” *Journal of Geophysical Research*, **79**, 1974, pp. 2821-2827.

29. C. G. Park and P. M. Banks, “Influence of Thermal Plasma Flow on the Mid-latitude Night-time F2 Layer: Effects of Electric Fields and Neutral Winds Inside the Plasmasphere,” *Journal of Geophysical Research*, **79**, 1974, pp. 4661-4668.

30. D. L. Carpenter and K. Stone, “Direct Detection by a Whistler Method of the Magnetospheric Electric Field Associated with a Polar Substorm,” *Planetary and Space Science*, **15**, 1967, pp. 395-397.

31. D. L. Carpenter and A. J. Smith, “The Study of Bulk Plasma Motions and Associated Electric Fields in the Plasmasphere by Means of Whistler-Mode Signals,” *Journal of Atmospheric and Solar-Terrestrial Physics*, **63**, 2001, pp. 1117-1132.

32.D. L. Carpenter, C. G. Park, and T. R. Miller, “A Model of Substorm Electric Fields in the Plasmasphere Based on Whistler Data,” *Journal of Geophysical Research*, **84**, 1979, pp. 6559-6563.

33.D. L. Carpenter, “New Whistler Evidence of a Dynamo Origin of Electric Fields in the Quiet Plasmasphere, *Journal of Geophysical Research*, **83**, 1978, pp. 1558-1564.

34.N. R. Thomson, “Causes of the Frequency Shift of Whistler-Mode Signals,” *Planetary and Space Science*, **24**, 1976, pp. 447-454.

35.H. F. Balmforth, M. A. Clilverd, and A. J. Smith, “A Case Study of Storm Commencement and Recovery Plasmaspheric Electric Fields Near L = 2.5 at Equinox,” *Annales Geophysicae*, **12**, 1994, pp. 625-635.

36.A. J. Smith, “Whistler Observations of the Plasmasphere/plasmapause from Stations of the British Antarctic Survey,” *Journal of Atmospheric and Solar-Terrestrial Physics*, **63**, 2001, pp. 1149-1156.

37.E. W. Paschal, “Phase Measurements of Very Low Frequency Signals From the Magnetosphere,” PhD Thesis, Stanford University, 1988, pp. 90-97.

38.R. L. Smith, “Propagation Characteristics of Whistlers Trapped in Field-Aligned Columns of Enhanced Ionization,” *Journal of Geophysical Research*, **66**, 1961, pp. 3699-3707.

39.C. Béghin and C. Siredey, “Un Procédé d’Analyse Fine des Sifflements Atmosphérique,” *Annales de Géophysique*, **20**, 1964, pp. 301-308.

40.D. Hamar, Gy. Tarcsai, J. Lichtenberger, A. J. Smith, and K. H. Yearby, “Fine Structure of Whistlers Recorded Digitally at Halley, Antarctica,” *Journal of Atmospheric and Terrestrial Physics*, **52**, 1990, pp. 801-810.

41.D. Hamar, C. S. Ferencz, J. Lichtenberger, Gy. Tarcsai, A. J. Smith, and K. H. Yearby, “Trace Splitting of Whistlers: A Signature of Fine Structure or Mode Splitting in Magnetospheric Ducts?” *Radio Science*, **27**, 1992, pp. 341-346.

42.A. D. Richmond, “Self-Induced Motions of Therma Plasma in the Magnetosphere and the Stability of the Plasmapause,” *Radio Science*, **8**, 1973, pp. 1019-1027.

43.J. Lemaire, “The Mechanisms of Formation of the Plasmapause,” *Annales de Géophysique*, **31**, 1975, pp. 175-189.

44.P. A. Bernhardt and C. G. Park, “Protonospheric-Ionospheric Modeling of VLF Ducts,” *Journal of Geophysical Research*, **82**, 1977, pp. 5222-5230.

45.D. Hamar and J. Lichtenberger, “Methods of Signal Analysis,” in Cs. Ferencz, O. E. Ferencz, D. Hamar, and J. Lichtenberger (eds.), *Whistler Phenomena*, Dordrecht, Kluwer Academic Publishers, 2001, pp. 176-230.

46.E. W. Paschal, L. J. Lanzerotti, and C. G. Maclennan, “Correlation of Whistler Mode Phase Delay with Transient Hydromagnetic Waves,” *Journal of Geophysical Research*, **95**, 1990, pp. 15059-15072.

47.R. M. Gallet, “The Very Low Frequency Emissions Generated in the Earth’s Exosphere,” *Proceedings of the IRE*, **47**, 1959, pp. 211-231.

48.R. L. Dowden, “Doppler-Shifted Cyclotron Radiation from Electrons, A Theory of Very Low Frequency Emissions from the Exosphere,” *Journal of Geophysical Research*, **67**, 1962, pp. 1745-1750.

49.R. A. Helliwell, “Whistler-Triggered Periodic VLF Emissions,” *Journal of Geophysical Research*, **68**, 1963, pp. 5387-5395.

50.R. A. Helliwell, *Whistlers and Related Ionospheric Phenomena*, Stanford, California, Stanford University Press, 1965.

51.N. M. Brice, “Fundamentals of VLF Emission Generation Mechanisms,” *Journal of Geophysical Research*, **69**, 1964, pp. 4515-4522.

52.T. H. Stix, *The Theory of Plasma Waves*, New York, McGraw-Hill, 1962, pp. 131-260.

53.R. A. Helliwell, J. P. Katsufrakis, M. Trimpi, and N. M. Brice, “Artificially Stimulated VLF Radiation from the Ionosphere,” *Journal of Geophysical Research*, **69**, 1964, pp. 2391-2394.

54.R. L. Dowden, A. D. McKay, L. E. S. Amon, H. C. Koons, and M. H. Dazy, “Linear and Nonlinear Amplification in the Magnetosphere During a 6.6 –kHz Transmission,” *Journal of Geophysical Research*, **83**, 1978, pp. 169-181.

55.R. A. Helliwell, “VLF Wave Stimulation Experiments in the Magnetosphere from Siple Station, Antarctica,” *Reviews of Geophysics*, **26**, 1988, pp. 551-578.

56.R. A. Helliwell and J. P. Katsufrakis, “VLF Wave Injection into the Magnetosphere from Siple Station, Antarctica,” *Journal of Geophysical Research*, **79**, 1974, pp. 2511-2518.

57.R. A. Helliwell, “A Tale of Two Magnetospheres – The Cold and the Hot,” *Journal of Atmospheric and Solar-Terrestrial Physics*, **63**, 2001, pp. 1107-1116.

58.V. S. Sonwalkar, D. L. Carpenter, R. A. Helliwell, M. Walt, U. S. Inan, D. L. Caudle, and M. Ikeda, “Properties of the Magnetospheric Hot Plasma Distribution Deduced from Whistler Mode Wave Injection at 2400 Hz: Ground-based Detection of Azimuthal Structure in Magnetospheric Hot Plasmas,” *Journal of Geophysical Research*, **102**, 1997, pp. 14363-14380.

59.R. A. Helliwell and U. S. Inan, “VLF Wave Growth and Discrete Emission Triggering in the Magnetosphere: A Feedback Model,” *Journal of Geophysical Research*, **87**, 1982, pp. 3537-3550.

60.C. W. Carlson, R. A. Helliwell, and U. S. Inan, “Space-Time Evolution of Whistler Mode Wave Growth in the Magnetosphere,” *Journal of Geophysical Research*, **95**, 1990, pp. 15073-15089.

61.D. Nunn, “A Self-consistent Theory of Triggered VLF Emissions, *Planetary and Space Science*, **22**, 1974, pp. 349-378.

62.D. Nunn, “The Quasi-static Theory of Triggered VLF Emissions, *Planetary and Space Science*, **32**, 1984, pp. 325-350.

63.R. A. Helliwell and K. F. Walworth, “Whistler Mode Wave Intensities in the Radiation Belts,” in G. D. Reeves (ed.), *Workshop on the Earth’s Trapped Particle Environment*, New York, American Institute of Physics, 1996, pp. 61-63.

64.R. A. Helliwell, “Intensity of Discrete VLF Emissions,” in B. M. McCormac (ed.), *Particles and Fields in the Magnetosphere*,

D. Reidel Publishing Company, Dordrecht, Holland, 1970, pp. 292-301.

65.J. Dungey, "Loss of Van Allen Electrons due to Whistlers," *Planetary and Space Science*, **11**, 1963, pp. 591-595.

66.J. Dungey, "Effects of Electromagnetic Perturbations on Particles Trapped in the Radiation Belts," *Space Science Reviews*, **4**, 1965, pp. 199-222.

67.C. F. Kennel and H. E. Petschek, "Limit on Stably Trapped Particle Fluxes," *Journal of Geophysical Research*, **71**, 1966, pp. 1-28.

68.C. S. Roberts, "Pitch Angle Diffusion of Electrons in the Magnetosphere," *Reviews of Geophysics*, **7**, 1969. pp. 305-337.

69.U. S. Inan, T. F. Bell, and R. A. Helliwell, "Nonlinear Pitch Angle Scattering of Energetic Electrons by Coherent VLF Waves in the Magnetosphere," *Journal of Geophysical Research*, **83**, 1978, pp. 3235-3254.

70.R. A. Helliwell, J. P. Katsufrakis, and M. Trimpi, "Whistler-induced Amplitude Perturbations in VLF Propagation," *Journal of Geophysical Research*, **78**, 1973, pp. 4679-4688.

71.M. J. Rycroft, "Enhanced Energetic Electron Intensities at 100 km Altitude and a Whistler Propagating Through the Plasmasphere," *Planetary and Space Science*, **21**, 1973, pp. 239-251.

72.R. Lohrey and A. B. Kaiser, "Whistler-induced Anomalies in VLF Propagation," *Journal of Geophysical Research*, **84**, 1979, pp. 5122-5130.

73.D. L. Carpenter and J. W. LaBelle, "A Study of Whistlers Correlated with Bursts of Electron Precipitation near L = 2," *Journal of Geophysical Research*, **87**, 1982, pp. 4427-4434.

74.R. L. Dowden and C. D. D. Adams, "Phase and Amplitude Perturbations on Subionospheric Signals Explained in Terms of Echoes from Lightning-induced Electron Precipitation Ionization Patches," *Journal of Geophysical Research*, **93**, 1988, pp. 11543-11550.

75.W. C. Burgess and U. S. Inan, "The Role of Ducted Whistlers in the Precipitation Loss and Equilibrium Flux of Radiation Belt Electrons," *Journal of Geophysical Research*, **98**, 1993, pp. 15643-15666.

76.D. S. Lauben, U. S. Inan, and T. F. Bell, "Precipitation of Radiation Belt Electrons Induced by Obliquely Propagating Lightning-generated Whistlers," *Journal of Geophysical Research*, **106**, 2001, pp. 28841-28856.

77.J. Bortnik, U. S. Inan, and T. F. Bell, "L Dependence of Energetic Electron Precipitation Driven by Magnetospherically Reflecting Whistler Waves," *Journal of Geophysical Research*, **107**, A8, 10.1029/2001JA000303, 2002.

78.T. J. Rosenberg, R. A. Helliwell, and J. P. Katsufrakis, "Electron Precipitation Associated with Discrete Very-Low-Frequency Emissions," *Journal of Geophysical Research*, **76**, 1971, pp. 8445-8452.

79.J. C. Foster and T. J. Rosenberg, "Electron Precipitation and VLF Emissions Associated with Cyclotron Resonance Interactions near the Plasmapause," *Journal of Geophysical Research*, **81**, 1976, pp. 2183-2192.

80.R. A. Helliwell, S. B. Mende, J. H. Doolittle, W. C. Armstrong, and D. L. Carpenter, "Correlations Between ë4278 Optical Emissions and VLF Wave Events Observed at L~4 in the Antarctic," *Journal of Geophysical Research*, **85**, 1980, pp. 3376-3386.

81.M. P. Johnson, U. S. Inan, S. J. Lev-Tov, and T. F. Bell, "Scattering Pattern of Lightning-induced Ionospheric Disturbances Associated with Early/Fast VLF Events," *Geophysical Research Letters*, **26**, 1999, pp. 2363-2366.

82.M. A. Clilverd, D. Nunn, S. J. Lev-Tov, U. S. Inan, R. L. Dowden, C. J. Rodger, and A. J. Smith, "Determining the Size of Lightning-induced Electron Precipitation Patches," *Journal of Geophysical Research*, **107**, A8, 10.1029/2001JA00301, 2002.

83.T. A. Potemra and T. J. Rosenberg, "VLF Propagation Disturbances and Electron Precipitation at Mid-latitudes," *Journal of Geophysical Research*, **78**, 1973, pp. 1572-1580.

84.D. L. Carpenter, J. C. Foster, T. J. Rosenber, and L. J. Lanzerotti, "A Subauroral and Mid-latitude View of Substorm Activity," *Journal of Geophysical Research*, **80**, 1975, pp. 4279-4286.

85.W. D. Cummings, R. J. O'Sullivan, and P. J. Coleman, Jr., "Standing Alfven Waves in the Magnetosphere," *Journal of Geophysical Research*, **74**, 1969, pp. 778-793.

86.V. A. Troitskaya and A. V. Gul'yel'mi, "Hydromagnetic Diagnostics of Plasma in the Magnetosphere," *Annales de Géophysique*, **26**, 1970, pp. 893-902.

87.D. C. Webb, L. J. Lanzerotti, and C. G. Park, "A Comparison of ULF and VLF Measurements of Magnetospheric Cold Plasma Density Profiles, *Journal of Geophysical Research*, **82**, 1977, pp. 5063-5072.

88.L. J. Lanzerotti, C. G. Maclennan, and D. C. Webb, "Comparisons of Inferred Total Plasmasphere Content with Measured Plasma Density Profiles, *Journal of Geophysical Research*, **84**, 1979, pp. 2648-2650.

89.L. N. Baransky, J. E. Borovkov, M. B. Gokhberg, S. M. Krylov, and V. A. Troitskaya, "High Resolution Method of Direct Measurement of the Magnetic Field Lines' Eigen Frequencies," *Planetary and Space Science*, **33**, 1985, pp. 1369-1374.

90.F. W. Menk, D. Orr, M. A. Clilverd, A. J. Smith, C. L. Waters, and B. J. Fraser, "Monitoring Spatial and Temporal Variations in the Dayside Plasmasphere using Geomagnetic Field Line Resonances," *Journal of Geophysical Research*, **104**, 1999, pp. 19955-19970.

91.F. W. Menk, C. L. Waters, and B. J. Fraser, "Field Line Resonances and Waveguide Modes at Low Latitudes, 1. Observations," *Journal of Geophysical Research*, **105**, 2000, pp. 7747-7761.

92.A. W. Green, E. W. Worthington, L. N. Baransky, E. N. Fedorov, N. A. Kurneva, V. A. Pilipenko, D. N. Shvetzov, A. A. Bektemirov, and G. V. Philipov, "Alfven Field Line Resonances at Low Latitudes (L = 1.5)," *Journal of Geophysical Research,* **98**, 1993, pp. 15693-15699.

93.C. L. Waters, J. C. Samson, and E. F. Donovan, "Variation of Plasmatrough Density Derived from Magnetospheric Field Line Resonances, *Journal of Geophysical Research*, **101**, 1996, pp. 24737-24746.

94.D. K. Milling, I. R. Mann, and F. W. Menk, “Diagnosing the Plasmapause with a Network of Closely Spaced Ground-based Magnetometers,” *Geophysical Research Letters*, **28**, 2001, pp. 115-118.

95.M. A. Clilverd, F. W. Menk, G. Milinevski, B. R. Sandel, J. Goldstein, B. W. Reinisch, C.R. Wilford, M. C. Rose, N. R. Thomson, K. H. Yearby, G. J. Bailey, I. R. Mann, and D. L. Carpenter, “In-situ and Ground-Based Intercalibration Measurements of Plasma Density at L = 2.5,” *Journal of Geophysical Research*, **108**, 2003, submitted.

96.C. R. Chappell, K. K. Harris, and G. W. Sharp, “OGO 5 Measurements of the Plasmasphere During Observations of Stable Auroral Red Arcs,” *Journal of Geophysical Research*, **76**, 1971, pp. 2357-2365.

97.D. L. Carpenter, “Ogo 2 and 4 VLF Observations of the Asymmetric Plasmapause Near the Time of SAR Arc Events,” *Journal of Geophysical Research*, **76**, 1971, pp. 3644-3650.

98.H. A. Taylor, Jr., H. C. Brinton, D. L. Carpenter, F. M. Bonner, and R. L. Heyborne, “Ion Depletion in the High-latitude Exosphere. Simultaneous OGO 2 Observations of the Light Ion Trough and the VLF Cutoff,” *Journal of Geophysical Research*, **74**, 1969, pp. 3517-3528.

99.L. H. Brace and R. F. Theis, “The Behavior of the Plasmapause at Mid-latitudes: ISIS-1 Langmuir Probe Measurements,” *Journal of Geophysical Research*, **79**, 1974, pp. 1871-1884.

100.J. C. Foster, C. G. Park, L. H. Brace, J. R. Burroughs, J. H. Hoffman, E. J. Meier, and J. H. Whitteker, “Plasmapause Signatures in the Ionosphere and Magnetosphere,” *Journal of Geophysical Research*, **83**, 1978, pp. 1175-1182.

101.J. C. Foster, “Storm-Time Plasma Transport at Middle and High Latitudes,” *Journal of Geophysical Research*, **98**, 1993, pp. 1675-1689.

102.J. C. Foster, P. J. Erickson, A. J. Coster, J. Goldstein, and F. J. Rich, “Ionospheric Signatures of Plasma Tails,” *Geophysical Research Letters*, **29**, (13), 10.1029/2002GL015067, 2002.

103.A. J. Coster, E. M. Gaposchkin, and L. E. Thornton, “Real-time Ionospheric Monitoring System Using GPS,” *Navigation: Journal of he Institute of Navigation*, **39**, 2, Summer 1992, pp. 191-204.

104.D. L. Carpenter, B. L. Giles, C. R. Chappell, P. M. E. Décréau, R. R. Anderson, A. M. Persoon, A. J. Smith, Y. Corcuff, and P. Canu, “Plasmasphere Dynamics in the Duskside Bulge Region: A New Look at an Old Topic,” *Journal of Geophysical Research*, **98**, 1993, pp. 19243-19271.

105.D. L. Carpenter and J. Lemaire, “Erosion and Recovery of the Plasmasphere in the Plasmapause Region,” *Space Science Reviews*, **80**, 1997, pp. 153-179.

106.B. R. Sandel, A. L. Broadfoot, C. C. Curtis, R. A. King, T. C. Stone, R. H. Hill, J. Chen, O. H. W. Siegmund, R. Raffanti, D. D. Allred, R. S. Turley, and D. L. Gallagher, “The Extreme Ultraviolet Imager Investigation for the IMAGE Mission,” *Space Science Reviews*, **91**, 2000, 197-242.

107.B. W. Reinisch, D. M. Haines, K. Bibl, G. Cheney, I. A. Galkin, X. Huang, S. H. Myers, G. S. Sales, R. F. Benson, S. F. Fung, J. L. Green, W. W. L. Taylor, J.-L. Bougeret, R. Manning, N. Meyer-Vernet, M. Moncuquet, D. L. Carpenter, D. L. Gallagher, and P. H. Reiff, “The Radio Plasma Imager Investigation on the IMAGE Spacecraft,” *Space Science Reviews*, **91**, 2000, pp. 319-359.

108.J. Goldstein, M. Spasojeviæ, P. H. Reiff, B. R. Sandel, W. T. Forrester, D. L. Gallagher, and B. W. Reinisch, “Identifying the Plasmapause in IMAGE EUV data using IMAGE RPI *in situ* Steep Density Gradients,” *Journal of Geophysical Research*, **108**(A4), 1147, doi:10.1029/2002JA009475, 2003.

109.J. Goldstein, R. W. Spiro, P. H. Reiff, R. A. Wolf, B. R. Sandel, J. W. Freeman, and R. L. Lambour, “IMF-Driven Overshielding Electric Field and the Origin of the Plasmaspheric Shoulder of May 24, 2000,” *Geophysics Research Letters*, **29**(16), 10.1029/ 2001GL014534, 2002.

110.J. Goldstein, B. R. Sandel, W. T. Forrester, and P. H. Reiff, “IMF-Driven Plasmasphere Erosion of 10 July 2000,” *Geophysics Research Letters*, **30**(A3), 1146, doi:10.1029/ 2002GL016478, 2003.

111.C. R. Chappell, “Detached Plasma Regions in the Magnetosphere,” *Journal of Geophysical Research*, **79**, 1974, pp. 1861-1870.

112.B. Higel and L. Wu, “Electron Density and Plasmapause Characteristics at 6.6 RE: A Statistical Study of the GEOS 2 Relaxation Sounder Data,” *Journal of Geophysical Research*, **89**, 1984, pp. 1583-1601.

113.M. B. Moldwin, M. F. Thomsen, S. J. Bame, D. J. McComas, and K. R. Moore, “An Examination of the Structure and Dynamics of the Outer Plasmasphere Using Multiple Geosynchronous Satellites,” *Journal of Geophysical Research*, **99**, 1994, pp. 11475-11481.

114.D. L. Carpenter, “Whistler Evidence of the Dynamic Behavior of the Duskside Bulge in the Plasmasphere,” *Journal of Geophysical Research*, **75**, 1970, pp. 3837-3847.

115.D. Ho and D. L. Carpenter, “Outlying Plasmasphere Structure Detected by Whistlers,” *Planetary and Space Science*, **24**, 1976, pp. 987-994.

116.D. L. Carpenter, A. J. Smith, B. L. Giles, C. R. Chappell, and P. M. E. Décréau, “A Case Study of Plasma Structure in the Dusk Sector Associated With Enhanced Magnetospheric Convection,” *Journal of Geophysical Research*, **97**, 1992, pp. 1157-1166.

117.J. M. Grebowsky, “Model Study of Plasmapause Motion,” *Journal of Geophysical Research*, **75**, 1970, pp. 4329-4333.

118.B. W. Reinisch, X. Huang, D. M. Haines, I. A. Galkin, J. L. Green, R. F. Benson, S. F. Fung, W. W. L. Taylor, P. H. Reiff, D. L. Gallagher, J.-L. Bougeret, R. Manning, D. L. Carpenter, and S. A. Boardsen, “First Results from the Radio Plasma Imager on IMAGE,” *Geophysical Research Letters*, **28**, 6, 2001, pp. 1167-1170.

119.J. L. Green, R. F. Benson, S. F. Fung, W. W. L. Taylor, S. A. Boardsen, B. W. Reinisch, D. M. Haines, K. Bibl, G. Cheney, I. A. Galkin, X. Huang, S. H. Myers, G. S. Sales, J.-L. Bougeret, R. Manning, N. Meyer-Vernet, M. Moncuquet, D. L. Carpenter, D. L. Gallagher, and P. H. Reiff, “Radio Plasma Imager Simulations and Measurements,” *Space Science Reviews*, **91**, 2000, pp. 361-389.

120.D. L. Carpenter, M. A. Spasojeviæ, T. F. Bell, U. S. Inan, B. W. Reinisch, I. A. Galkin, R. F. Benson, J. L. Green, S. F. Fung, and S. A. Boardsen, “Small-scale Field Aligned Plasmaspheric Density Structures Inferred from the Radio Plasma Imager on IMAGE,” *Journal of Geophysical Research*, **107**, A9, 1258, doi:10.1029/2001JA009199, 2002.

121.H. G. James, “ISIS-1 Measurements of High-Frequency Backscatter Inside the Ionosphere,” *Journal of Geophysical Research*, **94**, 1989, pp. 2617-2630.

122.B. W. Reinisch, X. Huang, P. Song, G. S. Sales, S. F. Fung, J. L. Green, D. L. Gallagher, and V. M. Vasyliunas, “Plasma Density Distribution Along the Magnetospheric Field: RPI Observations from IMAGE,” *Geophysical Research Letters*, **28**, 24, 2001, pp. 4521-4524.

123.X. Huang, B. W. Reinisch, P. Song, J. L. Green, and D. L. Gallagher, “Developing an Empirical Plasma Density Model of the Plasmasphere Using IMAGE/RPI Observations,” *Advances in Space Research*, 2003, in press.

124.S. F. Fung, R. F. Benson, D. L. Carpenter, J. L. Green, V. Jayanti, I. A. Galkin, and B. W. Reinisch, “Guided Echoes in the Magnetosphere: Observations by Radio Plasma Imager on IMAGE,” *Geophysics Research Letters*, **30**, A11, 1509, doi:10.1029/2002GL016531, 2003.

125.V. S. Sonwalkar, D. L. Carpenter, T. F. Bell, U. S. Inan, R. F. Benson, W. W. L. Taylor, and B. W. Reinisch, “Whistler Mode Echoes from Radio Sounding on the IMAGE Satellite,” *Journal of Geophysical Research*, **108,** 2003, submitted.

126.D. L. Carpenter, T. F. Bell, U. S. Inan, R. F. Benson, V. S. Sonwalkar, B. W. Reinisch, and D. L. Gallagher, “Z Mode Sounding Within Propagation ‘Cavities’ and Other Inner Magnetospheric Regions by the RPI Instrument on the IMAGE Satellite,” *Journal of Geophysical Research*, **108**, 2003, in press.

127.J.-N. Tu, J. L. Horwitz, P. Song, X.-Q. Huang, B. W. Reinisch, and P. G. Richards, “Simulating Plasmaspheric Field-aligned Density Profiles Measured with IMAGE/RPI: Effects of Plasmasphere Refilling and Ion Heating,” *Journal of Geophysical Research*, **108**, A1, 1017, doi:10.1029/2002JA009468, 2003.

128.R. W. Fredricks, L. R. O. Storey, T. F. Bell, R. F. Benson, F. W. Crawford, O. K. Garriott, M. D. Grossi, H. Koons, A. Pedersen, H. G. James, T. R. Buckner, S. P. Kirkner, and W. W. L. Taylor, “Report of the AMPS Wave Injection Facility Definition Team,” TRW Report no. 32747-6002-RU-01, 1978.

129.C. T. Russell, “A Brief History of Solar-Terrestrial Physics,” in C. T. Russell and M. G. Kivelson (eds.), *Introduction to Space Physics*, Cambridge, Cambridge University Press, 1995, pp. 1-26.

130.E. Kolesnikova, C. Béghin, R. Grard, and C. P. Escoubet, “The Electrical Stability of the Electric Field Antennas in the Plasmasphere,” *Journal of Atmospheric and Solar-Terrestrial Physics*, **63**, 2001, pp. 1217-1224.

131.W. J. Hughes, “The Magnetopause, Magnetotail, and Magnetic Reconnection,” in M. G. Kivelson and C. T. Russel (eds.), *Introduction to Space Physics*, Cambridge, Cambridge University Press, 1995, pp. 227-287.

132.M. Roth, D. S. Evans, and J. Lemaire, “Theoretical Structure of a Magnetospheric Plasma Boundary: Application to the Formation of Discrete Auroral Arcs,” *Journal of Geophysical Research*, **98**, 1993, pp. 11411-11423.

133.C. E. McIlwain, “Substorm Injection Boundaries,” in B. M. McCormac (ed.), *Magnetospheric Physics*, Dordrecht, D. Reidel, Holland, 1974, pp. 143-154.

134.M. F. Thomsen, D. J. McComas, J. E. Borovsky, and R. C. Elphic, “The Magnetospheric Trough,” in J. L. Horwitz, D. L. Gallagher and W. K. Peterson (eds.), *Encounter Between Global Observations and Models in the ISTP Era, Geophysical Monograph Series*, **104**, American Geophysical Union, Washington, D. C., 1998, pp. 355-369.

135.L. Block, “On the Distribution of Electric Fields in the Magnetosphere,” *Journal of Geophysical Research*, **71**, 1966, pp. 855-864.

135.R. K. Jaggi and R. A. Wolf, “Self Consistent Calculation of the Motion of a Sheet of Ions in the Magnetosphere,” *Journal of Geophysical Research*, **78**, 1973, pp. 2852-2866.

136.R. A. Wolf, “The Quasi-Static (Slow-Flow) Region of the Magnetosphere,” in R. L. Carovillano and J. M Forbes (eds.), *Solar-Terrestrial Physics, Principles and Theoretical Foundations*, Dordrecht, D. Reidel, Holland, 1983, pp. 303-329.

137.G. Parks, *Physics of Space Plasmas, An Introduction*, Addison-Wesley Publishing Company, Redwood City, California, 1991, pp. 229-237.

138.R. D. Hunsucker and J. K. Hargreaves, *The High-Latitude Ionosphere and its Effects on Radio Propagation*, Cambridge, Cambridge University Press, 2003.

139.“Physics of the Plasmapause”, M. J. Rycroft and J. Lemaire (eds.), *Annales de Geophysique*, **31**, 1975, pp. 1-193.

140.J. L. Green and J. L. Horwitz, “A Meeting Report on: The Fundamental Magnetospheric Processes in the Plasmapause Region Conference,” *EOS, Transactions, American Geophysical Union,* **65**, March 1984, p. 110.

Microwave Remote Sensing of Land

P. Pampaloni
K. Sarabandi

Abstract

Considering the rapid growth of population, its impact on the environment, and limited available resources on our planet, the need for monitoring the environmental processes and managing our resources is unequivocal. Microwave remote sensing provides a unique capability towards achieving this goal. Over the past decade, significant progress has been made in microwave remote sensing of land processes through development of advanced airborne and space-borne microwave sensors, and the tools – such as physics-based models and advanced inversion algorithms – needed for analyzing the data. These activities have sharply increased in recent years since the launch of the ERS-1/2, JERS-1, and RADARSAT satellites, and with the availability of radiometric data from SSM/I. A new era has begun with the recent space missions ESA-ENVISAT, NASA-AQUA, and NASDA-ADEOSII, and the upcoming PALSAR and RADARSAT2 missions, which open new horizons for a wide range of operational microwave remote-sensing applications. This paper highlights major activities and important results achieved in this area over the past years.

1. Introduction

The application of microwaves for remote sensing of terrestrial targets is motivated by the all-weather, day/night, and target-penetrating attributes of such systems. Though traditional optical and multi-spectral imaging systems can be used effectively in principle, issues related to the atmospheric effects often render such systems less desirable. In the past decade, several satellite-borne synthetic-aperture radars (SAR) were launched for the remote sensing of the environment.

The successful application of SAR technology to address a wide range of remote-sensing problems helped the advancement of SAR systems to include polarization diversity and operation in interferometric mode. The first remote-sensing space-borne polarimetric SAR system, and the first single-pass interferometric SAR, were flown aboard the Space Shuttle in 1994 [1] and 2000 [2], respectively. was given in [3]. A very good review of radar polarimetry techniques and interferometric SAR systems and applications can be found in [4] and [5].

The most significant event in recent years was the launch, performed by the European Space Agency, of the ENVISAT satellite, carrying onboard a set of innovative sensors, including the Advanced Synthetic Aperture Radar (ASAR) [6]. This C-band radar is a significant improvement over the ERS-1/2 SAR, in that it makes observations at different incidence angles and polarizations possible, and allows for scanSAR operations. The satellite was launched on March 1, 2002, but data were made available to the scientific community in the fall of 2002, only after the commissioning phase. Thus, most of the work performed so far with satellite radar still involves the use of data from the currently in-orbit ERS-2 and RADARSAT, or from archives of ERS-1 (C band) and JERS (L band).

The combined active microwave instrument (AMI), operating at C band (5.3 GHz) and with vertical polarization, is aboard the European remote-sensing satellite ERS-2. AMI is composed of a SAR and a scatterometer (SCAT), operating in an interleaved mode. In SAR wave mode, 10 km × 5 km images are acquired at a nominal incidence angle of 23°, with a spatial resolution of about 30 m. The ERS-1/2 scatterometer continuously illuminates a 500 km-wide swath with a resolution of 45 km [7]. A first interferogram, using radar data from the ERS-2's SAR instrument and Envisat's ASAR instrument, has already been produced by scientists from the German Aerospace Centre (DLR). They analyzed images taken in 1999 (ERS-2) and 2002 (Envisat) over the town of Las Vegas in the US [6]. Producing an interferogram with data from these two

Paolo Pampaloni is with the Institute of Applied Physics (IFAc) of National Research Council (CNR), via Panciatichi 64 50127 Florence, Italy; Tel: +39 055 4235205; Fax: +39 055 4235290; e-mail: P.Pampaloni@ifac.cnr.it.
Kamal Sarabandi is with the Department of Electrical Engineering & Computer Science, Radiation Laboratory, 1301 Beal Ave., University of Michigan, Ann Arbor, MI 48104-6462 USA; Tel: +1 (734) 936-1575; Fax: +1 (734) 647-2106; e-mail: saraband@eecs.umich.edu

Editors Note: This paper is one of the invited *Reviews of Radio Science*, from Commission F.

satellites was not initially considered to be feasible, since the SARs on ERS-2 and Envisat operate at slightly different frequencies, and this was enough to complicate the joint processing of data from the ERS and Envisat sensors. However, generation of interferograms using ERS and ENVISAT by the application of permanent scatterers with very stable scattering phase centers was proposed in [8, 9].

RADARSAT-1 was launched in November, 1995, circling the Earth in a sun-synchronous polar orbit [10]. RADARSAT-1 operates at C band, and offers users a wide variety of beam selections. The satellite's SAR has the unique ability to shape and steer its beam from an incidence angle of 10° to 60°, in swaths from 45 to 500 km in width, with resolutions ranging from eight to 100 m.

As far as passive systems are concerned, two space-borne microwave radiometers, called the Advanced Microwave Scanning Radiometer, were launched in 2002 to provide new observational data. One sensor is the AMSR-E, aboard the Earth Observing System (EOS) Aqua of the US National Aeronautics and Space Administration (NASA) [11]. The other is the AMSR [12], aboard the Advanced Earth Observing Satellite-II (ADEOS-II) of the National Space Development Agency of Japan (NASDA). AMSR and AMSR-E are almost identical sensors, and have lower frequencies of 6 GHz and 10 GHz, and much better ground resolution compared to previous sensors. Indeed, the ground resolution ranges from $43 \times 75\ km^2$ at the lower frequency, to $3.5 \times 5.9\ km^2$ at the highest frequency. We expect to retrieve soil moisture and vegetation biomass on a global scale with reasonable accuracy from the lower-frequency channels of these sensors. Geophysical products are currently being validated by means of several methods, such as the use of existing in-situ data, and by comparing data with data from other sensors [13].

Among the near-future space-borne radar remote-sensing systems, the Japanese fully polarimetric Phased Array type L-band Synthetic Aperture Radar (PALSAR), operating at 1.27 GHz, and RADARSAT-2, operating at C band, can be mentioned. In high-resolution mode (~10 m) the system can be used in fully polarimetric mode over a swath width of 70 km. PALSAR offers another attractive observational mode, called the ScanSAR mode. By sacrificing spatial resolution (~100 m), PALSAR can provide a swath width of the order of about 250-350 km, most appropriate for monitoring targets of large extent, such as sea ice and rain forests [14]. Scheduled for launch in 2004, RADARSAT-2 will provide data continuity to RADARSAT-1 users and offer data for new applications. The RADARSAT-2 Synthetic Aperture Radar (SAR) is fully polarimetric, and will be able to acquire data at all or any of HH, VV, and HV/VH polarizations over a range of resolutions from 3 m to 100 m [15].

Apart from the contributions made in the preparation of these missions, the microwave remote-sensing community has been deeply involved in improving the knowledge in the field by analyzing experimental data collected from satellite, airborne, and ground-based sensors, and is engaged in developing more advanced forward models and inversion algorithms. To this end, studies have also been performed by using data from sensors not specifically designed for land, use such as SSM/T, AMSU [16], and TRMM [17].

The literature concerning microwave remote-sensing terrestrial targets and Earth processes is rather extensive, and cannot be entirely covered here. This article attempts to highlight major activities and important results in this area over the past decade.

2. Retrieval of Land Parameters

The availability of a considerable amount of Synthetic Aperture Radar (SAR) and multi-frequency radiometric data, obtained in recent years from airborne and space-borne systems, has stimulated significant research in interpreting data and investigating their potential in various applications. For environmental studies, the focus of research on microwave remote-sensing of land processes can be categorized into: 1) land classification, 2) soil-moisture retrieval, 3) forest and crop biomass estimation, and 4) ice- and snow-pack parameter estimation.

2.1 Image Processing and Land Classification

The first step in most retrieval algorithms is image classification, where the domain of the imaged scene is divided into different general categories, which, in turn may each be subdivided into statistically homogeneous domains. Several different types of microwave image classifiers are now routinely in use. The classification techniques implemented so far can be categorized into statistical-based approaches, such as the maximum-likelihood classifier [18], unsupervised and knowledge-based classifiers [19, 20], and neural-network classifiers, which use a non-parametric classification technique [21-23]. A methodology known as the "decision tree" classification technique has also been used successfully for a wide range of classification problems, but it has not been tested in detail by the remote-sensing community [24]. Algorithms for edge and change detection, using polarimetric and/or multi-frequency SAR data, have been developed, and were reported in [25, 26].

Microwave land-coverage studies have been performed at high resolution with airborne sensors, such as JPL AirSAR [27] and CCRS C/X SAR [28]; satellite SAR; and at global scale, mainly with the ERS-1/2 Wind scatterometer and the SSM/I. The potential of multi-frequency polarimetric SAR data for separating agricultural fields from other types of surfaces, and in discriminating among classes of agricultural species, has been demonstrated by various authors [e.g., 28]. Lee et al. [30] exploited the land-use classification capabilities of fully polarimetric synthetic-aperture radar (SAR) versus dual-polarization and single-polarization SAR for P-, L-, and C-band frequencies. A variety of polarization combinations was investigated for application to crop and tree-age classification. The authors found that L-band fully polarimetric SAR data are best for crop classification, but that P band is best for forest-age classification. This is because longer-wavelength electromagnetic waves provide higher penetration. Moreover, the HH and VV phase difference is important for crop classification, but less important for tree-age classification

Recent research addressed to urban areas by using multi-temporal analysis of SAR data has demonstrated that the coarse resolution of ERS images does not prevent the possibility of characterizing these areas [31, 32]. Tupin et al. [33] established the usefulness of multiple SAR views in road detection.

Significant efforts have also been devoted to addressing land-cover characterization on a global scale by using ERS scatterometer data. These studies showed that the radar backscattering, $\sigma°$, was able to describe the vegetation cycle in a semi-arid region and in boreal forests [34, 35]. A few significant studies for distinguishing land surfaces and estimating quantitative parameters with the use of space-borne microwave radiometers were conducted using data from the Scanning Multi-channel Microwave Radiometer (SMMR) and the Special Sensor Microwave Imager (SSM/I). This research led to establishing empirical or semi-empirical rules for land-surface classification [e.g., 36, 37]. The 19-37 GHz spectral gradient and the 37 GHz brightness temperature, Tb, were effective for freeze/thaw classification in the northern prairies and for characterizing the land surface in Greenland [38, 39]. Convenient indices, derived by the observed backscattering and brightness temperature from the ERS scatterometer and the SSM/I, made possible the monitoring of seasonal variations in various types of land surfaces [40, 41].

2.2 Soil Moisture

Soil moisture, and its temporal and spatial variations, are influential parameters in both climatic and hydrologic models. The measurement of soil-moisture content (SMC) is one of the most important targets of remote sensing, and significant amounts of experimental and theoretical studies have been carried out since the late 1970s. The soil dielectric constant at microwave frequencies exhibits a strong dependence on the soil's moisture content. For example, at L band, the real part of the dielectric constant ranges from 3 for dry soil to about 25 for saturated soil. This variation can result in a change on the order of 10 dB in the magnitude of the radar-backscatter coefficient [42], and of 100 K in the magnitude of the brightness temperature. An important component required in the soil-moisture inverse problem is the knowledge of the relationship between the soil dielectric constant and its moisture content. Accurate empirical models and measurements for soil dielectric constant were given in [43-45].

As mentioned earlier, the radar backscatter and thermal emission at low microwave frequencies are both sensitive to soil-moisture content. Vegetation cover is one major difficulty encountered in practice, which masks the soil surface and reduces the radiometric and radar sensitivities to soil-moisture content. Controversial opinions have been expressed regarding the superiority of the radiometric technique over radar, or vice-versa. Du et al. [46] investigated the question by using radiative-transfer models for three types of canopies, all at 1.5 GHz, and this led to the conclusion that as far as vegetation effects are concerned, neither sensor can claim superiority over the other. From an experimental point of view, a certain conclusion on this point has not yet been reached. Surface roughness is the other disturbing factor that may significantly affect the measurement of soil moisture. This quantity has also been the subject of many investigations. In general, it has been stated that backscatter is more sensitive to this factor than emission.

2.2.1 Passive Systems

Soil-moisture-content research with microwave radiometers has been active since the late 1970s, and has recently been revitalized by new missions: the already-in-orbit AMSR-E and AMSR, and the planned SMOS, selected by the European Space Agency (ESA) in the framework of the Earth Explorer Opportunity Missions; and AQUARIUS, selected by NASA as part of the Earth System Science Pathfinder small-satellite program. The SMOS mission [47] is based on a dual-polarized L-band radiometer that uses aperture synthesis to achieve a ground resolution of 50 km. AQUARIUS [48], based on a combination of L-band active and passive conical-scanning instruments, will have similar performance, and will use radar data to correct for surface roughness.

Most experimental research on soil moisture with passive systems has been carried out in the US at GSFC in Greenbelt (Maryland), USDA in Beltsville (Maryland), JPL in Pasadena (California), MIT in Cambridge (Massachusetts), the University of Michigan (Michigan), and Princeton University (New Jersey); and in Europe at INRA in Avignon (France), the University of Amsterdam (The Netherlands), and the CNR in Florence (Italy). An excellent summary of recent research can be found in the special issue on "Large Scale Passive Microwave Remote Sensing of Soil Moisture" of the *IEEE Transactions on Geoscience and Remote Sensing*, published in August, 2001. Large airborne experiments, called the Southern Great Plains Hydrology Experiments, were conducted in the US in 1997 (SGP97) and 1999 (SGP99) to address significant gaps in the knowledge, and to validate retrieval algorithms designed for the AMSR and the AMSR-E. In 1997, the L-band Electronically Scanned Thinned Array

Radiometer (ESTAR) was used for daily mapping of soil-moisture content over an area greater than 10000 km^2 for a one-month period. Results showed the consistency of both the retrieval algorithm and the instrument. Error levels were on the order of 3% [49, 50]. In the SGP99, the Passive and Active L- and S-band airborne sensor (PALS) [51, 52] was used together with the C-band Polarimetric Scanning Radiometer (PSR/C). The acquired data provided information on the sensitivities of multi-channel low-frequency measurements to soil-moisture content for various vegetation conditions with water contents in the 0-2.5 kg m^2 range. The 1.41 GHz horizontal-polarization channel showed the greatest sensitivity, with a retrieval accuracy of 2.3%. PSR/C images showed spatial and temporal patterns consistent with meteorological and soil conditions, and indicated that the AMSR instrument can provide useful soil-moisture information.

As a part of the same SGP experiment, an observing-system simulation experiment (OSSE) was carried out to assess the impact of land-surface heterogeneity on the large-scale retrieval and validation of soil-moisture products, using the 6.925 GHz channel on the AMSR-E sensor. To do this, a high-resolution hydrologic model, a land-surface microwave-emission model (LSMEM), and an explicit simulation of the orbital and scanning characteristics for the AMSR-E were used. Results within the 575000 km^2 Red-Arkansas River basin showed that for surfaces with vegetation water content below 0.75 kg/m^2, two scale effects induced rms errors of 1.7% into daily 60 km AMSR-E soil moisture products, and rms differences of 3.0% into 60 km comparisons of AMSR-E soil-moisture products and in-situ field-scale measurements sampled on a fixed 25 km grid [53].

In the same area of SGP99, SSM/I and TMI satellite data were acquired over a two-week period under excellent meteorological conditions [10]. The analysis of the resulting maps showed that consistent satellite-based SMC retrieval is possible, and that data provided by the 6.9 GHz AMSR channel should offer significant improvements.

The problem of the effective temperature of the emitting surface at 6.6 GHz was investigated in [54], in which the magnitude of the long-term mean difference between actual and effective temperature was estimated by using data from the Scanning Microwave Multi-channel Radiometer (SMMR).

Various approaches have been considered for retrieving SMC from multi-frequency radiometric data, and, in particular, from the AMSR-E measurements [55]. These approaches differ primarily in the methods used to correct for the effects of soil texture, roughness, vegetation, and surface temperature. A common assumption is that over most land areas at the AMSR-E footprint scale, the effects of variability in soil texture and roughness on the observed brightness temperature are small compared with the effect of variability in soil—moisture content. This has been demonstrated in a number of model sensitivity studies [e.g., 56]. These parameters may therefore be approximated as non-variable. The vegetation-opacity coefficient can also be approximated as non-time-varying. However, it exhibits some dependence on crop type at the field scale, and the assumption of spatial uniformity must be considered a potential source of error. Soil-moisture-content retrieval approaches that have been investigated in previous studies include:

- Single-channel retrieval with sequential corrections using ancillary data [57, 58];
- Iterative forward model corrections using multi-channel brightness temperatures [56];
- Correction using multi-frequency polarization indices [59];
- Variations or combinations of the above methods [60, 61].

Other methods, based on Bayesian iterative inversion of a forward model [62] or neural networks [63, 64], have also been investigated.

The algorithm implemented for AMSR-E [56] was based on a radiative-transfer (RT) model; it used an iterative, least-squares algorithm, based on six radiometric channels. The primary rationale for this choice was that of minimizing the dependence on external ancillary data. The retrieval model assumes that temperature and moisture are uniform over the sensing depths of the frequencies used, and that the frequency dependence of the vegetation attenuation factor can be adequately characterized. The first factor is aided by using nighttime (1:30 a.m., descending-pass) measurements when the temperature and moisture profiles are reasonably uniform. Analysis of SMMR data taken over deserts and forests was used to obtain pre-launch estimates for AMSR-E.

Another algorithm, developed within the framework of the AMSR project, has been proposed in [59]. This algorithm is based on the sensitivity to moisture of both the brightness temperature, *Tb*, and the polarization index, *PI*, at C band, and uses the polarization index at X band to correct for the effect of vegetation by means of a semi-empirical model. Comparing the values of SMC retrieved from airborne measurements with those measured on the ground, the authors found a correlation coefficient of 0.78 with the standard error of estimate SE = 4.31 . The algorithm was further validated by using data from the SMMR and the SSM/I. Another approach, based on polarization difference, which used a radiative-transfer model to solve for soil-moisture content and vegetation optical depth simultaneously, was tested with SMMR observations over several test sites in Illinois. Results compared well with field observations of soil-moisture content and vegetation-index data from satellite optical sensors [60].

Due to the coarse ground resolution of space-borne microwave measurements, the resolution cell may include a non-homogeneous surface. The effects of within-pixel variability were exploited by several authors, who found that errors in the retrieved soil-moisture content were generally negligible for a heterogeneous bare soil, and less than 3% of the actual soil moisture for a pixel that was heterogeneous in vegetation and soil moisture [65-71].

The thickness of the soil layer through which moisture can be directly estimated by means of a microwave radiometer has been investigated by many experimental studies. Most researchers have come to the conclusion that at L band this layer is about 5-10 cm. This result matches well with the requirements of those processes such as infiltration and evapotranspiration that take place within this first layer of the soil medium. In other applications, where soil-moisture profiles down to several decimeters are necessary, microwave must be coupled to appropriate hydrological models. The effectiveness of the Kalman filter for retrieving such a quantity was demonstrated in [72] by using field observations and a simulation study. The usefulness of assimilating remotely sensed measurements into land-surface models was discussed in [73-75]. Burke et al. [70] explored the potential for using low-resolution passive microwave in a two-dimensional Land Data Assimilation System (LDAS) for estimating deep-soil moisture from surface-soil moisture. Houser et al. [73] investigated four-dimensional (4-D) soil-moisture assimilation using in-situ and remote-sensing observations. A refined four-dimensional algorithm that accounts for model errors and fully incorporates process dynamics into the estimates was developed in [75].

Simultaneously with experimental research, theoretical investigations were performed to interpret experimental data and to provide tools for the retrieval of land parameters. The classical approach to computing the brightness temperature of soils is the radiative-transfer theory, which can treat multiple scattering in a medium consisting of random discrete scatterers. However, the theory assumes independent scattering, and then disregards coherent effects. If the temperature of the medium is constant and energy conservation holds, the emissivity can be expressed as one minus the reflectivity, and the problem of computing the brightness temperature is brought back to the computation of the bistatic scattering coefficients. Most of the models developed for soil and vegetation are based on this method. The problem of computing the brightness temperature of land surfaces has been extensively treated in the three volumes of the recent book by Tsang and Kong and their collaborators [76-78]

An evaluation of classical methods (Physical Optics, small perturbations, and integral equations) to compute the emissivity of rough soils from the bistatic scattering coefficient was performed by comparing model simulations with experimental data obtained at C and X bands on an artificial dielectric surface with the same statistical properties used in the model [79]. The results showed that on relatively smooth surfaces (height standard deviation HStD = 0.4 cm), all the models fitted the vertical component of emissivity quite well, and underestimated the horizontal component of emissivity. On rougher surfaces (HStD = 2.5 cm), the IEM model slightly underestimated the horizontal component and overestimated the vertical component.

Li et al. [80] have recently proposed a rigorous solution of the problem of computing emissivity from a two-dimensional (2D) wet soil with a random rough surface by applying a physics-based two-grid method, combined with a sparse-matrix canonical-grid method. The advantage of this approach is that unlike analytic approximations, such as the Kirchhoff method and the Small Perturbation Method, this method solves the three-dimensional Maxwell's equations numerically. The use of the fast numerical method presented in the paper shows that numerical simulations of emissivities can be calculated with modest CPU resources. Thus, the results of extensive numerical simulations can be directly applied to passive microwave remote sensing of soil moisture.

2.2.2 Active Systems

This possibility of monitoring soil-moisture changes using SAR data has stimulated a large number of studies focused on establishing a relationship between the observed SAR response and surface soil-moisture content. For a homogeneous soil with a perfectly smooth surface, the scattering of electromagnetic waves is totally forward, and depends on permittivity of the medium. For a rough surface, radiation is scattered in various directions, and also generates backscattering. Thus, two basic properties determine the backscatter response observed by the SAR system: the permittivity of the medium and the roughness characteristics of the surface. Both parameters are, in turn, related to different geophysical parameters of the soil. With the advent of the polarimetric SAR, radar remote sensing of soil moisture has attained significant prominence in the past two decades. Initially, extensive experimental studies using polarimetric scatterometers were carried to establish a relationship between radar response and the surface roughness and soil moisture [81]. Extensive field experiments have also been conducted to examine retrieval algorithms ranging from simple analytical to regression/empirical models [82-84]. For example, the already mentioned SGP97 was conducted using a variety of active and passive remote-sensing tools on different platforms (truck, aircraft, and satellite) [85, 86].

Careful experiments under laboratory conditions or large field experiments all indicate that in order to retrieve soil-moisture content, more than a single backscatter observation is needed to separate the effects of surface-roughness parameters from the moisture content. Often times, only the surface rms height – and, in some cases, the surface correlation length – are sought for the surface-roughness parameters. In reality, the surface power spectral density is the quantity that affects the radar response;

however, retrieving surface parameters other than the rms height and correlation coefficient seems to be beyond the realm of possibility for radar remote-sensing tools. This implies that the experimental regressions between backscattering coefficient and soil-moisture content presented in the literature are both time and site dependent, and, thus, difficult to generalize.

SIR-C/X-SAR data pointed out that in the scale of surface roughness typical of agricultural areas, a co-polar L-band sensor provided the highest information content for estimating soil-moisture content and surface roughness. The sensitivity to soil-moisture content and surface roughness for individual fields was rather low, since both parameters affected the radar signal. However, in considering data averaged over a relatively wide area that included several fields, the correlation with the temporal variation of soil-moisture content was significant, since the effects of spatial roughness variations were smoothed [87]. On the other hand, the sensitivity to surface roughness was better manifested at a spatial scale, integrating in time to reduce the effects of moisture variation [87]. The retrieval of both soil moisture and surface roughness from multi-frequency polarimetric data was performed with good results by means of semi-empirical models [88, 89], or by inverting the IEM model [90].

The current limits of soil-moisture retrieval from ERS-SAR data were analyzed in [89] by using synthetic datasets, as well as a large pan-European database of ground and ERS-1 and ERS-2 measurements. The results from this study indicated that no more than two soil-moisture classes could be reliably distinguished using the ERS configuration, even for the limited roughness range considered.

In hydrological modeling of runoff and water balance, various input data – such as land use, soil moisture, and digital elevation terrain models (DEM) –can be acquired or estimated by the use of remote-sensing techniques. A good example of ERS SAR data assimilation in an integrated flood-forecasting model to translate rainfall into runoff was given in [91]. In the model, digital elevation terrain models derived from interferometric SAR data are used for a static description of a watershed, and dynamic model variables are obtained from the surface soil-moisture distribution estimated from SAR backscattering data.

Several scientists investigated the retrieval of soil-moisture content on a large scale by using ERS Wind Scatterometer data [e.g. 92, 93]. The results illustrated the applicability of these data for measuring land parameters, and offered the potential for deriving a physically-based alternative to empirical indices for estimating regionally-variable parameters.

As mentioned earlier, apart from surface-roughness parameters, the existence of short vegetation on the surface makes the retrieval of soil-moisture content very complicated. Vegetation cover and its temporal variations are believed to be the major stumbling blocks in monitoring soil-moisture-content variations using microwave. A very complicated coherent-scattering model, which accounts for scattering from rough surfaces, vegetation cover, and their near-field interaction, was demonstrated in [94]. The inverse of this model was then used to demonstrate its ability for estimating the physical parameters of a soybean field, including soil moisture from a polarimetric set of AIRSAR images.

2.3 Snow

Snow cover constitutes the largest component of any of the cryosphere, and plays a significant role in the global climate and climate response to global changes. It can be viewed as a sensitive indicator of variations in the climate system. Remote-sensing instruments have been shown to be the most appropriate tools for monitoring snow parameters over large extended areas. In addition to global-climate studies, remote sensing of snow packs is of great importance in forecasting the snow-water runoff. The currently available snow products are based on single sensors; thus, the temporal and spatial limitations are given by the sensor characteristics. For users to be able to utilize remote-sensing data in operational monitoring and management of snow, the data must fulfill the temporal and spatial resolution and accuracy requirements. The availability of data from new satellite sensors, such as ENVISAT, AQUA, and ADEOSII, should provide the scientific community with important tools for developing and bringing into operational use remote-sensing systems, for both regional and global mapping.

From the electromagnetic point of view, a snow medium can be considered to be a dense, heterogeneous medium, composed of an amorphous interconnected matrix of ice particles, air voids, a thin film of water on ice surfaces, and pockets of water among ice particles. Existing theoretical-modeling techniques for the snow medium can be categorized into two major groups: 1) field-based techniques (Maxwell's equations), and 2) techniques based on the law of conservation of power (radiative transfer). Field-based techniques are formulated either based on single scattering or dielectric fluctuations, and then the distorted Born approximation (DBA) is used to find the solution [77]. Although obtaining the solution for the distorted Born approximation is straightforward, some particular material characteristics, such as the dielectric correlation function, are exceedingly difficult to obtain. Measurement techniques for characterizing this correlation function involve a very arduous process [77]. It has been shown [95] that the correlation function must be known with high accuracy, including its tail region, to obtain an accurate prediction of scattering. At higher frequencies (X band and up), formulations based on the single-scattering theory fail because the size of the particles forming a snow medium becomes a considerable fraction of the wavelength, and they occupy an appreciable volume fraction ($>10\%$).

In this case, an appropriate approach is the radiative-transfer technique. Dense Medium Radiative Transfer Theory (DMRT), under the quasi-crystalline approximation with a coherent potential, and Strong Fluctuation Theory (SFT) are the most rigorous approaches to modeling microwave emission and scattering from snow packs at high frequencies [77, 96-98]. These approaches take into account the coherence of the scattering from random scatterers, and satisfy the energy-conservation constraint. An exhaustive description of the two theories can be found in [76-78]. Recent measurements, performed in the Italian Alps using multi-frequency passive sensors, demonstrated the capability of the DMRT to represent experimental data [99].

An approach to computing the effective permittivity of wet snow by using strong fluctuation theory was shown in [100]. In this work, snow was treated as a two-phase mixture where the water was considered to be inclusions embedded in dry snow. The shape of the scatterers was taken into account by using an anisotropic azimuthally symmetric correlation function. Model results were found to be in good agreement with experimental data. Although the DMRT method is quite rigorous, accurate determination of fundamental quantities of this formulation, such as extinction matrix and phase matrices, is not straightforward. Recently, numerical approaches for the determination of these quantities have been developed [101, 102]. In addition to numerical methods, quantities such as the extinction matrix can be measured experimentally, as shown in [103]. Apart from the theoretical approaches addressed above, purely empirical approaches may be considered [104]; these, however, have the obvious limitation that the entire parameter space of the target cannot be sufficiently well known to allow estimation of more-specific target properties. To circumvent the difficulties associated with the above-mentioned techniques and to offer some means by which realistic modeling of dense media might be accomplished, a new hybrid experimental /theoretical modeling scheme was introduced in [105]

2.3.1 Passive Systems

The capability of microwave radiometers to monitor snow parameters and seasonal variations in snow cover has been the subject of several experimental activities carried out since the late 1970s, using ground-based, airborne, and satellite systems [e.g., 106-111]. Measurements carried out between 3 GHz and 90 GHz pointed out the sensitivity of microwave emission to snow type and to snow-water equivalent (SWE). At the lower frequencies of the microwave band, emission from a layer of dry snow is mostly influenced by the soil conditions below the snow pack and by snow layering. However, at the higher frequencies the role played by volume scattering increases, and emissivity appears sensitive to snow-water equivalent. If snow melts, the presence of liquid water in the surface layer causes a strong increase in emissivity, especially at high frequencies [106, 108]. The average spectra of the brightness temperature show that the brightness temperature, *Tb*, of dry and refrozen snow decreases with frequency, whereas the *Tb* of wet snow increases [99, 106].

In general, microwave radiometers tend to underestimate the snow area compared with estimates from visible-infrared maps [109]. In addition, the errors in estimates of snow volume tend to be large, with standard errors of 20 mm snow-water equivalent or more [110]. For proper water-resource management and climate modeling, greater accuracy in a local scale and on a daily basis is required. Unfortunately, the spatial resolution of the SMMR and SSM/I instruments tends to limit their effective use to global-scale studies. Furthermore, currently available SSM/I data are acquired twice daily only at high latitudes, with a more restrictive coverage at lower latitudes. The AMSR and AMSR-E will help to overcome some of these drawbacks.

In general, high-frequency microwave emission from dry snow increases as snow depth (SD) increases. However, *Tb* measured by the SSM/I within the former Soviet Union during the 1987-1988 winter period showed dramatic deviations from this pattern. Indeed, in the middle of winter, *Tb* approached a minimum and then began to increase, despite the fact that the snow depth remained constant or continued to grow [111]. Model results suggested that the increase in *Tb* was due to a decrease in the single-scattering albedo as the snow pack aged. This decrease in the albedo was related to changes in the snow's crystalline structure, due to metamorphism. The midwinter minimum of *Tb* caused ambiguity in the relationship between snow-water equivalent and snow depth on *Tb* at high frequencies, and substantial nonlinearity of this dependence at intermediate frequencies. This midwinter minimum of *Tb* prevents the use of a simple, regression-type algorithm to derive the snow depth and snow-water equivalent from *Tb* measurements.

Several approaches have been proposed for retrieving snow parameters by means of empirical algorithms, such as the Spectral Polarization Difference (SPD), linear regressions, or iterative inversion of forward models [110, 112-114]. The inversion technique based on the HUT snow microwave emission model, developed in [115] and tested with SSM/I data, showed snow-water equivalent retrieval accuracies higher than those obtained with empirical approaches.

Since microwave radiation is sensitive to both snow depth and density, estimating snow depth alone requires that assumptions be made about the snow density. For average seasonal and global snow-depth estimation, "static" algorithms, which assume temporally constant grain size and density, have worked reasonably well [116]. However, in the cases of rapid changes in internal snow pack properties, estimates have been subject to errors. Dynamic algorithms, based on DMRT combined with density and grain-radius evolution models, have demonstrated their superiority, in that they tend to underestimate the snow depth less than do the static algorithms [117, 118].

Other studies were addressed to the combined use of electromagnetic and hydrological models [119, 120]. A three-component retrieval algorithm, developed in [120], included a DMRT model, a physically-based snow hydrology model (SHM) that incorporated meteorological and topographical data, and a neural network (NN). The DMRT model related physical snow parameters to *Tb*. The snow hydrology model simulated the mass and heat balance, and provided initial guesses for the neural network; the neural network was used to speed up the inversion of parameters. Inversion results obtained by applying the algorithm to measurements at 19 GHz and 37 GHz V and H polarizations compared favorably with ground-truth observations.

2.3.2 Active Systems

A great deal of experimental and theoretical work has been carried out pertaining to the radar response of snow. Similar to the soil-moisture problem, very careful experimentation with snow using radar systems over a wide range of radar attributes and snow conditions have been carried out initially to examine the feasibility, sensitivity, and accuracy of radar snow-parameter retrievals [121-124]. In addition, substantial efforts have been devoted to characterizing and measuring the very complex dielectric-constant behavior of snow with varying snow wetness [125-127].

Snow-parameter retrieval is mainly confounded by the complexity and dynamics of its structure and dielectric properties. To elaborate on this, consider a typical target of snow-covered ground. Target parameters that influence the radar response and that must be potentially considered include: 1) rough-surface parameters associated with the top surface of the snow; 2) the snow volume itself, i.e., density and particle-size distribution, and vertical distributions of these properties within the snow pack; 3) snow wetness, when present, may well be a very complex function of time and depth; and, finally, 4) the parameters of the ground beneath, such as dielectric constant, roughness parameters, and local slope.

Controlled experiments have concluded that microwave frequencies offer the highest potential for the retrieval of gross snow properties, such as depth or water equivalence, parameters that are especially important for hydrological applications. More specifically, a combination of L- and Ku-band radars – with the lower-frequency system measuring the parameters of the underlying ground surface and the higher-frequency radar monitoring the snow volume – was found the be an optimal configuration [122].

To examine the potential of active systems in mapping the extent of wet snow, experiments have been carried out by using both airborne and satellite SAR systems. For example, significant seasonal changes of Radarsat and ERS SAR backscatter from snow-covered surfaces in the Austrian Alps have been observed. These were mainly caused by variations of the snow liquid-water content and of the surface roughness [128]. A comparison of snow maps from SAR and Landsat-5 Thematic Mapper images showed good agreement in areas of continuous snow cover, whereas near the snow line, the SAR data slightly underestimated the snow extent.

Algorithms have been implemented for deriving the snow-covered areas (SCA) using change detection [128-130]. These studied showed that contrary to wet snow, the effect of dry snow in Alpine regions on C-band backscattering is too small to detect snow cover, and that a higher frequency would be necessary for snow retrievals [129]. However, the snow-water equivalent of dry snow was successfully retrieved on relatively smooth surfaces from the difference between the signal of the snow-free surfaces and the signal of the soil below the snow cover, which depends on the depth of the frozen soil layer. The latter is, in turn, related to the mass of snow [130]. Simulations obtained on a global scale with a model developed on the basis of data obtained from the Topex Poseidon Altimeter showed that Ku band provided more accurate snow-depth determinations than did C band [131], as predicated earlier by the controlled experiments.

The analysis of multi-frequency polarimetric SIR-C/X-SAR data showed that the frequency and polarization behavior of the radar-backscattering coefficients of a snow pack are very important for characterizing the physical state of snow and ice, and for separating the accumulation and ablation areas on glaciers [132]. The same data pointed out that the relationship between snow-water equivalent and backscattering coefficients at C and X band can be either positive or negative [133, 134]. Therefore, development of a simple empirical relationship between radar and snow parameters is unrealistic. Instead, snow depth and particle size were estimated from a physics-based first-order backscattering model, through the analysis of the importance of each scattering term and its sensitivity to snow properties.

In addition to the conventional backscattering analysis, recent work demonstrated the potential of the interferometric SAR techniques (InSAR) for separating bare soil from wet snow, and wet snow from dry snow. A new approach to retrieve information on the changes in snow-water equivalent from the phase difference in InSAR data was introduced in [135]. In the case of dry snow, the backscattering was from the snow-ground interface. However, the refraction of a radar wave in dry snow results in an interferometric phase difference, which is related to changes in snow depth and density. InSAR was also found to be a useful tool for monitoring the motion of glaciers [136, 137]. When this approach was limited by phase noise, intensity tracking, based on patch-intensity cross-correlation optimization, and coherence tracking, based on patch-coherence optimization, were successfully employed [138]

The utility of SAR data in estimating snow-cover area under wet-snow conditions is important for river-flow prediction, especially in applications such as hydro-power production and flood prevention.

Global observations with active systems were carried out by using scatterometric and altimetric data from satellites. The potential of a space-borne Ku-band scatterometer for monitoring global snow cover was demonstrated by using data from the National Aeronautics and Space Administration (NASA) scatterometer (NSCAT), operated on the Advanced Earth Observing Satellite (ADEOS) from September, 1996, to June, 1997 [140]. Sensitivity of Ku-band backscatter to snow conditions was illustrated with the dramatic change over the US northern plains and the Canadian prairie region corresponding to the snow event leading to the 1997 "Flood of the Century."

2.4 Forest Stands

A large portion of the Earth's surface is covered with vegetation of many different species and canopy configurations. Vegetation cover on the Earth's surface is an important factor in the study of global change. The total vegetation biomass is the most influential input to models for terrestrial ecosystems and atmospheric chemistry. The ability to monitor canopy parameters – such as total vegetation biomass, total leaf area index, and soil moisture content – is of vital importance to the study of the carbon cycle and global warming. Microwave remote-sensing techniques offer a unique opportunity to probe vegetation canopies at various depths by operating at different frequencies.

2.4.1 Passive Systems

Theoretical investigations have shown that passive microwave remote sensing can contribute significantly to the global study of soil and vegetation parameters in forests [141, 142]. However, microwave radiometers on satellites are hampered by the coarse ground resolution. On the other hand, airborne sensors provide much better resolution, and can be useful for detailed analyses of some particular areas and surveillance of forests subject to fires or other sudden changes. Moreover, the next-generation sensors (SMOS, AMSR, AMSR-E) will be able to attain a much more enhanced resolution. At present, only some experimental data are available. These data have been collected mostly in northern Europe on boreal coniferous forests using satellite [143, 144] and airborne data [145]. Recently, L-band radiometer measurements of coniferous forests were performed by flying the ESTAR radiometer over loblolly pine stands in eastern Virginia. The images of the area showed a strong correlation between forest biomass and the measured brightness temperature, *Tb* [146].

Airborne radiometric measurements in a frequency range from L to Ka band were carried out over six broad-leaved forests and one coniferous forest in Italy [147]. Ground-truth data of the major tree parameters were available for the same tree stands. The analysis of the collected data indicated that the use of microwave emission at the highest frequencies made it possible to identify some forest types, whereas L-band emission was more closely related to tree biomass. Other relationships were found between emission and leaf-area index, basal area, woody volume, and crown transparency. The significant relationship between L-band emission and woody volume was further analyzed by means of a discrete-element radiative-transfer model. The analysis showed that the main contribution to the total emission was due to the elements in tree crowns and, in particular, to primary and medium branches, while double reflection from soil was negligible. Simulations performed at L band by using a model validated with experimental data at C band confirmed these results, and pointed out an appreciable sensitivity to soil moisture, even under developed forests [148].

2.4.2 Active Systems

The use of polarimetric, interferometric, and polarimetric-interferometric SARs to survey forested areas has become increasingly important in recent years [149-153]. Experimental studies conducted since the early 1990s with space-borne and airborne SAR systems led to the conclusion that the radar-backscatter results from scattering and/or attenuation of leaves, branches, and trunks, leading to an indirect relationship between the radar measurements and the biomass parameters. The greater temporal stability of forest compared with many other types of land cover presented a means of mapping forest areas using multi-temporal data [154, 155]. However, the comparison of results obtained over different forest sites is difficult, due to differences in stand characteristics, validation procedures, parameters used as evaluation criteria, selection of stands, etc. Stand size seems to explain most of the variability of the results, and although an attempt has been made to suggest procedures to convert results from one stand size to another, there still are open issues to be addressed [156].

It has been shown that the radar measurements are no longer sensitive to biomass variation after a certain amount of biomass value, which depends on the electromagnetic frequency. This limit was estimated to be about 30-50 tons/ha at C and L band (5 GHz and 1.2 GHz), and about 150-200 tons/ha at P band (0.4 GHz), for both evergreen and coniferous forests [151, 157-159]. In general, the use of P-band channels can provide better estimates of stem biomass, while L-band channels can estimate the crown biomass more accurately [29, 153]. However, the most appropriate approach for estimating forest biomass is the use of lower-frequency systems, such as the VHF (20-90 MHz) airborne imaging radar CARABAS. Using this radar, signal saturation was not observed up to 900 m^3 ha. However, the sensitivity to the volume was high in the range of 0-500 m^3 ha (e.g., 1 dB to 1.5 dB for 50 m^3 ha), whereas it was reduced beyond 500 m^3 ha [160]. The accuracy of the estimated stem volume retrieved using these data and a new textural method based on the variations of the standard deviation of the backscattering coefficient was comparable to that of the ground truth [161]. The other forest parameters could not be estimated with such good accuracy, but this was partly due to using the dominant values instead of averages. Also, it was found that in the case of storms, the backscattering for a given stem volume was considerably higher for wind-thrown forests than for unaffected forests. This indicates that VHF SAR imagery has potential for mapping wind-thrown forests [162].

A key component in the study of microwave remote sensing of vegetation is the understanding of the spectral behavior of the dielectric constant of vegetation. Through careful experimentation and examination of the dielectric properties of water, bound water, and dry vegetation, an approximate empirical formulation for the dielectric constant of vegetation as a function of moisture content and temperature was reported in [163]. The validity of this model was examined by independent measurement techniques, and its accuracy was found to be with 10% of the measured quantities [164]. Extensive measurements of complex permittivity for various parts of a conifer were reported in [165].

In the early forest-scattering models, the forest structure was simplified in terms of a homogeneous random medium, and the single-scattering theory was applied to account for scattering and propagation in the random medium [166-168]. For example, in [166] and [167], vector radiative transfer was used to calculate the bistatic scattering from a forest stand, represented by a two-layer random medium. In a medium where particle size – such as tree trunks and large branches – is comparable to the extent of the medium, a radiative transfer model may not produce satisfactory results. Furthermore, an important feature of a high-fidelity scattering model is to preserve the structure of vegetation, as different species of vegetation have their own unique structures, and this has been shown to have considerable effect at P and L band. An important effect of the vegetation structure is the coherence effect, caused by the relative position of the vegetation particles, which produce certain interference patterns. To preserve the coherence effects and the nonuniform attenuation and scattering profile, a Monte Carlo coherent-scattering model for forest canopies was also presented in [169]. In this model, realistic-looking tree structures were constructed using a stochastic fractal algorithm, and the distorted Born approximation was used for scattered-field calculations. Common in all forest scattering and emission models are scattering formulations for broad leaves, needles, twigs, branches, and tree trunks [170 -175].

Recent advancements in the field of radar interferometry have opened a new door to the radar remote sensing of vegetation. In addition to the backscattering coefficient, radar interferometers measure two additional quantities that contain target information [176]. These quantities are the correlation coefficient and the interferogram phase. The premise of this investigation with regard to retrieving vegetation parameters from INSAR data stems from the fact that the location of the scattering phase center of a target is a strong function of the target's structure. For example, the scattering phase centers of non-vegetated terrain are located at or slightly below the surface, whereas for vegetated terrain, these scattering phase centers lie at or above the surface, depending upon the wavelength of the SAR and the attributes of the vegetation. In recent years, some experimental and theoretical studies have been carried out to demonstrate the potential of InSAR in retrieving forest parameters. For example in [177-180], experimental data using ERS-1 SAR repeat-pass and DO-SAR single-pass were employed to show the applications of SAR interferometry for classification of forest types and retrieval of tree heights. The accuracy achieved in separating forest/non-forest areas by using a single pair of repeat-pass SAR interferometry was on the order of 80%-85%. Similar or slightly better classification accuracies were reported with multi-temporal backscattering coefficients using C-band ERS data [154].

Simplified theoretical models have also been developed to establish relationships between the interferogram phase and coefficient of correlation with the physical parameters of vegetation and the underlying soil surface [181, 182]. A far more accurate model for estimation of scatter phase-center location, based on the Monte Carlo simulation of fractal trees, was developed later [183]. This model accounted for the exact structure, shape, size, number density, and orientation distributions of vegetation in desired forest stands, and its accuracy was tested against JPL TOPSAR [184] data.

Whereas radar polarimetry provides an enhanced capability in recovering target-structure anisotropy (preferred orientation), and SAR interferometry reveals the target's penetrability and vertical extent, a polarization-agile interferometric SAR has this combined capability, and can provide the target-structure parameters far more conveniently than can the individual sensors. Polarimetric target decomposition techniques have also been suggested and successfully demonstrated using polarimetric/interferometric SARs [185, 186]. More sophisticated techniques, using interferometric SARs – such as multi-baseline INSAR – have also been tried, and showed significant potential for retrieving vegetation parameters [187, 188].

The retrieval of target parameters in an imaged scene is possible through the use of multi-frequency observations, polarization diversity of imaging polarimetry, estimation of the scattering phase-center height, and textural information.

The study of the inversion problems has been of great importance from the onset of remote-sensing science [189, 190]. To make the inverse-scattering problem tractable, overly simplistic forward models were initially used [191]. With the availability of significant SAR and accurate ground-truth data, statistical and regression inversion methods have been investigated [192]. Like most empirical models, the success of these techniques is somewhat limited to the range of system and measured target-parameter space. Other systematic inversion algorithms, such as neural-network approaches [193] and genetic algorithms [194], using more sophisticated forward models, have been developed.

2.5 Short Vegetation Crops

As mentioned in the previous section, vegetation biomass plays a very important role in the Earth's climate dynamics and the atmosphere's carbon cycle. However, another vegetation class that must not be overlooked is the category of herbaceous vegetation, both natural and cultural. At approximately 30 million square kilometers, this vegetation type covers 20% of the Earth's dry surface, accounting for more than 30 billion metric tons of total biomass. An understanding on a global scale of the biophysical parameters that describe this vegetation is thus highly desirable.

Although the sensitivity of microwave emission to crop type and biomass has been demonstrated in several investigations, the ground resolution of passive systems is inadequate for operational systems, and recent research has mostly been addressed to the study of SAR data.

The large amount of SAR data collected at different times made it possible to evaluate the potential of multi-temporal analysis in timing critical phases of the crop-growth cycle, and in separating broad-leaf crops from cereals (small leaf) [29, 195, 196]. The radar response of these two types of crops to biomass showed that for crops characterized by small-plant constituents, such as wheat (narrow-leaf crops), σ° decreased as the biomass increased, whereas the trend was quite the opposite in plants with bigger leaves and stems, such as sunflowers (broad-leaf crops) [197]. Model simulations confirmed the trends of the experimental data, and made it possible to evaluate the contribution of single-plant constituents to total backscattering. In "broad-leaf" crops, σ° from stalks dominated at L band, while at C band, leaves made a significant contribution to scattering and attenuated the contribution of stems. In "narrow-leaf" crops, the contributions of leaves and stalks were comparable and close to total backscattering. The analysis of the contributions of each scattering mechanism showed that in general, double scattering was the most important contribution for stalks, direct scattering prevailed for leaves, and soil contribution was appreciable even for well-developed crops [198].

On the other hand multi-frequency observations pointed out that for remote sensing of crops, low microwave frequencies (< 5 GHz) are recommended, and therefore one must carefully account for the coherence effects. The model developed in [199] may be among the first to address the coherence effects caused by the vegetation structure. A very careful coherent model for grass-type vegetation, such as a wheat field, and measurements over the entire growing season are reported in [200-202]. Simulations performed with a coherent model confirmed the experimental relations found between backscattering and the biomass of broad- and narrow-leaf crops, and demonstrated the contribution of the InSAR observation in crop discrimination [203].

A model based on the Method of Moments and Monte Carlo simulation for similar crops showed the importance of near-field scattering and coherence to the target radar response [204]. In [205], an analytical polarimetric coherent scattering model for short branching vegetation – such as a soybean crop – was developed that accounted for the second-order near-field interaction among particles, as well as the underlying rough surface and particles. In this paper, retrieval of soil moisture and vegetation parameters was demonstrated, using data obtained from JPL AIRSAR.

A number of studies have been carried out aimed at using remote-sensing data to improve the accuracy of crop-functioning models in predicting the yield and the evolution of canopy variables through the crop cycle. Two main approaches have been used and reported in [206]. In the first approach, some crop variables were retrieved by inverting the radiative-transfer models, and used to force or to recalibrate some well-identified parameters of the crop-functioning model. In the second approach, a crop model was coupled with a radiative transfer model to simulate the whole process from canopy functioning to remote-sensing data, by fitting simulated results to observed results. The assimilation of optical and radar data in a coupled crop-plus-radiative-transfer model was tested by [207], using data acquired over wheat fields. The study showed that assimilating optical and radar data into a crop model is feasible. However, in this case, the introduction of radar data did not improve the accuracy of the results.

3. Final Remarks

In this article, we tried to provide the reader with a comprehensive overview of the recent techniques and approaches in microwave remote sensing of land. Both analytical and experimental remote-sensing methods for active and passive systems were surveyed. It is important to mention here that the wealth of knowledge in this area is overwhelming, and it quickly became obvious to us that we could not possibly include all the significant contributions reported in the literature in the limited space of this article. This fact also indicates the great progress made in the science and technology of microwave remote sensing over the past decade, such as that related to the operational applications of SAR interferometry. Despite this significant progress, there are still considerable challenging problems for which the existing remote-sensing tools and methodologies do not provide solutions with desirable accuracies, as requested by the users. It is on these problems – such as land classification and the measurement of land hydrological parameters on a routine basis – that further research need to be focused. It is believed that further investments in advanced space-based remote-sensing instrumentations, with new functionalities and modalities – such as low-frequency active and passive systems aboard satellites with short revisit time – will provide the scientific community with sufficiently large, precise, and frequent databases to allow for accurate and consistent retrieval of target parameters.

4. References

1. http://southport.jpl.nasa.gov/desc/SIRCdesc.html.

2. http://www.jpl.nasa.gov/srtm.

3. F. M. Anderson and A. J. Lewis, *Manual of Remote Sensing, Principles and Applications of Imaging Radar*, New York, John Wiley & Sons, third Edition, 1998.

4. S. R. Cloude and E. Pottier, **"A Review of Target Decomposition Theorems in Radar Polarimetry**," *IEEE Transactions on Geoscience and Remote Sensing*, **GRS-34**, 2, March 1996, pp. 498-518.

5. P. A. Rosen, S. Hensley, I. R. Joughin, F. K. Li, S. N. Madsen, E. Rodriguez, and R. M. Goldstein, "**Synthetic Aperture Radar Interferometry**," *Proceedings of the IEEE*, **88**, 3, March 2000, pp. 333-382.

6. http://envisat.esa.int/

7. A. Bentamy, Y. Quilfen, and P. Queuffeulou, "Calibration of the ERS-1 Scatterometer C-Band Model," Technical. Rep., IFREMER DRO/OS, Institute Francaise de Recherche pour l'Exploitation de la Mer, France, January 1994.

8. A. Ferretti, C. Prati, F. Rocca, "Permanent Scatterers in SAR Interferometry," *IEEE Transactions on Geoscience and Remote Sensing*, **GRS-39**, 1, January 2001, pp. 8-20.

9. C. Colesanti, A. Ferretti, C. Prati, F. Rocca, "Full Exploitation of the ERS Archive: Multi Data Set Permanent Scatterers Analysis," *IEEE Transactions on Geoscience and Remote Sensing*, **GRS-41**, 7, July 2003, pp. 1685-1701.

10. http://www.space.gc.ca/csa_sectors/earth_environment/radarsat/default.asp

11. T. Kawanishi, T. Seyai, Y. Ito, K. Imaoka, T. Takeshima, Y. Ishido, A. Shibata, M. Miura, H. Inahata, and R. W. Spencer, "The Advanced Microwave Scanning Radiometer for the Earth Observing System (AMSR-E), NASDA's Contribution to the EOS for Global Energy and Water Cycle Studies," *IEEE Transactions on Geoscience and Remote Sensing*, **GRS-41**, 2, February 2003, pp. 184-194.

12. A. Shibata, "AMSR/AMSR-E Algorithm Development and Data Distribution," *Proceedings of the IEEE 2000 International Geoscience and Remote Sensing Symposium (IGARSS 2000)*, Honolulu, Hawaii, 24-28 July 2000.

13. http://sharaku.eorc.nasda.go.jp/AMSR/index_e.htm.

14. http://alos.nasda.go.jp/2/palsar-e.html.

15. http://www.ccrs.nrcan.gc.ca/ccrs/data/satsens/radarsat/rsat2/radnews_e.html.

16. C. Prigent, J.-P. Wigneron, W. B. Rossow, and J. R. Pardo-Carrion, "Frequency and Angular Variations of Land Surface Microwave Emissivities: Can We Estimate SSM/T and AMSU Emissivities from SSM/I Emissivities?," *IEEE Transactions on Geoscience and Remote Sensing*, **GRS-38**, 5, September 2000, pp. 2373-2386.

17. T. J. Jackson and A. Y. Hsu, "Soil Moisture and TRMM Microwave Imager Relationships in the Southern Great Plains 1999 (SGP99) Experiment," *IEEE Transactions on Geoscience and Remote Sensing*, **GRS-39**, 8, August 2001, pp. 1632-1642.

18. Y. Jhung and P. H. Swain, "Bayesian Contextual Classification Based on Modified M-Estimates and Markov Random Fields," *IEEE Transactions on Geoscience and Remote Sensing*, **GRS-34**, 1, January 1996, pp. 68-75.

19. L. E. Pierce, F. T. Ulaby, K. Sarabandi, and M. C. Dobson," Knowledge-Based Classification of Polarimetric SAR Images," *IEEE Transactions on Geoscience and Remote Sensing*, **GRS-32**, 5, September 1994, pp. 1081-1086.

20. J. J. van Zyl, "Unsupervised Classification of Scattering Behavior Using Radar Polarimetry Data," *IEEE Transactions on Geoscience and Remote Sensing*, **GRS-27**, 1, January 1989, pp. 36-45.

21. J. A. Benediction, P. H. Swain, and O. K. Erase, "Neural Network Approaches Versus Statistical Methods in Classification of Multisource Remote Sensing Data," *IEEE Transactions on Geoscience and Remote Sensing*, **GRS-28**, 4, July 1990, pp. 540-551.

22. L. E. Pierce, K. Sarabandi, and F. T. Ulaby, "Application of an Artificial Neural Network in a Canopy Scattering Model Inversion," *International Journal of Remote Sensing*, **15**, 16, 1994, pp. 3263-3270.

23. P. M. Atkinson and A. R. L. Tatnall, "Neural Networks in Remote Sensing," *International Journal of Remote Sensing*, **18**, 4, 1997, pp. 699-709.

24. R. S. Safavian and D. Landgrebe, "A Survey of Decision Tree Classifier Methodology," *IEEE Transactions of Systems, Man, and Cybernetics*, **21**, 1991, pp. 660-675.

25. J. Schou, H. Skriver, A. A Nielsen, and K. Conradsen, "CFAR Edge Detector for Polarimetric SAR Images," *IEEE Transactions on Geoscience and Remote Sensing*, **GRS-41**, 1, January 2003, pp. 20-32.

26. K. Conradsen, A. A Nielsen, J. Schou, and H. Skriver, "A Test Statistics in the Complex Wishart Distribution and its Applications to Change Detection in Polarimetric SAR Data," *IEEE Transactions on Geoscience and Remote Sensing*, **GRS-41**, 1, January 2003, pp. 4-19.

27.http://airsar.jpl.nasa.gov/data/.

28.http://www.ccrs.nrcan.gc.ca/ccrs/data/satsens/airborne/sarbro/sbmain_e.html

29.P. Ferrazzoli, S. Paloscia, P. Pampaloni, G. Schiavon, S. Sigismondi, and D. Solimini, "The Potential of Multifrequency Polarimetric SAR in Assessing Agricultural and Arboreous Biomass," *IEEE Transactions on Geoscience and Remote Sensing*, **GRS-35**, 1, January 1997, pp. 5-17.

30.J. S. Lee, M. R. Grunes and Eric Pottier, "Quantitative Comparison of Classification Capability: Fully Polarimetric Versus Dual and Single-Polarization SAR," *IEEE Transactions on Geoscience and Remote Sensing*, **GRS-39**, 11, November 2001, pp. 2343-2351.

31.F. Dell'Acqua and P. Gamba, "Texture-Based Characterization of Urban Environments on Satellite SAR Images," *IEEE Transactions on Geoscience and Remote Sensing*, **GRS-41**, 1, January 2003, pp. 153-159.

32.G. Franceschetti, A. Iodice, D. Riccio, "**A Canonical Problem in Electromagnetic Backscattering from Buildings,**" *IEEE Transactions on Geoscience and Remote Sensing*, **GRS-40**, 8, August 2002, pp 1787-1801.

33.F. Tupin, B. Houshmand, and M. Dactu, "Road Detection in Dense Urban Areas Using SAR Imagery and the Usefulness of Multiple Views," *IEEE Transactions on Geoscience and Remote Sensing*, **GRS-40**, 11, November 2002, pp. 2405-2414.

34.P. L. Frison and E. Mougin, "Monitoring Seasonal Vegetation Dynamics in the Sahel with ERS Wind Scatterometer Data, ESA SP-414," *IEEE Transactions on Geoscience and Remote Sensing*, **GRS-35**, 1997, pp. 163-168.

35.C. Schmullius, "Monitoring Siberian Forests and Agriculture with the ERS-1 Windscatterometer," *IEEE Transactions on Geoscience and Remote Sensing*, **GRS-35**, 5, September 1997, pp. 1363-1366.

36.C. M. U. Neale, M. J. McFarland, and K. Chang, "Land-Surface-Type Classification Using Microwave Brightness Temperatures from the Special Sensor Microwave/Imager," *IEEE Transactions on Geoscience and Remote Sensing*, **GRS-28**, 5, September 1990, pp. 829-838.

37.J. V. Fiore and N. C. Grody, "Classification of Snow Cover and Precipitation Using SSM/I Measurements: Case Studies," *International Journal of Remote Sensing*, **13**, 1992, pp. 3349-3361.

38.J. Judge, J. F. Galantowicz, A. W. England, and P. Dahl, "Freeze/Thaw Classification for Prairie Soils Using SSM/I Radiobrightnesses," *IEEE Transactions on Geoscience and Remote Sensing*, **GRS-35**, 4, July 1997, pp. 827-832.

39.N. C. Grody and Alan N. Basist, "Interpretation of SSM/I Measurements over Greenland," *IEEE Transactions on Geoscience and Remote Sensing*, **GRS-35**, 2, March 1997, pp. 360-366.

40.P.-L. Frison, E. Mougin, L. Jarlan, M. A. Karam, and P. Hiernaux, "Comparison of ERS Wind-Scatterometer and SSM/I Data for Sahelian Vegetation Monitoring," *IEEE Transactions on Geoscience and Remote Sensing*, **GRS-38**, 4, July 2000, pp. 1794-1803.

41.G. Macelloni, S. Paloscia, P. Pampaloni, and E. Santi, "Global Scale Monitoring of Soil and Vegetation Using Active and Passive Sensors," *International Journal Remote Sensing*, 2003, pp. 2409-2425.

42.Y. Oh, K. Sarabandi, and F. T. Ulaby, "An Empirical Model and an Inversion Technique for Radar Scattering from Bare Soil Surfaces," *IEEE Transactions on Geoscience and Remote Sensing*, **GRS-30**, 2, March 1992, pp. 370-381.

43.M. C. Dobson, F. T. Ulaby, M. T. Hallikainen, and M. A. El-Rayes, "Microwave Dielectric Behavior of Wet Soil – Part II – Dielectric Mixing Models," *IEEE Transactions on Geoscience and Remote Sensing*, **GRS-23**, 1, January 1985, pp. 35-46.

44.N. R. Peplinski, F. T. Ulaby, and M. C. Dobson, 1995, "Dielectric Properties of Soil in the 0.3 - 1.3 GHz Range," *IEEE Transactions on Geoscience and Remote Sensing*, **GRS-33**, 3, May 1995, pp. 803-806.

45.K. Sarabandi and E. S. Li, "A Microstrip Ring Resonator for Non-Invasive Dielectric Measurements," *IEEE Transactions on Geoscience and Remote Sensing*, **GRS-35**, 5, September 1997, pp. 1223-1231.

46.G. Du, F. T. Ulaby, and M. C. Dobson, "Sensitivity to Soil Moisture by Active and Passive Microwave Sensors," *IEEE Transactions on Geoscience and Remote Sensing*, **GRS-38**, 1, January 2000, pp. 105-114.

47.Y. H. Kerr, Ph. Waldteufel, J.-P. Wigneron, J.-M. Martinuzzi, J. Font, and M. Berger, "Soil Moisture Retrieval from Space: The Soil Moisture and Ocean Salinity (SMOS) Mission," *IEEE Transactions on Geoscience and Remote Sensing*, **GRS-39**, 8, August 2001, pp. 1729-1735.

48.D. Le Vine, C. Koblinsky, and F. Pellerano, "The Measurement of Salinity from Space: Sensor Concept," IEEE International Geoscience and Remote Sensing Symposium, Sidney, Australia, July 9-13, 2001.

49.T. J. Jackson, D. M. Le Vine, A. Y. Hsu, A. Oldak, P. J. Starks, C. T. Swift, J. D. Isham, and M. Haken, "Soil Moisture Mapping at Regional Scales Using Microwave Radiometry: The Southern Great Plains Hydrology Experiment," *IEEE Transactions on Geoscience and Remote Sensing*, **GRS-37**, 5, September 1999, pp. 2136-2452.

50.R. Bindlish, W. P. Kustas, A. N. French, G. R. Diak, and J. R. Mecikalski, "Influence of Near-Surface Soil Moisture on Regional Scale Heat Fluxes: Model Results Using Microwave Remote Sensing Data from SGP97," *IEEE Transactions on Geoscience and Remote Sensing*, **GRS-39**, 8, August 2001, pp. 1719-1728.

51.E. G. Njoku, W. J. Wilson, S. H. Yueh, St. J. Dinardo, F. K. Li, T. J. Jackson, V. Lakshmi, and J. Bolten, "Observations of Soil Moisture Using a Passive and Active Low-Frequency Microwave Airborne Sensor During SGP99," *IEEE Transactions on Geoscience and Remote Sensing*, **GRS-40**, 12, December 2002, pp. 2659-2673.

52.T. J. Jackson, A.. J. Gasiewski, A. Oldak, M. Klein, E. G. Njoku, A. Yevgrafov, S. Christiani, and R. Bindlish, "Soil Moisture Retrieval Using the C-Band Polarimetric Scanning Radiometer During the Southern Great Plains 1999 Experiment," *IEEE Transactions on Geoscience and Remote Sensing*, **GRS-40**, 10, October 2002, pp. 2151-2161.

53.W. T. Crow, M. Drusch, and E. F. Wood, "An Observation System Simulation Experiment for the Impact of Land Surface Heterogeneity on AMSR-E Soil Moisture Retrieval," *IEEE Transactions on Geoscience and Remote Sensing*, **GRS-39**, 8, August 2001, pp. 1622-1631.

54.A. Van de Griend, "The Effective Thermodynamic Temperature of the Emitting Surface at 6.6 GHz and Consequences for Soil Moisture Monitoring from Space," *IEEE Transactions on Geoscience and Remote Sensing*, **GRS-39**, 8, August 2001, pp. 1673-1679.

55.E. G. Njoku, T. J. Jackson, V. Lakshmi, T. K. Chan, and S.V. Nghiem, "Soil Moisture Retrieval from AMSR-E," *IEEE Transactions on Geoscience and Remote Sensing*, **GRS-41**, 2, February 2003, pp. 215-229.

56.E. G. Njoku and Li Li, "Retrieval of Land Surface Parameters Using Passive Microwave Measurements at 6-18 GHz," *IEEE Transactions on Geoscience and Remote Sensing*, **GRS-37**, 1, January 1999, pp. 79-93.

57.T. J. Jackson, D. M. Le Vine, A. J. Griffis, D. C. Goodrich, T. J. Schmugge, C. T. Swift, and P. E. O'Neill, "Soil Moisture and Rainfall Estimation Over a Semiarid Environment with the ESTAR Microwave Radiometer," *IEEE Transactions on Geoscience and Remote Sensing*, **GRS-31**, 4, July 1993, pp. 836-841.

58.K. Vinnikov, A. Robock, S. Qiu, J. Entin, M. Owe, B. Choudhury, S. Hollinger, and E. Njoku, "Satellite Remote Sensing of Soil Moisture in Illinois, USA," *Journal Geophysical Research*, **GRS-104**, 1999, pp. 4145-4168.

59.S. Paloscia, G. Macelloni, E. Santi, and T. Koike, "A Multifrequency Algorithm for the Retrieval of Soil Moisture on a Large Scale Using Microwave Data from SMMR and SSM/I Satellites," *IEEE Transactions on Geoscience and Remote Sensing*, **GRS-39**, 8, August 2001, pp. 1655-1661.

60.M. Owe, R. de Jeu, and J. Walker, "A Methodology for Surface Soil Moisture and Vegetation Optical Depth Retrieval Using the Microwave Polarization Difference Index," *IEEE Transactions on Geoscience and Remote Sensing*, **GRS-39**, 8, August 2001, pp. 1643-1654.

61.T. J. Jackson and A. Y. Hsu, "Soil Moisture and TRMM Microwave Imager Relationships in the Southern Great Plains 1999 (SGP99) Experiment," *IEEE Transactions on Geoscience and Remote Sensing*, **GRS-39**, 8, August 2001, pp. 1632-1642.

62.D. T. Davis, Z. Chen, J.-N. Hwang, L. Tsang, and E. G. Njoku, "Solving Inverse Problems by Bayesian Iterative Inversion of a Forward Model with Applications to Parameter Mapping Using SMMR Remote Sensing Data," *IEEE Transactions on Geoscience and Remote Sensing*, **GRS-33**, 5, September 1995, pp. 1182-1193.

63.Y. Liou, S. Liu, and W. Wang, "Retrieving Soil Moisture from Simulated Brightness Temperatures by a Neural Network," *IEEE Transactions on Geoscience and Remote Sensing*, **GRS-39**, 8, August 2001, pp. 1662-1672.

64.S. Liu, Y. Liou, W. Wang, J.-P. Wigneron, and J.-B. Lee, "Retrieval of Crop Biomass and Soil Moisture From Measured 1.4 and 10.65 GHz Brightness Temperatures," *IEEE Transactions on Geoscience and Remote Sensing*, **GRS-40**, 6, June 2002, pp. 1260-1268.

65.J. F. Galantowicz, D. Entekhabi, and E. G. Njoku, " Estimation of Soil-Type Heterogeneity Effects in the Retrieval of Soil Moisture from Radiobrightness," *IEEE Transactions on Geoscience and Remote Sensing*, **GRS-38**, 1, January 2000, pp. 312-315.

66.Y. A. Liou, J. Kim, and A. W. England, "Radiobrightness of Prairie Soil and Grassland During Dry-Down Simulations," *Radio Science*, **33**, 1998, pp. 259-265.

67.M. Drusch, E. F. Wood, and C. Simmer, "Up-scaling Effects in Passive Microwave Remote Sensing: ESTAR 1.4 GHz Measurements during SGP '97," *Geophysical Research Letters*, **26**, 2001, pp. 879-882.

68.W. T. Crow, M. Drusch, and E. F. Wood, "An Observation System Simulation Experiment for the Impact of Land Surface Heterogeneity on AMSR-E Soil Moisture," *IEEE Transactions on Geoscience and Remote Sensing*, **GRS-39**, 2001, pp. 1622-1631.

69.A. Guha and V. Lakshmi, "Sensitivity, Spatial Heterogeneity, and Scaling of C-Band Microwave Brightness Temperatures for Land Hydrology Studies," *IEEE Transactions on Geoscience and Remote Sensing*, **GRS-40**, 12, December 2002, pp. 2626-2635.

70.E. J. Burke and L. P. Simmonds, "Effects of Sub-Pixel Heterogeneity on the Retrieval of Soil Moisture from Passive Microwave Radiometry," *International Journal of Remote Sensing*, **24**, 10, May 2003, pp. 2085-2104.

71.E. J. Burke, R. J. Gurney, L. P. Simmonds, and T. J. Jackson, "Calibrating a Soil Water and Energy budget Model with Remotely Sensed Data to Obtain Quantitative Information about the Soil," *Water Resources Research*, **33**, 1997, pp. 1689-1697.

72.J. F. Galantowicz, D. Entekhabi, and E. G. Njoku, "Tests of Sequential Data Assimilation for Retrieving Profile Soil Moisture and Temperature from Observed L-Band Radiobrightness," *IEEE Transactions on Geoscience and Remote Sensing*, **GRS-37**, 4, July 1999, pp. 1860-1870.

73.P. R. Houser, W. J. Shuttleworth, J. S. Famiglietti, H. V. Gupta, K. H. Syed, and D. C. Goodrich, "Integration of Soil Moisture Remote Sensing and Hydrological Modeling Using Data Assimilation," *Water Resources Res.*, **34**, 1998, pp. 3405-3420

74.E. J. Burke, W. J. Shuttleworth, K. Lee, and L. A. Bastidas, "Using Area-Average Remotely Sensed Surface Soil Moisture in Multipatch Land Data Assimilation Systems," *IEEE Transactions on Geoscience and Remote Sensing*, **GRS-39**, 10, October 2001, pp. 2091-2100.

75.R. H. Reichle, D. B. McLaughlin, and D. Entekhabi, "Variational Data Assimilation of Microwave Radiobrightness Observations for Land Surface Hydrology Applications," *IEEE Transactions on Geoscience and Remote Sensing*, **GRS-39**, 8, August 2001, pp. 1708-1718.

76.L. Tsang, J. A. Kong, and K.-H. Ding, *Scattering of Electromagnetic Waves*, *Vol. I: Theories and Applications*, New York, John Wiley & Sons, 2000.

77.L. Tsang, J. A. Kong, K.-H. Ding, and C. O. Ao, *Scattering of Electromagnetic Waves*, *Vol. II*: *Numerical Simulations*, New York, John Wiley & Sons, 2001.

78.L. Tsang and J. A. Kong, *Scattering of Electromagnetic Waves*, *Vol. III: Advanced Topics*, New York, John Wiley & Sons, 2001.

79.G. Macelloni, G. Nesti, P. Pampaloni, S. Sigismondi, D. Tarchi, and S. Lolli, "Experimental Validation of Surface Scattering and Emission Models," *IEEE Transactions on Geoscience and Remote Sensing*, **GRS-38**, 1, January 2000, pp. 459-469.

80.Q. Li, L. Tsang, J. Shi, and C. H. Chan, "Application of Physics-Based Two-Grid Method and Sparse Matrix Canonical Grid Method for Numerical Simulations of Emissivities of

Soils With Rough Surfaces at Microwave Frequencies," *IEEE Transactions on Geoscience and Remote Sensing*, **GRS-38**, 4, July 2000, pp. 1635-1643.

81. K. Sarabandi, Y. Oh, and F. T. Ulaby, "Measurement and Calibration of Differential Mueller Matrix of Distributed Targets," *IEEE Transactions on Antennas and Propagation*, **AP-40**, 12, December 1992, pp. 1524-1532.

82. Y. Oh, K. Sarabandi, and F. T. Ulaby, "An Empirical Model and an Inversion Technique for Radar Scattering from Bare Soil Surfaces," *IEEE Transactions on Geoscience and Remote Sensing*, **GRS-30**, 2, March 1992, pp. 370-381.

83. P. C. Dubois, J. van Zyl, and T. Engman, "Measuring Soil Moisture with Imaging Radars," *IEEE Transactions on Geoscience and Remote Sensing*, **GRS-33**, 4, July 1995, pp. 915-926.

84. Y. Kim and J.J. van Zyl, "On the Relationship Between Polarimetric Parameters and Soil Moisture," *Proceedings of the IEEE 2002 International Geoscience and Remote Sensing Symposium (IGARSS 2002)*, Toronto, June 2002.

85. A. J. Wickel and T. J. Jackson, "Multitemporal Monitoring of Soil Moisture with RADARSAT SAR during the 1997 Southern Great Plains Hydrology Experiment," *International Journal of Remote Sensing*, **22**, 8, 2001, pp. 1571-1583.

86. http://hydrolab.arsusda.gov/sgp97/gsm.html

87. G. Macelloni, S. Paloscia, P. Pampaloni, S. Sigismondi, P. De Matthaeis, P. Ferrazzoli, G. Schiavon and D. Solimini, "The SIR-C/X-SAR Experiment on Montespertoli Supersite: The Sensitivity to Hydrological Parameters," *International Journal of Remote Sensing*, **13**, 1999, pp. 2597-2612.

88. R. Bindlish and A. P. Barros, "Multifrequency Soil Moisture Inversion from SAR Measurements with the Use of IEM," *Remote Sensing of Environment*, **71**, 1, January 2000, pp. 67-88.

89. G. Satalino, F. Mattia, M. W. J. Davidson, T. Le Toan, G. Pasquariello, and M. Borgeaud, "On Current Limits of Soil Moisture Retrieval from ERS-SAR Data," *IEEE Transactions on Geoscience and Remote Sensing*, **GRS-40**, 11, November 2002, pp. 2438-2447.

90. L. Jarlan, P. Mazzega, and E. Mougin, "Retrieval of Land Surface Parameters in the Sahel From ERS Wind Scatterometer Data: A "Brute Force" Method," *IEEE Transactions on Geoscience and Remote Sensing*, **GRS-40**, 9, September 2002, pp. 2056-2062.

91. H. Bach and W. Mauser, "Methods and Examples for Remote Sensing Data Assimilation in Land Surface Process Modeling," *IEEE Transactions on Geoscience and Remote Sensing*, **GRS-41**, 7, July 2003, pp. 1629-1637.

92. I. H. Woodhouse and D. H. Hoekman, "Determining Land-Surface Parameters from the ERS Wind Scatterometer," *IEEE Transactions on Geoscience and Remote Sensing*, **GRS-38**, 1, January 2000, pp. 126-140.

93. W. Wagner and K. Scipal, "Large-Scale Soil Moisture Mapping in Western Africa Using the ERS Scatterometer," *IEEE Transactions on Geoscience and Remote Sensing*, **GRS-38**, 4, July 2000, pp. 1777-1782.

94. T. C. Chiu and K. Sarabandi, "Electromagnetic Scattering from Short Branching Vegetation," *IEEE Transactions on Geoscience and Remote Sensing*, **GRS-38**, 2, March 2000, pp. 911-925.

95. P. Siqueira, K. Sarabandi, and F. T. Ulaby, "Numerical Simulation of Scatterer Positions in a Very Dense Medium with an Application to the Two-dimensional Born Approximation," *Radio Science*, **30**, 5, 1995, pp. 1325-1339.

96. R. West, L. Tsang, and D. P. Winebrenner "Dense Medium Radiative Transfer Theory for Two Scattering Layers with a Rayleigh Distribution of Particle Sizes," *IEEE Transactions on Geoscience and Remote Sensing*, **GRS-31**, 2, March 1993, pp. 426-437.

97. L. Tsang, L. and J. A. Kong, "Scattering of Electromagnetic Waves from a Dense Medium Consisting of Correlated Mie Scatterers with Size Distributions and Applications to Dry Snow," *Journal of Electromagnetic Waves and Applications*, **6**, 3, 1992, pp. 265-296.

98. A. N. Arslan, H. Wang, J. Pulliainen, and M. Hallikainen, "Effective Permittivity of Wet Sow Using Strong Fluctuation Theory," *Progress In Electromagnetic Research, PIERS 31*, 2001, pp. 273-290.

99. G. Macelloni, S. Paloscia, P. Pampaloni, and M. Tedesco, "Microwave Emission from Dry Snow: A Comparison of Experimental and Model Result," *IEEE Transactions on Geoscience and Remote Sensing*, **GRS-39**, 12, December 2001, pp. 2649-2656.

100. K. Sarabandi and P. Siqueira, "Numerical Scattering Analysis for Two Dimensional Dense Random Media: Characterization of Effective Permittivity," *IEEE Transactions on Antennas and Propagation*, **AP-45**, 5, May 1997.

101. P. Siqueira and K. Sarabandi, "T-Matrix Determination of Effective Permittivity for Three-dimensional Dense Random Media," *IEEE Transactions on Antennas and Propagation*, **AP-48**, 2, February 2000, pp. 317-327.

102. A. Nashashibi A. and K. Sarabandi, "Experimental Characterization of the Effective Propagation Constant of Dense Random Media," *IEEE Transactions on Antennas and Propagation*, **AP-47**, 9, September 1999, pp. 1454-1462.

103. F. T. Ulaby, P. R. Siqueira, A. Nashashibi, and K. Sarabandi, "Semi-Empirical Model for Radar Backscatter from Snow at 35 and 95 GHz," *IEEE Transactions on Geoscience and Remote Sensing*, **GRS-34**, 5, September 1996, pp. 1059-1065.

104. F. T. Ulaby, R. K. Moore and A. K. Fung, *Microwave Remote Sensing: Active and Passive*, *Vol. III: Surface Scattering and Emission Theory*, Norwood, MA, Artech House, 1986.

105. J. R. Kendra and K. Sarabandi, "A Hybrid Experimental/Theoretical Scattering Model for Dense Random Media," *IEEE Transactions on Geoscience and Remote Sensing*, **GRS-37**, 1, January 1999, pp. 21-35.

106. E. Schanda, C. Mätzler and K. Künzi, "Microwave Remote Sensing of Snow Cover," *International Journal of Remote Sensing*, **4**, 1983, pp. 149-158.

107. H. Rott, K. Strum, and H. Miller. "Active and Passive Microwave Signatures of Antarctic Firn by Means of Field Measurements and Satellite Data." *Annals of Glaciology*, **17**, 1993, pp. 337-342.

108. P. Pampaloni, G. Macelloni, S. Paloscia, M. Tedesco, R. Ranzi, M. Tomirotti, A. Cagnati, A. Crepaz, "The Microwave

Alpine Snow Melting Experiment (MASMEx 2002): A Contribution to the ENVISNOW Project," *Proceedings of the IEEE 2003 International Geoscience and Remote Sensing Symposium IGARSS 2003*, Toulouse, France, 2003.

109.L. Armstrong and M. J. Brodzik, "Recent Northern Hemisphere Snow Extent: a Comparison of Data Derived from Visible and Microwave Satellite Sensors," *Geophysical Research Letters*, **28**, 2001, pp. 3673-3676.

110.J. Pulliainen and M. Hallikainen, "Retrieval of Regional Snow Water Equivalent from Space/borne Passive Microwave observations," *Remote Sensing of Environment*, **75**, 2001, pp. 76-85.

111.S. Rosenfeld and N. C. Grody, "Metamorphic Signature of Snow Revealed in SSM/I Measurements," *IEEE Transactions on Geoscience and Remote Sensing*, **GRS-38**, 1, January 2000, pp. 53-63.

112.D. T. Davis, Z. Chen, L. Tsang, J. N. Hwang, and A. T. C. Chang, "Retrieval of Snow Parameters by Iterative Inversion of a Neural Network," *IEEE Transactions on Geoscience and Remote Sensing*, **GRS-31**, 4, July 1993, pp. 842-851.

113.M. Hallikainen, P. Jolma, "Comparison of Algorithms for Retrieval of Snow Water Equivalent from Nimbus-7 SMMR Data in Finland, " *IEEE Transactions on Geoscience and Remote Sensing*, **GRS-30**, 1, January 1992, pp. 124-131.

114.P. R. Singh and T. Y. Gan, "Retrieval of Snow Water Equivalent Using Passive Microwave Brightness Temperature Data," *Remote Sensing of Environment*, **74**, 2, November 2000, pp. 275-286.

115.J. T. Pulliainen, J. Grandell, and M. Hallikainen, "HUT Snow Emission Model and its Applicability to Snow Water Equivalent Retrieval," *IEEE Transactions on Geoscience and Remote Sensing*, **GRS-37**, 3, May 1999, pp. 1378-1390.

116.J. L. Foster, A. T. C. Chang, and D. K. Hall, "Comparison of Snow Mass Estimates from a Prototype Passive Microwave Snow Algorithm, a Revised Algorithm and Snow Depth Climatology," *Remote Sensing of Environment*, **62**, 1997, pp. 132-142.

117.R. E. Kelly, A. T. Chang, L. Tsang and J. L. Foster, "A Prototype AMSR-E Global Snow Area and Snow Depth Algorithm," *IEEE Transactions on Geoscience and Remote Sensing*, **GRS-41**, 2, February 2003, pp. 230-242.

118.J. Guo, L. Tsang, E. G. Josberger, A. W. Wood, J. N. Hwang, and D. P. Lettenmaier, "Mapping the Spatial Distribution and Time Evolution of Snow Water Equivalent With Passive Microwave Measurements," *IEEE Transactions on Geoscience and Remote Sensing*, **GRS-41**, 3, March 2003, pp. 612-621.

119.L. L. Wilson, L. Tsang, J.-N. Hwang, and C.-T. Chen, "Mapping Snow Water Equivalent by Combining a Spatially Distributed Snow Hydrology Model with Passive Microwave Remote-Sensing Data," *IEEE Transactions on Geoscience and Remote Sensing*, **GRS-37**, 2, March 1999, pp. 690-704.

120.C. T. Chen, B. Nijssen, J. Guo, L. Tsang, A. W. Wood, J.-N. Hwang, and D. P. Lettenmaier, "Passive Microwave Remote Sensing of Snow Constrained by Hydrological Simulations," *IEEE Transactions on Geoscience and Remote Sensing*, **GRS-39**, 8, August 2001, pp. 1744-1756.

121.W. H. Stiles and F. T. Ulaby, "The Active and Passive Microwave Response to Snow Parameters 1. & 2. Wetness," *Journal Geophysical Research*, **85**, C2, 1980.

122.C. Maetzler, E. Schanda, and W. Good, "Towards the Definition of Optimum Sensor Specifications for Microwave Remote Sensing of Snow," *IEEE Transactions on Geoscience and Remote Sensing*, **GRS-20**, 1, January 1982, pp. 57-66.

123.A. T. C. Chang, J. L. Foster, M. Owe, and D. K. Hall, "Passive and Active Microwave Studies of Wet Snowpack Properties," *Nordic Hydrology*, **16**, 1985, pp. 57-66.

124.J. R. Kendra, K. Sarabandi, and F. T. Ulaby, "Radar Measurements of Snow: Experiment and Analysis," *IEEE Transactions on Geoscience and Remote Sensing*, **GRS-36**, 3, May 1998, pp. 864-879.

125.M. Hallikainen, F. T. Ulaby, and M. Abdelrazik, "Dielectric Properties of Snow in the 3 to 37 GHz Range," *IEEE Transactions on Antennas and Propagation*, **AP-34**, 1986, pp. 1329-1339.

126.M. E. Tiuri, A. H. Sihvola, E. G. Nyfors, and M. T. Hallikainen, "The Complex Dielectric Constant of Snow at Microwave Frequencies," *IEEE Journal of Oceanic Engineering*, **9**, 1984, pp. 377-382.

127.J. R. Kendra, F. T. Ulaby, and K. Sarabandi, "Snow Probe for *in situ* Determination of Wetness and Density," *IEEE Transactions on Geoscience and Remote Sensing*, **GRS-32**, 6, November 1994, pp. 1152-1159.

128.T. H. Nagler, H. Rott, and G. Glendinning, "Snowmelt Runoff Modelling by Means of Radarsat and ERS SAR," *Canadian Journal of Remote Sensing*, **26**, 6, 2000, pp. 512-520.

129.T. Nagler and H. Rott, "Retrieval of Wet Snow by Means of Multitemporal SAR Data," *IEEE Transactions on Geoscience and Remote Sensing*, **GRS-38**, 2, March 2000, pp. 754-765.

130.M. Bernier, J-P. Fortin, Y. Gauthier, R. Gauthier, R. Roy, and P. Vincent, "Determination of Snow Water Equivalent Using Radarsat SAR data in Eastern Canada," *Hydrological Processes*, **13**, 18, 1999, pp. 3041-3051.

131.F. Papa, B. Legresy, N. M. Mognard, E. G. Josberger, and F. Remy, "Estimating Terrestrial Snow Depth With the Topex-Poseidon Altimeter and Radiometer," *IEEE Transactions on Geoscience and Remote Sensing*, **GRS-40**, 10, October 2002, pp. 2162-2169.

132.D. Floricioiu and H. Rott, "Seasonal and Short-Term Variability of Multifrequency, Polarimetric Radar Backscatter of Alpine Terrain from SIR-C/X-SAR and AIRSAR Data," *IEEE Transactions on Geoscience and Remote Sensing*, **GRS-39**, 12, December 2001, pp. 2634-2648.

133.J. Shi and J. Dozier, "Estimation of Snow Water Equivalence Using SIR-C/X-SAR, Part I: Inferring Snow Density and Subsurface," *IEEE Transactions on Geoscience and Remote Sensing*, **GRS-38**, 6, November 2000, pp. 2465-2474.

134.J. Shi and J. Dozier, "Estimation of Snow Water Equivalence Using SIR-C/X-SAR, Part II: Inferring Snow Depth and Particle Size," *IEEE Transactions on Geoscience and Remote Sensing*, **GRS-38**, 6, November 2000, pp. 2475-2488.

135.T. Guneriussen, K. A. Høgda, H. Johnsen, and I. Lauknes, " InSAR for Estimation of Changes in Snow Water Equivalent of Dry Snow," *IEEE Transactions on Geoscience and Remote Sensing*, **GRS-39**, 10, October 2001, pp. 2101-2108.

136.R. Goldstein, R. Engelhard, B. Kamb, and R. Frolich, "Satellite Radar Interferometry for Monitoring Ice Sheet Motion:

Application to an Antarctic Ice Stream," *Science*, **262**, December 1993, pp. 1525-1530.

137. J. J. Mohr, N. Reeh, and S. Madsen, "Three-Dimensional Glacial Flow and Surface Elevation Measured with Radar Interferometry," *Nature*, **391**, January 1998, pp. 273-276.

138. T. Strozzi, A. Luckman, T. Murray, U. Wegmüller and C. L. Werner, "Glacier Motion Estimation Using SAR Offset-Tracking Procedures," *IEEE Transactions on Geoscience and Remote Sensing*, **GRS-40**, 11, November 2002.

139. J.-P. Kärnä, J. Pulliainen, M. Huttunen and J. Koskinen, "Assimilation of SAR data to operational hydrological runoff and snow melt forecasting model," *Proceedings of the IEEE 2002 International Geoscience and Remote Sensing Symposium (IGARSS 2002)*, 2002.

140. S. V. Nghiem and W.-Y. Tsai, "Global Snow Cover Monitoring With Spaceborne Ku-band Scatterometer," *IEEE Transactions on Geoscience and Remote Sensing*, **GRS-39**, 10, October 2001, pp. 2118-2134.

141. P. Ferrazzoli and L. Guerriero, "Passive Microwave Remote Sensing of Forests: A Model Investigation," *IEEE Transactions on Geoscience and Remote Sensing*, **GRS-34**, 2, March 1996, pp. 433-443.

142. M. A. Karam, "A Physical Model for Microwave Radiometry of Vegetation," *IEEE Transactions on Geoscience and Remote Sensing* **GRS-35**, 4, 1997, pp. 1045-1058.

143. M. T. Hallikainen, P. A. Jolma, and J. M. Hyyppa, "Satellite Microwave Radiometry of Forest and Surface Types in Finland," *IEEE Transactions on Geoscience and Remote Sensing*, **GRS-26**, 5, September 1988, pp. 622-628.

144. L. Kurvonen, J. Pulliainen, and M. Hallikainen, "Monitoring of Boreal Forests with Multitemporal Special Sensor Microwave Imager," *Radio Science*, **33**, 1998, pp. 731-744.

145. N. Kruopis, J. Praks, A. N. Arslan, H. M. Alasalmi, J. Koskinen, and M. T. Hallikainen, "Passive Microwave Measurements of Snow-Covered Forest Areas in EMAC'95," *IEEE Transactions on Geoscience and Remote Sensing*, **GRS-37**, 6, November 1999, pp. 2699-2705.

146. R. H. Lang, P. de Matthaeis, D. M. Le Vine, S. Bidwell, M. Haken, and N. Chauhan, "L-Band Radiometer Measurements of Conifer Forests," *Proceedings of the IEEE 2000 International Geoscience and Remote Sensing Symposium (IGARSS 2000)*, Honolulu, Hawaii, July 2000, pp. 1930-1932.

147. G. Macelloni, S. Paloscia, P. Pampaloni, and R. Ruisi, "Airborne Multi-Frequency L- to Ka - Band Radiometric Measurements over Forests," *IEEE Transactions on Geoscience and Remote Sensing*, **GRS-39**, 11, November 2001, pp. 2507-2513.

148. P. Ferrazzoli, L. Guerriero, J. P. Wigneron, "Simulating L-band Emission of Forests in View of Future Satellite Applications," *IEEE Transactions on Geoscience and Remote Sensing*, **GRS-40**, 12, December 2002, pp. 2700-2708.

149. S. J. Durden, J. J. van Zyle, and H. A. Zebker, "Modeling and Observation of the Radar Polarization Signature of Forested Areas," *IEEE Transactions on Geoscience and Remote Sensing*, **GRS-27**, 3, May 1989, pp. 290-301.

150. M. C. Dobson, F. T. Ulaby, T. Le Toan, A. Beaudoin, and E. S. Kasischke, "Dependence of Radar Backscatter on Conifer Forest Biomass," *IEEE Transactions on Geoscience and Remote Sensing*, **GRS-30**, 2, March 1992, pp. 402-415.

151. M. L. Imhoff, "A Theoretical Analysis of the Effect of Forest Structure on SAR Backscatter and the Remote Sensing of Biomass", *IEEE Transactions on Geoscience and Remote Sensing*, **GRS-33**, 2, 1995, pp. 341-352.

152. M. C. Dobson, F. T. Ulaby, L. E. Pirece, T. L. Sharik, K. M. Bergen, J. Kellndorfer, J. R. Kendra, E. Li, Y. C. Lin, A. Nashashibi, K. Sarabandi, and P. Siqueira, "Estimation of Forest Biomass," *IEEE Transactions on Geoscience and Remote Sensing*, **GRS-33**, 4, July 1995, pp. 887-895.

153. S. S. Saatchi and M. Moghaddam, "Estimation of Crown and Stem Water Content and Biomass of Boreal Forest Using Polarimetric SAR Imagery," *IEEE Transactions on Geoscience and Remote Sensing*, **GRS-38**, 2000, pp. 697-708.

154. S. Quegan, T. Le Toan, J. J. Yu, F. Ribbes, and N. Floury, "Multitemporal ERS SAR Analysis Applied to Forest Mapping," *IEEE Transactions on Geoscience and Remote Sensing*, **GRS-38**, 2, March 2000, pp. 741-753.

155. J. T. Pulliainen, L. Kurvonen, and M. T. Hallikainen, "Multitemporal Behavior of L- and C-Band SAR Observations of Boreal Forests," *IEEE Transactions on Geoscience and Remote Sensing*, **GRS-37**, 2, March 1999, pp. 927-937.

156. H. J. Hyyppä and J. M. Hyyppä, "Effects of Stand Size on the Accuracy of Remote Sensing-Based Forest Inventory," *IEEE Transactions on Geoscience and Remote Sensing*, **GRS-39**, 12, December 2001, pp. 2613-2621.

157. T. Le Toan, A. Beaudoin, J. Riom, and D. Guyon, "Relating Forest Biomass to SAR Data," *IEEE Transactions on Geoscience and Remote Sensing*, **GRS-30**, March 1992, pp. 403-411.

158. M. C. Dobson, F. T. Ulaby, T. Le Toan, A. Beaudoin, E. Kasischke, and N. L. Christensen, "Dependence of radar backscatter on coniferous biomass," *IEEE Transactions on Geoscience and Remote Sensing*, **GRS-30**, 2, March 1992, pp. 412-415.

159. A. Beaudoin, T. Le Toan, S. Goze, E. Nezry, A. Lopes, E. Mougin, C. C. Hsu, H. C. Han, J. A. Kong, and R. T. Shin, "Retrieval of Forest Biomass from SAR Data," *International Journal of Remote Sensing*, **15**, March 1994, pp. 2777-2796.

160. P. Melon, J. M. Martinez, T. Le Toan, L. M. H. Ulander, and A. Beaudoin, "On the Retrieving of Forest Stem Volume From VHF SAR Data: Observation and Modeling," *IEEE Transactions on Geoscience and Remote Sensing*, **GRS-39**, 11, November 2001, pp. 2364-2372.

161. A. T. Manninen and L. M. H. Ulander, "Forestry Parameter Retrieval From Texture in CARABAS VHF-Band SAR Images," *IEEE Transactions on Geoscience and Remote Sensing*, **GRS-39**, 12, December 2001, pp. 2622-2633.

162. J. E. S. Fransson, F. Walter, K. Blennow, A. Gustavsson, and L. M. H. Ulander, "Detection of Storm-Damaged Forested Areas Using Airborne CARABAS-II VHF SAR Image Data," *IEEE Transactions on Geoscience and Remote Sensing*, **GRS-40**, 10, October 2002, 2170-2175.

163. F. T. Ulaby and M. A. El-Rayes, "Microwave Dielectric Spectrum of Vegetation, Part II: Dual-Dispersion Model," *IEEE Transactions on Geoscience and Remote Sensing*, **GRS-25**, 5, September 1987, pp. 550-557.

164.K. Sarabandi, “A Technique for Dielectric Measurement of Cylindrical Objects in a Rectangular Waveguide,” *IEEE Transactions on Instrumentation Measurements*, **43**, 6, December 1994, pp. 793-798.

165.A. Franchois, Y. Piñeiro and R. H. Lang Microwave Permittivity Measurements of Two Conifers *IEEE Transactions on Geoscience and Remote Sensing* **GRS- 36**, 5, 1998, pp. 1384-1394.

166.F. T. Ulaby, K. Sarabandi, K. MacDonald, M. Whitt, and M. C. Dobson, “Michigan Microwave Canopy Scattering Model,” *International Journal of Remote Sensing*, **11**, 7, 1990, pp. 1223-1253.

167.M. A. Karam and A. K. Fung, “Electromagnetic Scattering from a Layer of Finite Length, Randomly Oriented, Dielectric Circular Cylinders over a Rough Interface with Application to Vegetation,” *International Journal of Remote Sensing*, **9**, 1988, pp. 1109-1134.

168.R. H. Lang and J. S. Sidhu, “Electromagnetic Backscattering from a Layer of Vegetation: a Discrete Approach,” *IEEE Transactions on Geoscience and Remote Sensing*, **GRS-21**, 1, January 1983, pp. 62-71.

169.Y. C. Lin and K. Sarabandi, “A Monte Carlo Coherent Scattering Model For Forest Canopies Using Fractal-Generated Trees,” *IEEE Transactions on Geoscience and Remote Sensing*, **GRS-37**, 1, January 1999, pp. 440-451.

170.R. Schiffer and K. O. Thielheim, “Light Scattering by Dielectric Needles and Disks,’“ *Journal of Applied Physics*, **50**, 4, April 1979.

171.K. Sarabandi and T. B. A. Senior, “Low-frequency Scattering from Cylindrical Structures at Oblique Incidence,” *IEEE Transactions on Geoscience and Remote Sensing*, **GRS-28**, 5, September 1990, pp. 879-885.

172.S. S. Seker and A. Schneider, “Electromagnetic Scattering from a Dielectric Cylinder of Finite Length,” *IEEE Transactions on Antennas and Propagation*, **AP-36**, 2, February 1988, pp. 303-307.

173.K. Sarabandi, T. B. A. Senior, and F. T. Ulaby, “Effect of Curvature on the Backscattering from a Leaf,” *Journal of Electromagnetic Waves and Applications*, **2**, 1988, pp. 653-670.

174.T. B. A. Senior, K. Sarabandi, and F.T. Ulaby, “Measuring and Modeling the Backscattering Cross Section of a Leaf,” *Radio Science*, **22**, 1987, pp. 1109-1116.

175.Y. C. Lin, and K. Sarabandi, “Electromagnetic Scattering Model for a Tree Trunk above a Ground Plane,” *IEEE Transactions on Geoscience and Remote Sensing*, **GRS-33**, 4, July 1995, pp. 1063-1070.

176.E. Rodriguez and J. M. Martin, “Theory and Design of Interferometric Synthetic Aperture Radars,” *Proceedings of the IEEE*, **F139**, 2, 1992, pp. 147-159.

177.J. O. Hagberg, L. M. H. Ulander, and J. Askne, “Repeat-pass SAR Interferometry over forested terrain,” *IEEE Transactions on Geoscience and Remote Sensing*, **GRS-33**, 2, March 1995, pp. 331-340.

178.U. Wegmueller and C. L. Werner, “SAR Interferometry Signature of Forest,” *IEEE Transactions on Geoscience and Remote Sensing*, **GRS-33**, 5, September 1995, pp. 1153-1161.

179.T. Strozzi, P. B. G. Dammert, U. Wegmüller, J.-M. Martinez, J. I. H. Askne, A. Beaudoin, and M. T. Hallikainen, “Land Use Mapping with ERS SAR Interferometry,” *IEEE Transactions on Geoscience and Remote Sensing*, **GRS-38**, 2, March 2000, pp. 766 -775.

180.N. P. Faller and E. H. Meier, “First Results with the Airborne Single-Pass DO-SAR Interferometer,” *IEEE Transactions on Geoscience and Remote Sensing*, **GRS-33**, 5, September 1995, pp. 1230-1237.

181.K. Sarabandi, “D*K*-Radar Equivalent of Interferometric SARs: A Theoretical Study for Determination of Vegetation Height,” *IEEE Transactions on Geoscience and Remote Sensing*, **GRS-35**, 5, September 1997, pp. 1267-1276.

182.R. N. Treuhaft, S. N. Madsen, M. Moghaddam, and J. J. van Zyl, “Vegetation Characteristics and Underlying Topography from Interferometric Radar,” *Radio Science*, **31**, 6, 1996, pp. 1449-1485.

183.K. Sarabandi and Y. C. Lin, “Simulation of Interferometric SAR Response for Characterization of Scattering Phase Center Statistics of Forest Canopies,” *IEEE Transactions on Geoscience and Remote Sensing*, **GRS-38**, 1, January 2000, pp. 115-125.

184.H. A. Zebker, S. N. Madsen, J. Martin, K. B. Wheeler, T. Miller, Y. Lou, G. Alberti, S. Vetrella, and A. Cucci, “The TOPSAR Interferometric Radar Topographic Mapping Instrument,” *IEEE Transactions on Geoscience and Remote Sensing*, **GRS-30**, 5, September 1992, pp. 933-940.

185.S. R. Cloude and K.P. Pathanassiou, “Polarimetric SAR interferometry,” *IEEE Transactions on Geoscience and Remote Sensing*, **GRS-34**, 2, March 1996, pp. 498-518.

186.R. Cloude, K. P. Papathanassiou, I. Woodhouse, J. Hope, J. C. Suarez Minguez, P. Osborne, and G. Wright, “The Glen-Affric Project: Forest Mapping using Polarimetric Radar Interferometry,” *Proceedings of the IEEE 2001 International Geoscience and Remote Sensing Symposium (IGARSS 2001)*, Sydney, Australia, 9-13, July, 2001.

187.R. Treuhaft, M. Moghaddam, J. van Zyl, and K. Sarabandi, “Estimating Vegetation and Surface Topographic Parameters from Multibaseline Radar Interferometry,” *Proceedings of the IEEE 1996 International Geoscience and Remote Sensing Symposium (IGARSS 1996)*, Lincoln, Nebraska, May 1996.

188.A. Reigber and A. Moreira, “First Demonstration of Airborne SAR Tomography Using Multibaseline L-Band Data,” *IEEE Transactions on Geoscience and Remote Sensing*, **GRS-38**, 5, September 2000, pp. 2142-2152.

189.V. Dimri, *Deconvolution and Inverse Theory: Application to Geophysical Problems*, New York, Elsevier, 1992.

190.M. K. Sen, *Global Optimization Methods in Geophysical Inversion*, New York, Elsevier, 1995.

191.E. P. W. Attema and F. T. Ulaby, “Vegetation Modeled as a Water Cloud,” *Radio Science*, **13**, 1978, pp. 357-364.

192.S. Quegan, T. Le Toan, J. J. Yu, F. Ribbes and N. Floury “Multitemporal ERS SAR Analysis Applied to Forest Mapping,” *IEEE Transactions on Geoscience and Remote Sensing*, **GRS-38**, 2, March 2000, pp. 741-753.

193.L. Pierce, K. Sarabandi, and F. Ulaby, “Application of an Artificial Neural Network in Canopy scattering inversion,” *International Journal of Remote Sensing*, **15**, 1994, pp. 3263-3270.

194. Y. C. Lin and K. Sarabandi, "Retrieval of Forest Parameters Using a Fractal-based Coherent Scattering Model and a Genetic Algorithm," *IEEE Transactions on Geoscience and Remote Sensing*, **GRS-37**, 3, May 1999, pp. 1415-1424.

195. H. Skriver, M. T. Svendsen, and A. G Thomsen, "Multitemporal C- and L-Band Polarimetric Signatures of Crops," *IEEE Transactions on Geoscience and Remote Sensing*, **GRS-37**, 5, September 1999, pp. 2413.

196. P. Saich and M. Borgeaud, "Interpreting ERS SAR Signatures of Agricultural Crops in Flevoland, 1993-1996," *IEEE Transactions on Geoscience and Remote Sensing*, **GRS-38**, 2, 2000, pp. 651-657.

197. G. Macelloni, S. Paloscia, P. Pampaloni, and S. Sigismondi, "The Potential of *C*-and *L*-Band SAR in Estimating Vegetation Biomass: The ERS-1 And JERS-1 Experiments," *IEEE Transactions on Geoscience and Remote Sensing*, **GRS-37**, 4, July 1999, pp. 2107-2110G.

198. Macelloni, S. Paloscia, P. Pampaloni, F. Marliani, and M. Gai, "The Relationship between the Backscattering Coefficient and the Biomass of Narrow and Broad Laf Crops," *IEEE Transactions on Geoscience and Remote Sensing*, **GRS-39**, 4, April 2001, pp. 873-884.

199. S. H. Yueh, J. A. Kong, J. K. Jao, R. T. Shin, and T. L. Toan, "Branching Model for Vegetation," *IEEE Transactions on Geoscience and Remote Sensing*, **GRS-30**, 2, March 1992, pp. 390-402.

200. J. M. Stiles and K. Sarabandi, "A Scattering Model for Thin Dielectric Cylinders of Arbitrary Cross-Section and Electrical Length," *IEEE Transactions on Antennas and Propagation*, **AP-44**, 2, February 1996, pp. 260-266.

201. J. M. Stiles, K. Sarabandi, and F.T. Ulaby, "Electromagnetic Scattering from Grassland: Part II, Measurement and Modeling Results," *IEEE Transactions on Geoscience and Remote Sensing*, **GRS-38**, 1, January 2000, pp. 349-356.

202. J. M. Stiles and K. Sarabandi, "Electromagnetic Scattering from Grassland: Part I, A Fully Coherent Scattering Model," *IEEE Transactions on Geoscience and Remote Sensing*, **GRS-38**, 1, January 2000, pp. 339-348.

203. F. Marliani, S. Paloscia, P. Pampaloni and J. A. Kong, "Simulating coherent backscattering from crops during the growing cycle," *IEEE Transactions on Geoscience and Remote Sensing*, **GRS-40**, 1, January 2002, pp. 162-177.

204. Y. Oh, Y. Jang, and K. Sarabandi, "Full-Wave Analysis of Microwave Scattering from Short Vegetation: An Investigation on the Effect of Multiple Scattering," *IEEE Transactions on Geoscience and Remote Sensing*, **GRS-40**, 11, November 2002, pp. 2522-2526.

205. T. C. Chiu and K. Sarabandi, "Electromagnetic Scattering from Short Branching Vegetation," *IEEE Transactions on Geoscience and Remote Sensing*, **GRS-38**, 2, March 2000, pp. 911-925.

206. M. Guérif and C. Duke, "Calibration of the SUCROS Emergence and Early Growth Module for Sugar Beet Using Optical Remote Sensing Data Assimilation," *European Journal of Agronomy*, **9**, 1998, pp. 127-136.

207. L. Prévot, F. Baret, and A. Chanzy, "Assimilation of Multi-Sensor and Multi-Temporal Remote Sensing Data to Monitor Vegetation and Soil: The Alpilles-ReSeDA Project," *Proceedings of the International Geoscience and Remote Sensing Symposium IGARSS'98*, Seattle, WA, July 6-10, 1998.

IUCAF Annual Report for 2003

1. Introduction

The Scientific Committee on Frequency Allocations for Radio Astronomy and Space Science, IUCAF, was formed in 1960 by URSI, IAU, and COSPAR. Its brief is to study and coordinate the requirements of radio frequency allocations for passive radio sciences, such as radio astronomy, space research and remote sensing, in order to make these requirements known to the national and international bodies that allocate frequencies. IUCAF operates as a standing inter-disciplinary committee under the auspices of ICSU, the International Council for Science, which works under the umbrella of the United Nations organization UNESCO.

2. Membership

At the end of 2003 the composition of membership for IUCAF was:

URSI	Y. Gupta	India
	A. Tzioumis	Australia
	W. van Driel (Chair)	France
	G. Wannberg	Sweden
IAU	H. Chung	Korea
	R.J. Cohen	UK
	D.T. Emerson	USA
	M. Ohishi	Japan
	K.F. Tapping	Canada
COSPAR	S. Gulkis	USA
	J. Romney	USA

ex officio members:

W.A. Baan	(former Chair)	The Netherlands
K. Ruf	(former Chair)	Germany

In June 2003, the chairmanship of IUCAF changed from Darrel Emerson to Wim van Driel.

The IAU GA in 2003 marked the completion of term with IUCAF of the IAU member S. Ananthakrishnan (India), who was replaced by H. Chung (Korea) at this meeting.

IUCAF is expanding its groups of Correspondents, in order to improve its global geographic representation (notably in South America and Africa) and for issues on spectrum regulation concerning astronomical observations in the optical and infrared domains.

3. International Meetings

During the period of January to December 2003, its Members and Correspondents represented IUCAF in the following international meetings:

January:	ITU-R Task Group 1/8 (ultra-wide band) in Geneva, Switzerland
June-July:	World Radiocommunication Conference WRC-03 in Geneva, Switzerland
August:	IAU General Assembly in Sydney, Australia
	International Square Kilometer Array Conference in Geraldton, Australia
September:	Space Frequency Coordination Group SFCG-23 in San Diego, CA, USA
October:	ITU-R Working Party 7D (radio astronomy) in Geneva, Switzerland
	ITU-R Task Group 1/8 (ultra-wide band) in Geneva, Switzerland

Additionally, many IUCAF members and Correspondents participated in numerous national or regional meetings (including CORF, CRAF, RAFCAP, the FCC etc.), dealing with spectrum management issues.

3.1 IUCAF Business Meetings

During the year 2003 IUCAF had a face-to-face meeting as a committee before each of the ITU meetings of Working Parties and Task Groups of relevance to IUCAF, as well as before the World Radiocommunication Conference, with the purpose of discussing important issues on the agenda of the respective meetings in preparation for the public sessions. During these ITU sessions, typically lasting a week to 10 days, a number of ad-hoc meetings of IUCAF are held to discuss further the IUCAF strategy. During the 4 weeks' duration of the WRC-03, daily IUCAF meetings were organized for discussion and decision taking on ongoing developments. Other IUCAF business such as changes in the membership, action plans for future workshops and summer schools or initiatives, and future contributions to international spectrum meetings were also discussed at these meetings.

Although such face-to-face meetings at the ITU venues and elsewhere have been convenient and effective, throughout the year much IUCAF business is undertaken via e-mail communications between the members and correspondents.

An open IUCAF meeting was held at the IAU General Assembly in Sydney in August.

4. Contact with the sponsoring Unions and ICSU

IUCAF keeps regular contact with the secretariats of the supporting unions and with the ICSU secretariat. The Unions play a strong supporting role for IUCAF and the membership is greatly encouraged by their support.

IUCAF was strongly represented at the IAU General Assembly, held in Sydney, Australia, in June-July. An open IUCAF meeting was held during the assembly, and new IAU members were elected.

IUCAF members actively participated in national URSI meetings and in IAU Seminars and Symposia.

ICSU initiated its first ever review of IUCAF in November, within the framework of its Priority Area Assessment on Scientific Data and Information. In its written input document, IUCAF stressed its aim to fulfill its brief and to operate as a truly inter-disciplinary committee within ICSU, coordinating the efforts of all passive radio science Services in frequency management matters.

5. Affairs of the International Radiocommunication Union

5.1 The 2003 World Radio-communication Conference, WRC-03

The 2003 World Radiocommunication Conference, WRC-03, lasted for 4 weeks and was attended by over 2200 Delegates, the largest number ever, from 138 ITU Member States, who considered some 2500 proposals, and over 900 numbered documents relating to 50 Agenda items. Seventeen radio astronomers, including practically all IUCAF members, from a total of 12 countries, attended the Conference.

Out of a total of 50 agenda items, about a dozen were of interest to radio astronomy, most of which involved allocations to satellite downlinks adjacent or close to radio astronomy allocations. For such scenarios, WRC-03 adopted regulatory measures to protect radio astronomy and called for further studies to be completed before the next WRC-07, in 2007.

On the two agenda items that were of particular interest to IUCAF the following conclusions were reached:

Agenda item 1.8.2 on unwanted emissions: This was one of the most difficult issues of the Conference. For the radio astronomy bands, the main thrust is a new Resolution for Consultation for six radio astronomy/satellite band-pairs with clear guidelines on how to deal with the radio astronomy band protection issue during the design and construction (pre-launch) phase of a satellite and after its launch. It contains design criteria based on radio astronomy protection levels without having the burden of pre-launch verification of these limits. A second new Resolution calls for further studies on bands that showed potential problems during the discussions and some band-pairs that have not yet been studied. ITU-R Task Group 1/9 will complete the necessary studies before WRC-07.

Agenda item 1.16 on Mobile Satellite Service feeder links around 1.4 GHz: around the 1 400 – 1 427 MHz radio astronomy band containing the 21-cm HI line, new secondary allocations were made in the bands 1 390 - 1 392 MHz and 1 430 - 1 432 MHz for feeder links in the (Earth-to space) and (space-to-Earth) directions, respectively, for non-GSO MSS satellite networks with service links operating below 1 GHz. The compromise reached concerns secondary allocations, that cannot be used until WRC-07 has reviewed the issue of compatibility with, e.g. radio astronomical observations.

5.2 ITU-R Working Parties and Task Groups

The work in the various ITU-R Working Parties of interest to IUCAF is getting in gear after WRC-03, in preparation for WRC-07. As a rule, the meetings of WP7D, specializing in radio astronomy, are also attended by numerous representatives of other interests, which has unavoidably lead to compromises within this working party, to accommodate the interests of other groups. In an attempt to compensate for this development, IUCAF in principle sends representatives to other ITU working parties of interest to it, notably WP4A (Efficient orbit & spectrum utilization) and WP8D (Mobile satellites & radio determination satellites).

Of particular concern to IUCAF in WP7D is the opposition to proposed studies concerning the operational conditions of future giant radio astronomy instruments (such as ALMA and SKA), including studies on the creation of Radio Quiet Zones around their sites.

Task Group 1/8 deals with the introduction of unregistered low power ultra-wide bandwidth devices transmitting across large parts of the radio spectrum, into bands that are already allocated to a variety of other services. Preliminary studies show that the operation of such devices would be very harmful to the radio astronomy service.

6. Publications and Reports

IUCAF has contributed a number of documents to the proceedings of ITU-R Study Group 7, which are all available on the ITU-R web pages. IUCAF has a permanent web address, http://www.iucaf.org , where the latest updates on the organization's activities will become available. The editing of the Proceedings of IUCAF's first Summer School in Radio Astronomy was completed, and the volume will be printed by NRAO and made available on the IUCAF website.

7. Conclusion

IUCAF interests and activities range from preserving what has been achieved through regulatory measures or mitigation techniques, to looking very far into the future of high frequency use and giant radio telescope use. Current priorities, which will certainly keep us busy through the next years, include band-by-band studies for cases where allocations are made to satellite down-links close in frequency to the radio astronomy bands, the possible detrimental effects of ultra-wide band transmissions, and studies on the operational conditions that will allow the successful operation of future giant radio telescopes.

IUCAF is thankful for the moral and financial support that has been given for these continuing efforts by ICSU, URSI, the IAU, and COSPAR during the recent years. IUCAF also recognizes the support given by radio astronomy observatories, universities and national funding agencies to individual members in order to participate in the work of IUCAF.

Wim van Driel, IUCAF Chair
Meudon, France
February 3rd 2004
IUCAF website: http://www.iucaf.org
IUCAF contact: iucafchair@iucaf.org

Radio-Frequency Radiation Safety and Health

James C. Lin

Human Electroencephalograms (EEG) and Mobile-Phone Radiation

The neurological system is an essential integrator of biological functions in all living organisms – playing an essential role in the vital processes of highly developed animals and humans. The neurological system adapts and regulates the whole body in relation to changes in the external environment, to maintain homeostasis within physiological limits. A disturbance in the normal functioning of the neurological system could also result in changes in other body systems.

The neurological system is divided into the central nervous system (CNS), which includes the brain and spinal cord; the peripheral nervous system (PNS); and the autonomic nervous system (ANS), which includes nerve fibers that innervate smooth and heart muscles, and the glands of the body. Anatomically, the brain has three main parts. (1) The brain stem or medulla is responsible for the unconscious and involuntary control of important reflex functions, such as heartbeat and respiration; the medulla also relays nerve impulses to other parts of the brain. (2) The cerebellum is the center of coordination and balance. (3) The cerebrum is the center for sensation, consciousness, and all voluntary actions.

The CNS is in communication with all of the peripheral nervous system, and is the integrator and processor into which information concerning the ambient environment, the surface of the body, and the environment inside the body is constantly being fed from sensors and receptors located in all parts of the body. This information may be processed and stored in the memory, or it may be processed and acted upon by sending appropriate impulses out via the motor nerve fibers. A very large part of this constant activity takes place at levels below consciousness.

The neurological system is probably the most vulnerable of all the body systems to adverse assaults. It is the first system to go when the oxygen supply is discontinued. Moreover, the cerebral cortex is the part of the brain that is most vulnerable. Thus, many functions associated with the cerebral cortex are among the first to be impaired. This vulnerability of the nervous system and the cerebral cortex accounts for the observation that a very low level of intoxication may not show effects in other organs or bodily systems, but may show effects in the activity of the nervous system.

Although sleep may seem like a mundane event, it actually consists of several fascinating stages, characterized by brain waves or electroencephalo-graphic (EEG) changes that cycle throughout sleep [1]. There are two distinct states of EEG activities during sleep: the non-rapid eye movement (NREM) state, commonly known as slow-wave sleep; and a rapid eye movement (REM) state. These two states last about 90 minutes per cycle, which is repeated approximately five times per night, and each cycle includes four stages of NREM and REM sleep. The predominant EEG characteristics are classified into several approximate frequency bands: slow or delta waves, for frequencies less than 4 Hz; theta wave, for frequencies between 5-8 Hz; alpha waves, for 9-12 Hz; and beta waves, for lower amplitudes but higher frequencies (above 13 Hz). Alpha waves occur during the transition period between sleep and alertness, and beta waves occur when the brain is quite active in the REM stage. Delta and theta waves appear during the NREM stage.

The occurrence of beta waves during REM stages is thought to be associated with information processing in the brain, especially concerning memory functions and learning processes. Also, major depressions are known to be associated with increased REM stages of sleep. The presence of slow delta and theta waves in the EEG of awake adults is symptomatic of pathology. Neural pathology typically enhances slow-wave activity and attenuates fast waves (alpha and beta frequency bands). For example, a localized brain tumor would be expected to increase delta- and theta-wave activity, and to decrease alpha or beta waves.

The effects of exposure to radio-frequency radiation from cellular mobile telephones on human brain-wave potentials or electroencephalograms have been the subject

James C. Lin is with the University of Illinois at Chicago 851 South Morgan Street (M/C 154), Chicago, Illinois 60607-7053 USA; Tel: +1 (312) 413-1052 (direct); +1 (312) 996-3423 (main office); Fax: +1 (312) 996-6465; E-mail: lin@uic.edu

of several investigations. The topic is of interest because of the implications of induced changes in the functional state or the well-being of the brain. In these studies, EEG activities in awake subjects and during various stages of sleep were examined by polysomnography in human volunteers.

All-night polysomnographs of healthy male subjects were recorded, both with and without exposure to GSM signals (900 MHz; pulse repetition frequencies of 2, 8, and 217 Hz; pulse width of 577 microseconds; and 0.5 W/m2). A shortening of sleep-onset latency, which was interpreted as a hypnotic effect, and a REM suppressive effect with reduction of duration and percentage of REM sleep, were observed under the pulse-field-exposure conditions [2]. Moreover, spectral analysis revealed an increased spectral power density of the EEG signal during REM stages in the alpha-frequency band. However, since then, a series of reports from the same laboratory gave conflicting results on the influence of radio-frequency radiation from mobile telephones on human-sleep EEG patterns at power densities that ranged from 0.5 to 50 W/m^2. Specifically, subsequent studies that involved 20-24 subjects failed to confirm these findings, although there was a trend toward a REM-suppressive effect [3-5].

In another laboratory, healthy young subjects were exposed all night to mobile telephone fields with base-station-like GSM signals (900 MHz; 2, 8, 217 Hz and associated harmonics, and burs-related components at 1736 Hz and 50 kHz) at a spatial peak specific absorption rate (SAR) of 1 W/kg averaged over 10 g, in alternating intervals of a 15-minute-on-15-minute-off schedule, during sleep [6]. It was found that the spectral power of the EEG in NREM sleep was increased. The maximum rise occurred in the alpha frequency (10-11 Hz and 13.5-14 Hz) bands during the initial part of sleep. Moreover, compared to a control night with sham exposure, the amount of waking after a sleep onset was reduced from 18 to 12 minutes. The results suggested that pulse-modulated microwaves from mobile phones may promote sleep and modify the sleep EEG.

A similar change was observed in a subsequent study from this laboratory, where the same cellular-phone fields were applied for 30 minutes during the waking period preceding sleep [7]. The maximum rise in the spectral power of the EEG during NREM sleep occurred in essentially the same alpha (9.75-11.25 Hz and 12.5-13.25 Hz) frequency bands during the first stage of sleep. Since these changes corresponded to those obtained in a previous study where a GSM field was intermittently applied during sleep, the present results showed that exposure during waking modifies the EEG during subsequent sleep. These EEG studies involved a double-blind design, and the order of conditions was balanced.

A more recent report from this laboratory provided further evidence for the effect on sleep EEG from exposure to radio-frequency fields with GSM-phone-like modulations [8]. A group of 16 young male human subjects was exposed to 30 minutes of handset-like GSM signals at the common carrier frequency of 900 MHz, and an SAR of 1 W/kg. Note that while the modulation schemes for base-station and handset-type signals are the same, the spectral power contents of the frequency components are considerably higher in the handset-type signal. In addition, a continuous-wave (CW) exposure regime was used in this study, as well.

A sleep-onset latency of 13-15 minutes was found to be not significantly different under sham and exposed conditions. There was an increased spectral-power density in the alpha frequency band of the EEG signal prior to a sleep onset, compared to sham exposure, but the effect was not evident under CW exposure. Furthermore, the exposure with GSM modulation was seen to increase the spectral power in the 12.25-13.5 Hz range of the subject's NREM sleep EEG. This increase is characteristic of the so-called "sleep spindles," in which peaks of oscillatory EEG events become higher and higher, in the shape of spindles. A detailed examination of the time course revealed a pronounced difference between exposure to GSM- or CW-modulated fields.

Aside from the difference in the effect of GSM and CW modulations, this study showed a long-lasting effect on the EEG, in contrast to their two earlier studies. A possible, albeit untested, explanation is the difference in the pulse architecture between handset and base-station type signals. The spectral power at 2 and 8 Hz for the handset-type signal was higher. Also, while the average SAR of 1 W/kg was the same for both, the peak SAR for the handset-type signal was four times higher than for the base-station type.

In another laboratory, the EEG activity was recorded and analyzed in awake subjects (men and women, 28-57 years old), who were exposed to five different mobile telephones (analog and digital models), operating at a carrier frequency of 900 MHz or 1800 MHz for 20 minutes [9]. The recording was made for each subject under the closed-eyes situation during six 30-minute experiments, including one sham exposure. No change was observed during exposure in any frequency band, except for one of the telephones. In that case, a statistically significant change in the absolute power at the delta-frequency band of the EEG recording was seen. Since presence of delta brain waves (< 4 Hz) in the EEG of awake adults is symptomatic of neural pathology, this finding could be of potential concern. However, no difference occurred in the relative power of the delta-frequency band between sham and exposed periods. The authors concluded that "the observed difference in one parameter was probably caused by statistical chance."

It should be mentioned that in a similar study, EEG recordings were made during a 60-minute session: 15 minutes of background; 15 minutes of field-exposure or sham-exposure; 30 minutes after the exposure [10]. A significant increase of the global correlation dimension – an indicator of functional state changes in the brain – was noticed during the exposure and after the exposure period, under the eyes-closed condition. (The global correlation dimension is a single-value quantitative estimate of the complexity of brain state, which describes the ensemble characteristics of all recorded channels, independent of amplitude and frequency measures.)

It appears that conventional polysomnography techniques were applied in all the studies mentioned. In particular, a large number of small metallic electrodes are typically placed upon a subject's scalp, with electrically conducting paste or a glue-like substance to hold them in place. Low-voltage signals (< 500 microvolts) are amplified by the electronics in the EEG recording system. The resulting polygraphic display is then read by unaided visual inspection, followed by spectral analysis.

The use of metallic electrodes raises some questions concerning cellular-phone-radiation-induced interference and field concentration on and in the vicinity of metallic electrodes. These electrodes are known to perturb the radio-frequency field, and to produce electrophysiological recording artifacts [11, 12]. The observation that pulse modulation was critical for cellular-phone-radiation-induced enhancement of EEG power in specific frequency ranges during waking and sleep, and the fact that the peak SAR delivered by pulse modulations was four times higher than by CW modulations, seem to support such a speculation. However, since EEG recording was made post-cell-phone exposure in the reference [8] study, this potential deficiency in methodology may or may not be a factor in the interpretation of the reported results. Nevertheless, the potential for field concentration on and in the vicinity of metallic electrodes should be a cause for concern during exposure.

Indeed, the most recent publication from this group reported studies conducted to assess, and measures taken to minimize, potential electrode-related artifacts [13]. The variations in local SAR distributions, with and without the presence of electrodes, were of the order of 40%. They also reported measuring a 35% higher peak SAR (spatially averaged over 1 g of tissue) from currents induced on electrode wires

In summary, these results imply that radio-frequency radiation from mobile telephones could modify certain brain electrical activity under both awake and sleep conditions. However, the results were inconsistent. In particular, the results of the two series of studies from two different laboratories were most intriguing. A series of reports from one laboratory gave conflicting results on the influence of radio-frequency radiation from mobile telephones on human EEG activity. In contrast, results from another laboratory not only extended its earlier findings that radio-frequency radiation from mobile telephones can affect human EEG activity, but also suggested that pulse-modulated (but not CW-modulated) microwaves from mobile phones may promote sleep and modify human-brain electrical activity. While the investigators emphasized that the observed effects were "subtle," they indicated that the observation may provide "important new insights into the mechanism" of the influence. Furthermore, it was suggested that future studies should explore "its potential as a noninvasive method of influencing the brain for experimental, diagnostic, and therapeutic purposes."

References

1. A. Rechtschaffen and A. Kales, *A Manual of Standardized Terminology, Techniques and Scoring System for Sleep Stages of Human Subjects*, NIH Publication No. 204, Washington, DC, US Government Printing Office, 1968.
2. K. Mann and J. Roschke, "Effects of Pulsed High-Frequency Electromagnetic Fields on Human Sleep," *Neuropsychobiology*, **33**, 1996, pp. 41-47.
3. P. Wagner, J. Roschke, K. Mann, W. Hiller, and C. Frank, "Human Sleep Under the Influence of Pulsed Radiofrequency Electromagnetic Fields: A Polysomnographic Study using Standardized Conditions," *Bioelectromagnetics*, **19**, 1998, pp. 199-202.
4. K. Mann, P. Wagner, G. Brunn, F. Hassan, C. Hiemke, and J. Roschke, "Effects of Pulsed High-Frequency Electromagnetic Fields on the Neuroendocrine System," *Neuroendocrinology*, 67, 1998, pp. 139-144.
5. K. Mann, J. Fell, W. Hiller, C. Frank, M. Grozinger, P. Wagner, and J. Roschke, "Human Sleep EEG Under the Influence of Pulsed Radio Frequency Electromagnetic Fields. Results from Polysomnographies using Submaximal High Power Flux Densities," *Neuropsychobiology*, **42**, 2000, pp. 207-212
6. A. A. Borbely, R. Huber, T. Graf, B. Fuchs, E. Gallmann, and P. Achermann, "Pulsed High-Frequency Electromagnetic Field Affects Human Sleep and Sleep Electroencephalogram," *Neurosci Lett.*, **275**, 1999, pp. 207-210.
7. R. Huber, T. Graf, K. A. Cote, L. Wittmann, E. Gallmann, D. Matter, J. Schuderer, N. Kuster, A. A. Borbely, and P. Achermann, "Exposure to Pulsed High-Frequency Electromagnetic Field During Waking Affects Human Sleep EEG," *Neuroreport.*, **11**, 2000, pp. 3321-3325.
8. R. Huber, V. Treyer, A. A. Borbely, J. Schuderer, J. M. Gottselig, H. P. Landolt, E. Werth, T. Berthold, N. Kuster, A. Buck, and P. Achermann, "Electromagnetic Fields, Such as Those from Mobile Phones, Alter Regional Cerebral Blood Flow and Sleep and Waking EEG," *J. Sleep Res.*, **11**, 2002, pp. 289-295.
9. M. Hietanen, T. Kovala, and A. M. Hamalainen, "Human Brain Activity during Exposure to Radiofrequency Fields Emitted by Mobilephones," *Scandinavian Journal of Work, Environment & Health*, **26**, 2000, pp. 87-92.
10. N. N. Lebedeva, A. V. Sulimov, O. P. Sulimova, T. I. Kotrovskaya, and T. Gailus, 2000, "Cellular Phone Electromagnetic Field Effects on Bioelectric Activity of Human Brain," *Crit. Rev. Biomed. Eng.*, **28**, 2000, pp. 323-337.
11. C. C. Johnson and A. W. Guy, "Nonionizing Electromagnetic Wave Effects in Biological Materials and Systems," *Proceedings IEEE*, **60**, 1972, pp. 692-718.
12. V. V. Tyazhelov, R. E. Tigranian, and E. P. Khizhnian, "New Artifact Free Electrodes for Recording of Biological Potentials in Strong Electromagnetic Fields," *Radio Science*, **14** (Supp. 6), 1977, pp. 121-123.
13. R. Huber, J. Schuderer, T. Graf, K. Jutz, A. A. Borbely, N. Kuster, and P. Achermann, "Radio Frequency Electromagnetic Field Exposure in Humans: Estimation of SAR Distribution in the Brain, Effects on Sleep and Heart Rate," *Bioelectromagnetics*, **24**, 2003, pp. 262-276.

News from ITU-R

The current status of studies within the ITU-R Study Groups

The year 2003 saw three major events in the ITU-R cycle:

· Radiocommunication Assembly, RA-03
· World Radiocommunication Conference, WRC-03
· Conference Preparatory Meeting (first meeting), CPM06-1.

It is on the outcome of these events that the overall study programme within the ITU-R Study Groups has been based for the period leading up to the next Radiocommunication Assembly in 2007.

The Radiocommunication Assembly (RA-03) confirmed the existing seven Study Groups as follows:

- Study Group 1: Spectrum management
- Study Group 3: Radiowave propagation
- Study Group 4: Fixed-satellite service
- Study Group 6: Broadcasting services
- Study Group 7: Science services
- Study Group 8: Mobile, radiodetermination, amateur and related satellite services
- Study Group 9: Fixed service

and adopted a work programme "defined" in 362 formal Questions, (see Resolution ITU-R 5-4). In general, response to the Questions leads to new or revised ITU-R Recommendations, Handbooks or Reports. In many cases, the Questions relate to items associated with the agenda of WRC-07 (see below).

Amongst the many tasks of the World Radiocommunication Conference (WRC-03) was the preparation of the draft agenda for the following WRC in 2007. Most of the agenda items call for technical studies to be undertaken by ITU-R which, in turn, involve the ITU-R Study Groups. The organization of these preparatory studies for WRC-07 was the task of the first meeting of the Conference Preparatory Meeting, CPM06-1, which took place immediately after WRC-03 and for which the results are published in Administrative Circular CA/128. These indicate the Study Group(s) (or subordinate group(s) such as Working Parties, Task Groups) that are to be involved with preparing text for the draft CPM Report to WRC-07 containing the necessary technical information on which WRC-07 will base its decisions. The structure of the Report is as follows:

Chapter 1: Mobile, aeronautical mobile, radionavigation, and radiolocation services
Chapter 2: Space science services
Chapter 3: Fixed-satellite, mobile-satellite and broadcasting-satellite services below 3 GHz
Chapter 4: Fixed service including HAPS and fixed-satellite service above 3 GHz
Chapter 5: Services in LF, MF and HF bands and maritime mobile service
Chapter 6: Regulatory procedures and associated technical criteria applicable to satellite networks
Chapter 7: Future WRC programmes and other issues

Some example topics amongst the (approximately 25 technical) agenda items are:

- Agenda item 1.2: Allocations and regulatory issues related to the Earth exploration satellite service (EESS) (passive), space research service (SRS) (passive) and the meteorological satellite service; (the issues concern allocations to science services around 18 GHz and 10 GHz, and the use of the frequency band 36-37 GHz);
- Agenda item 1.4: Studies on frequency-related matters for the future development of IMT-2000 and systems beyond IMT-2000;
- Agenda item 1.13: Review of the allocations to all services in the HF bands between 4 and 10 MHz (with certain exceptions);
- Agenda item 1.19: Spectrum requirement for global broadband satellite systems;
- Agenda item 1.20: Protection of the EESS (passive) from unwanted emissions of active services;
- Agenda item 1.21: Compatibility between the radio astronomy service and the active space services.

It is of interest to note that a new ITU-R Task Group, (TG 1/9), has been established to address the studies concerning passive services required under agenda items 1.20 and 1.21.

An up-to-date calendar of meetings of the ITU-R Study Groups and their subordinate groups can be accessed at: http://www.itu.int/events/upcomingevents.asp?sector=ITU-R .

It is expected that the preparatory work for WRC-07 will be finalized in 2006 when the second meeting of the CPM will adopt its Report for transmission to WRC-07 the following year.

Meetings of the Working Parties of Study Group 7 (Science services), Geneva, October 2003

The four Working Parties (WP) of Study Group 7 comprise:

- WP 7A: Time signals and frequency standard emissions
- WP 7B: Space radio systems
- WP 7C: Earth-exploration satellite systems and meteo rological elements
- WP 7D: Radio astronomy

At these meetings, the first of the study period, the WPs planned the work programmes necessary for them to respond to those agenda items of WRC-07 concerning the science services. In addition, a draft new ITU-R Recommendation was prepared concerning inter-planetary and deep-space systems around 283 THz.

Of particular note was the simultaneous holding of two meetings comprising representatives of URSI's Scientific Committee for Telecommunications, (SCT), and participants of the Study Group 7 Working Parties. Study Group 7 (together with Study Group 3) has always been recognized as covering many areas of interest to URSI and it was in this light that the meetings attempted to identify specific topics in which URSI scientists could potentially contribute towards the development of ITU-R studies. Appropriate mechanisms for achieving such liaison in the future were also discussed. *(cf. A more detailed account of these meetings appeared in RSB, December 2003, no 307, pp. 61-62)*

Meetings of the Working Parties of Study Group 3 (Radiowave propagation) and "ClimDiff 2003", Fortaleza (Brazil), November 2003

The four Working Parties (WP) of Study Group 3 comprise:

- WP 3J: Propagation fundamentals
- WP 3K: Point-to-area propagation
- WP 3L: Ionospheric propagation
- WP 3M: Point-to-point and Earth-space propagation

Amongst the many topics addressed at these meetings were:

- scattering of signals from terrestrial links into spaceborne passive sensors (relevant to WRC-07 agenda item 1.21)
- differential attenuation on Earth-satellite and terrestrial paths
- propagation aspects of power line telecommunication systems
- propagation aspects of UWB systems
- point-to-area prediction methods with emphasis on the needs of the forthcoming ITU Regional Radiocommunication Conference for the planning of bands for digital broadcasting
- prediction methods for digital HF systems
- rain scatter model for point-to-point paths on the Earth's surface.

The Working Party meetings benefited from the URSI workshop "ClimDiff 2003" held immediately beforehand and at the same venue. "ClimDiff 2003" was the latest in a series of similar URSI workshops held over a period of 13 years - previously called "Climpara" - at which presentations were made in two topic areas highly relevant to on-going work in ITU-R Study Group 3, namely the use of climatic parameters in propagation prediction, and diffraction modelling including the effects of terrain and buildings. Many of the papers presented at ClimDiff described basic scientific work from which subsequent ITU-R studies could potentially develop, leading to new or revised propagation prediction techniques for spectrum management purposes. Such workshops represent an excellent example of exploiting the synergy of the URSI and ITU-R communities and is precisely the kind of event that URSI's SCT is attempting to promote. *[cf. Report of the ClimDiff Meeting appears on pp. 59-62 of this issue]*

Kevin A. Hughes
ITU Radiocommunication Bureau

Conferences

CONFERENCE REPORTS

2003 IEEE International Symposium on EMC

Istanbul, Turkey, 11-16 May 2003

Introduction

Hundreds of engineers and scientists in the discipline of Electromagnetic Compatibility (EMC) attended the 2003 IEEE International Symposium on EMC, Istanbul, which took place on May 11 to May 16, 2003, in the cosmopolitan city of Istanbul, Turkey. This is the very first time that this very important and prestigious Symposium was held in Region 8 of the IEEE, encompassing Europe, Africa and the Middle East, marking, more than anything else, the globalization of the IEEE EMC Society.

The Symposium was organized by the Israel IEEE EMC Chapter, technically co-sponsored by the IEEE EMC Society, and co-sponsored by the Israel IEEE Section, IEE and URSI, Commission E as well as other international organizations.

The slogan of the Symposium was: "Radiating Compatibility from the East" or "Ex-Oriente Radians" in Latin, alluding to the historical Byzantine period, where Istanbul (or Constantinople, in its historical name) was the center of the ancient world. Today, as in ancient times, Istanbul is simultaneously an important and thriving tourist attraction, as well as a modern business and industry metropolis. For the week of May 11, 2003, Istanbul was also the international center of the global EMC Community.

During this week, spanning from Sunday to Friday, an exciting top-notch technical program with something for everyone attending the Symposium took place, including technical sessions, workshops and tutorials, innovative special "meet the expert" sessions and "Birds of a Feather" forums, EMC Demonstrations and Computer Simulations, as well as a short EMC Course - and this is not all!

There was an international attendance of more than 330 participants from 41 countries representing all continents (with the exception of Antarctica).

The Symposium took place in the convention center of the Hilton Istanbul Hotel, a spacious, elegant and comfortable hotel, featuring 13 acres of beautiful gardens and exclusive sporting facilities. The Hilton Istanbul offered an impressive surrounding, ideally situated, overlooking the spectacular view of the Bosphorus, magically attractive amid the glittering lights of the City.

Technical Program and Activities

As a prologue, an EMCS Standards Open House was held on Sunday, May 11, 2003, with the guidance and leadership of Don Heirman, VP for Standards. Elya B. Joffe, the Symposium General Chairman, chaired the opening ceremony on the morning of Monday, May 12. In his welcome address, Elya gave a brief overview of the Symposium, and particularly - the evolution of this event. Elya then introduced the Guest of Honor - His Excellency, Mr. Ali Müfit Gürtuna - the Lord Mayor of Istanbul, a metropolis of 14 million citizens, who spared some of his very valuable time to present a welcome address of behalf of the host city.

Greetings were then offered by Don Heirman, VP for Standards of the IEEE EMC Society, and Past President of the IEEE EMC Society, on behalf of Dr. Todd Hubing, President of the IEEE EMC Society as well as by Professor Arie Braunstein, Chairman of the Israel IEEE Section.

The technical portion of the opening session included two presentations. First, there was an interesting presentation by Professor Marcello D'Amore, Editor of the IEEE Transactions on Electromagnetic Compatibility, who spoke on "IEEE Transactions on Electromagnetic Compatibility: An Overview."

The second presentation was a highlight of the opening ceremony. This was the keynote address given by Dr. Nigel Carter, from QinetiQ, UK, who spoke on "Past, Present and Future Challenges of Aircraft EMC." This presentation was an introduction to a series of activities planned in the Symposium, commemorating 100 years of manned powered aviation, from 1903 to 2003.

An Awards Ceremony concluded the Opening Session, where Certificates of "Appreciation, Recognition and Acknowledgement" were presented. Other awards were presented at the Wednesday Awards Banquet.

Considerable efforts were exerted in the formulation of the scientific/technical program of the Symposium. The Editorial Board (EB), under the skilled and devoted leadership of Dr. Anatoly Tsaliovich, composed of 52 international experts and professionals in the field of EMC, performed a peer review of the 579 technical papers received from almost 50 countries in order to ensure a high quality technical program.

Under the skilled leadership and dedication of Dr. Alex Axelrod, the Technical Program Committee did a great job in selecting the best papers and grouping them as best as possible into the appropriate sessions, and lined up a top-notch Technical Program; more than 380 papers were included in the Symposium technical program and presented in 34 regular sessions and 10 open forums (poster) sessions. No doubt - a record! Those sessions covered a broad range of areas in the field of electromagnetic compatibility; particularly noteworthy are six sessions on Measurement and Standards, five sessions on Human Exposure and EMF and five sessions on Numerical Modeling. However, besides the more traditional EMC topics, this symposium also featured some very special topics, not regularly covered at the IEEE EMC Symposia, including sessions on Wave Propagation, Radar Cross Section, Power Quality, and EMC in Power Equipment and Systems (and this is only a very partial list).

A session noteworthy of special attention was that organized by Mr. Peter Kerry, CISPR President, entitled: "EMC Standardization - Quo Vadis." This session, with speakers representing a variety of countries and continents, discussed the present and future of International EMC Standardization. Presentations covered EMC Standardization activities in Russia, Turkey, Israel and the relationship between academia and EMC Standardization.

The regular sessions were supplemented by a wide variety of 16 outstanding workshops and tutorials, covering a broad spectrum of topics such as "Lightning Phenomena and Lightning Protection Systems", presented by Professor Arie Braunstein from Israel, giving special insight into the concepts (and misconceptions) of external lightning protection, "Partial Element Equivalent Circuit (PEEC) Approach" by Professor G. Antonini, Italy, "The Latest Updates in EMC Emission Measurement Standardization" by Don Heirman, USA and many, many other excellent presentations.

Furthermore, special "Birds of a Feather" discussion forums took place, focused on examining innovative, controversial, or otherwise mind-provoking issues of interest to the EMC Community. These included "Personal Electronic Devices (PED) on Aircraft - Are they Really a Source of Concern," "The Precautionary Principle with regard to EMF," and "Grounding from Chips to Systems." These forums comprised a platform for discussion between experts and the audience, each of whom held very different opinions on these issues, often leading to a lively, even "heated" discussion. No agreement was probably reached on these very controversial topics, but those present definitely benefited from the different opinions presented in the discussions.

Russ Carstensen led a "Preparation for NARTE Exam" workshop from NARTE and an exam also took place during the Symposium, thus creating several new NCEs (NARTE Certified EMC Engineers).

For both the veterans desiring to "brush up" their EMC knowledge, and for the novices who wanted to learn more on the discipline of EMC, a "Selected Topics on EMC" course took place in four half-day sessions during the Symposium. The course, organized by Dr. Heyno Garbe from Germany, Chairman of the Symposium Education and Student Activities Committee, covered the following topics:

- Fundamentals of EMC through Interpreting the EMI Control Specifications for the EMC Designer, by Mr. Oren Hartal, Israel
- Complex EM Problems and Numerical Simulation Approaches, by Dr. Levent Sevgi, Turkey
- EMC Measurement Technology, by Dr. Heyno Garbe, Germany
- Fundamental Concepts of Signal Integrity and EMC Related to Printed Circuit Boards, by Mr. Mark Montrose, USA
- Principle of Path of Least Inductance in Circuit, Cable and Grounding Design, by Mr. Elya B. Joffe, Israel.

Participants who took part in at least three sessions of the four also received beautiful "Certificates of Completion." The technical program was supplemented by experiments and computer simulation demonstrations, which attracted much attention among the attendees of the Symposium. This provided the opportunity to observe, with their own eyes, the "facts of (EMC) life."

The Symposium Committee would like to thank the companies Rohde & Schwarz and R.D.T. (Israel) for providing the necessary test equipment in support of the experiments.

All of the above took place in six (yes - 6!) parallel sessions! As one of the participants said: "The technical program posed a special difficulty and a major dilemma - where to go first, and what to subsequently give up…?"

Exhibition

A technical exhibition took place alongside the Symposium, thus forming the link between the ivory tower of science and the reality of EMC technology.

Over 20 exhibitors from Europe, Asia and North America were on site to provide hands-on demonstrations and explanations of their products and services.

Radio Amateurs Activities

We were especially thankful to Mr. Aziz Sasa, TA1E, President of TRAC, the Turkish Radio Amateurs Society, who assisted us in erecting and operating a radio amateur's station during the Symposium. For the duration of the Symposium, the station received a special "EMC call sign" - TA1EMC. Two dedicated attendees of the Symposium, Dr. Rod Perala and Dr. Diethard Hansen, operated the station for many hours. We are told that special QSLs were made by TRAC.

Awards

During the Awards Banquet, the Best Symposium Paper award was presented to E.S. Siah, T. Ozdemir, J.L. Volakis, P.Y. Papalambros and R.W. Wiese, from the USA, for their paper (selected out of 16 papers nominated for the award) "Optimization for RF Coupling and Interference Reduction of Devices in Complex Systems." The winners of the Best Student Paper Award were also announced at the banquet. Maolin Wu and Xiang Cui from China received the award for their paper (selected out of 18 papers nominated for the award), "Wide Frequency Model for Transfer Function of Potential Transformer in Substation."

The Symposium Record was dedicated to the memory of Don Bush - a Dear Friend, who passed away in 2001.

Summary

We hope that this Symposium, in the cosmopolitan city of Istanbul, will form the bridge between people, making EMC the bridge of cooperation and exchange of technical information between people and professional societies and enhancing the quality of life for all people throughout the world through the constructive application of technology.

At the conclusion of this article, I would like to express my deep gratitude to all members of the Organizing Committee and the Symposium Secretariat for their efforts spent in making this Symposium materialize, and for the success we believe it was, particularly under the special circumstances in which it took place. Special thanks are due to Professor Dr. Selim Seker from Istanbul Turkey, whose dedicated, unconditional support of the Symposium from the very day of the decision to relocate the Symposium to Istanbul to the very last day were essential for coordination in Turkey, and making the local arrangements so much easier. Thank you, Selim! It was a pleasure to work with you on this Symposium!

The 2003 IEEE International Symposium on EMC in Istanbul will long be remembered for the high quality technical program, the beautiful venue, the hospitality and the wonderful social program.

Elya B. Joffe, Symposium General Chairman
Oren Hartal, URSI Liaison
Moshe Merzer, Signal Integrity (SI) Coordinator

ClimDiff 2003

Fortaleza, Ceara, Brazil, 17-19 November 2003

ClimDiff 2003, a meeting sponsored by URSI Commission F and by the **SCT (URSI's Scientific Committee on Telecommunications),** extended the Climpara (Climatic Parameters in Radiowave Propagation Prediction) meetings linking URSI with ITU-R previously held in Rio de Janeiro (1990), Moscow (1994), Oslo (1996), Ottawa (1998), and Budapest (2001). In addition to addressing the use of climatic parameters in the prediction of radiowave propagation characteristics as in the previous meetings (the Clim part), this time it also incorporated diffraction modeling and its applications (the Diff part). ClimDiff 2003 was held at the Caesar Park Hotel in Fortaleza, Ceará, Brazil, November 17-19, 2003, immediately preceding parallel meetings of ITU-R Working Parties 3J, 3K, 3L, and 3M.

ClimDiff 2003 was organized by URSI and ANATEL (Agência Nacional de Telecomunicações: the Brazilian Government Regulatory Agency for Telecommunications). It was also sponsored by ABERT (Associação Brasileira de Emissoras de Rádio e Televisão), ACERT (Associação Cearense de Emissoras de Rádio e Televisão), CAPES (Coordenação do Aperfeiçoamento de Pessoal de Nível Superior), CPqD (Centro de Pesquisa e Desenvolvimento), PUC/Rio (Pontifícia Universidade Católica do Rio de Janeiro), Sistema Verdes Mares, and Wings Telecom.

The Organizing Committee consisted of Prof. Marlene Pontes (CETUC-PUC/Rio, Chair), Eng. José Afonso Cosmo Jr. (ANATEL), and the staff of Infoview Ltd. The Scientific Program Committee consisted of Prof. Emanoel Costa (CETUC-PUC/Rio, Chair), Prof. Erasmus Miranda (UCP), and Dr. Terje Tjelta (Telenor, Norway).

Sixty scientists and engineers from 15 countries and four continents attended ClimDiff 2003. Eight of the participants were young scientists. A total of 35 contributed papers were accepted for oral presentation, distributed within six Clim and three Diff sessions.

Figure 1. The opening ceremony: (l-r) Marlene Pontes, Bertram Arbesser-Rastburg, José Paulo André Arruda, Counsellor José Leite Pereira Filho, José Pierre Barreto de Lima, Kevin Hughes, and José Afonso Cosmo Jr.

Counsellor José Leite Pereira Filho (ANATEL) chaired the opening session (Monday morning, November 17, 2003), in the presence of Mr. José Paulo André Arruda (representing the Governor of the State of Ceará), Mr. José Pierre Barreto de Lima (representing the Mayor of the City of Fortaleza), Mr. Kevin Hughes (Radiocommunication Bureau, ITU), Dr. Bertram Arbesser-Rastburg (representing the Chair of URSI Commission F), Prof. Marlene Pontes (CETUC-PUC/Rio), and Eng. José Afonso Cosmo Jr. (ANATEL) (Figure 1). In his welcoming speech, Counsellor José Leite described the role of ANATEL in the regulation and the development of telecommunications in Brazil, and its close relationships with ITU and URSI, as well as with the regional organizations CITEL and Mercosul.

The opening session was immediately followed by a General Presentation by Dr. David Cole (an invited speaker from IPS Radio & Space Services, Australia; Figure 2), Chair of ITU-R Study Group 3 (Radiowave Propagation). Dr. Cole stated the principal objectives of Study Group 3, describing its structure and Working Parties. Next, he briefly discussed the main topics to be studied in the immediate future by Study Group 3, in collaboration with several URSI Commissions and the SCT.

During the ice-breaker cocktail party in the evening of the same day, the participants enjoyed Brazilian music and the view of the sea and of the city of Fortaleza from the 20th floor of the Caesar Park Hotel. An extended city tour took place on Tuesday afternoon, both for participants and their companions.

Figure 2. Dr. David Cole at the podium during his invited talk.

The contents of the scientific sessions will be briefly described in the next paragraphs.

Session Diff.1, "Coupling of Terrain and Building Databases with Propagation Models for Path Loss Predictions," was convened by Carol Wilson (CSIRO ICT Centre, Australia). Sérgio Maffra and Marcelo Gattass presented an efficient beam-tracing algorithm for propagation predictions in 2.5-dimensional environments. Fernando Perez-Fontan et al. described a method to couple terrain and building database information for ray-tracing applications. Emanoel Costa presented results from a study of interference from Earth stations onboard vessels to receivers in the fixed service using a simulation method and considering diffraction effects.

Session Diff.2, "Statistical and Fundamental Modeling of Radiowave Propagation in Wireless Systems," was convened by Luiz da Silva Mello (CETUC-PUC/Rio, Brazil). M. O. Al-Nuaimi et al. described a statistical model of radiowave propagation in fixed wireless access systems in urban multipath environments. Fumio Ohkubo et al. presented results from a study of shadowing characteristics in a millimeter-wave ad hoc wireless access system. Fernando Perez-Fontán et al. described a Markov model for urban blockage effects in LMS systems. Mauro Assis and Andréa Souza established conditions for considering terrain as a smooth surface and obstacles to be isolated.

Session Diff.3, "Area-Coverage Modeling, Shadowed Point-to-Point Links and Results," was convened by Emanoel Costa (CETUC-PUC/Rio, Brazil). Alexandre Kholod and Stéphane Ménard described a coverage model for country-wide broadcasting networks. Markus Liniger et al. applied different diffraction models to mountainous terrain, and compared calculation results with corresponding measurements. Luiz da Silva Mello and Johnderson Carvalho compared the results from area-

Figure 3. Prof. Fernando Perez-Fontán describing a synthetic rain-rate model during Session Clim.3.

coverage prediction models with field measurements at UHF. Hajime Suzuki reported on diurnal signal fading characteristics of IEEE 802.11b outdoor fixed links.

Session Clim.1, "Measurements and Modeling of Clear-air Parameters and their Effects," was convened by Chris Gibbins (Rutherford Appleton Laboratory, United Kingdom). Bertram Arbesser-Rastburg et al. presented new reference standard atmospheres based on numerical weather products. Ana Benarroch described the use of profiles of meteorological parameters to estimate the attenuation by gases and clouds in slant paths (the authors, Angelica Liste and Jose Riera, were not able to attend the meeting). Bertram Arbesser-Rastburg outlined an experiment designed to study propagation effects on a satellite-to-satellite radio-occultation link for remote sensing of temperature and water vapor (the authors, M. Sterenborg and José Pedro Baptista, were not able to attend the meeting). Hervé Sizun et al. described new software developed to predict the quality of service of FSO links.

Session Clim.2, "Clear-Air Effects on Terrestrial Paths," was convened by David Cole (IPS Radio & Space Services, Australia). Andrew Kerans et al. compared measured data and simulations of microwave propagation within the tropical maritime evaporation duct. Lars Bråten et al. presented results from measurements of diurnal and seasonal variations of attenuation on a fixed radio link on the western coast of Norway. Luiz da Silva Mello and Pedro Castellanos used the results from measurements of simultaneous multipath fading in tandem links to develop a prediction model. and Laurent Castanet presented the results from the comparison of several fade-duration and fade-slope models with measurements (the author, Max van de Kamp, was not able to attend the meeting).

Session Clim.3, "Measurements and Modeling of Rain Parameters," was convened by Bertram Arbesser-Rastburg (ESA-ESTEC, the Netherlands). Fernando Perez-Fontán et al. reported on a synthetic rain-rate time-series generation model for radio system simulation (Figure 3). Seok-Hee Bae et al. described a method for converting one-minute rain rates from various integration-time data. Chris Gibbins and Chris Walden reported on extensive calculations that led to the development of a new model for the specific attenuation of rain. Nikolay Ruzhentsev and Olga Dorovskaya described particularities of temperature and frequency dependencies of hydrometeoric absorption in the millimeter-wave band.

Session Clim.4, "Modeling of Rain Attenuation and Scattering," was convened by David Rogers (Communications Research Centre, Canada). Chris Gibbins presented a new method for rain-scatter interference evaluation. Alexandre da Costa discussed some problems that can be found in validating ITU-R P.618-7 Earth-space rain-attenuation prediction methods for high rain rate in low-latitude areas. Gilson Alencar and Mauro Assis reported the results from tradeoff analyses of time percentage, rain rate, and elevation angle against estimated rain attenuation on Earth-space paths by an artificial neural network. Erasmus Miranda et al. described a simulation and prediction method for rain attenuation in LEO satellite links.

Session Clim.5, "Rain Effects on Ka-Band and Millimeter-Wave Paths," was convened by Gert Brussaard (Radicom, the Netherlands). Ana Benarroch et al. described the variations of slant-path depolarization parameters at 50 GHz with meteorological parameters. Mio Ishida et al.

Figure 4. A view of the meeting room and of the audience during an interval between sessions.

Figure 5. ClimDiff 2003 participants, displaying a variety of the T-shirts traditionally associated with these meetings.

presented results from a study of rain-fade duration distribution characteristics on millimeter-wave radio links. Naoto Takahashi et al. described radio-propagation characteristics due to rain in the 32 GHz band. Laurent Castanet and Frédéric Cornet presented a simulator of the dynamic behavior of the propagation channel for Ka-band satellite communication systems.

Session Clim.6, "Rain Effects on Ku-band Paths," was convened by Laurent Castanet (ONERA-CERT, France). Vaclav Kvicera and Milos Mazanek presented results from the propagation measurement of XPD, absorption, and multipath fading on a 59.3 km path at 13 GHz. Luiz da Silva Mello et al. described a prediction model for differential rain attenuation in converging links. S. K. Sarkar et al. reported on precipitation studies over India for estimation of the performance of communication systems. Laurent Castanet et al. described a methodology to be used in the generation of two-dimensional spatially correlated rain-rate fields with the Hycell model, and applications to propagation studies for telecommunication systems.

The registered participants received an abstract book (hardcopy) and a CD-ROM with the full version of all the accepted papers. The URSI Secretariat has been provided with copies of both, and will establish conditions for their distribution.

Many comments and questions followed each talk (Figure 4). We left Fortaleza with the perception that ClimDiff 2003 was a successful workshop, helpful in promoting scientific progress in the field of radiowave propagation most relevant to the interests of ITU-R SG3 with respect to the influences of climate and diffraction.

Emanoel Costa
epoc@cetuc.puc-rio.br

[Editorial note: Since the first such meeting in Rio in 1990, there has been a long tradition with URSI/Climpara/ITU-R meetings of having T-shirts produced to commemorate the event. In addition to the first one, they came from Climpara meetings in Adelaide (1993), Oslo (1996), Ottawa (1998), and Budapest (2001), as well as a few from other associated ITU-R meetings. Figure 2 shows that the tradition continued into ClimDiff 2003, and that "the spirit of Rio" is strongly alive and well. It was at the 1990 meeting that a new attitude encouraged generosity of exchange of information between groups within ITU-R and URSI. A T-shirt was also kindly sent from ClimDiff 2003 to Martin Hall, seen wearing it in Figure 3, even though he was not at the meeting: it has inked on it the names and kind messages from 39 of those present. These meetings are an example of what the SCT can promote.]

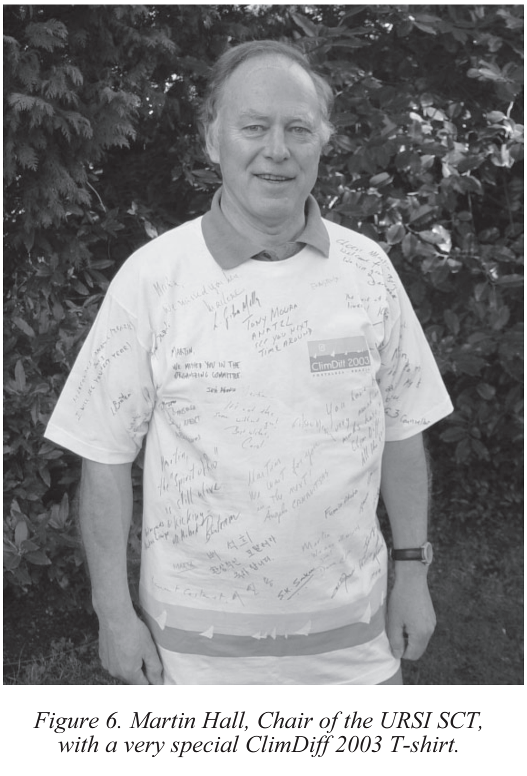

Figure 6. Martin Hall, Chair of the URSI SCT, with a very special ClimDiff 2003 T-shirt.

CONFERENCE ANNOUNCEMENT

URSI Commission F Open Symposium

Cairns, Great Barrier Reef, Australia, 1 - 4 June 2004

The URSI Commission F Triennium Open Symposium (URSI-F 2004) will be held in Cairns on the Great Barrier Reef of Australia, during 1-4 June 2004. See http://www.ursi-f2004.com

The Triennium Open Symposiums of URSI Commission F are established international conferences with a focus on the latest research in Radio Wave Propagation and Remote Sensing. URSI-F 2004 will build on the success of previous years in providing a premier forum for the scientific community to discuss the latest results and to identify developing trends. The conference programme will include a number of keynote presentations by leading researchers, intended to review recent progress in each field and define the current "state of the art". The programme will also include oral and poster papers published in the conference proceedings. The high degree of interaction between the Propagation and Remote Sensing represented by URSI Commission F is a particular strength that will be preserved and encouraged further.

Topics

URSI-F 2004 Open Symposium now welcomes from all those working in the research fields of URSI Commission F:

Propagation

- Terrestrial and slant path millimetre wave propagation
- Propagation for indoor (wireless local loop) and transport systems
- Tropospheric, ionospheric and trans-ionospheric propagation
- Propagation aspects of frequency management
- Propagation modelling and tools for system design
- Propagation in subsurface and biological media
- Radar application in propagation research
- Radio meteorology and climatology, including clear air and precipitation effects

Remote Sensing

- Radar and radiometer remote sensing of land, sea, ice, subsurface and atmosphere
- Applications on environmental and disaster management
- Forestry, agriculture and surface topography
- Radar meteorology
- Doppler radar, SAR, ISAR, InSAR, PolSAR
- Radar and radiometer design
- Propagation aspects of radar
- Remote sensing of buried objects

Prospective authors are invited to submit a photo-ready paper of length between 1 and 10 pages. Papers should present original work not submitted or published elsewhere. The paper should explain clearly the content and relevance of the contribution and include conclusions. E-mail submission of papers in PDF is preferred. Alternatively two hardcopies of the paper can be posted. Please indicate your preference for oral or poster presentation.

Contact

URSI-F 2004 Conference Secretariat
c/- Unit 13,
Milton Village43 Lang Parade
Milton, Qld 4064,
AUSTRALIA
Fax: +61-7-3721-6667
E-Mail: registration@ursi-f2004.com
(preferred option)
Website: http://www.ursi-f2004.com
Deadline for Paper Submission: 26 March 2004
Notification of Acceptance: 30 April, 2004

EUROEM 2004
EuroElectromagnetics

Magdeburg, Germany, 12 - 16 July 2004

EUROEM 2004 will continue the EUROEM/AMEREM tradition of bringing together the 14 th High Power Electromagnetics Conference (**HPEM14**), the 7 th Ultra-Wideband, Short-Pulse Electromagnetics Conference (**UWB SP 7**) and the 7 th Unexploded Ordnance Detection and Range Remediation Conference (**UXO 7**).
We are pleased to invite you to join us for the EUROEM 2004 Symposium. It provides a forum within the international scientific and engineering community for Electromagnetics. An attractive program of the highest standard, including speakers from many countries will await you. We look forward to seeing you in Magdeburg. Please register via the website **http://www.euroem.org** .

Steering Committee

J. Nitsch (Symposium Chair), Z. A. Styczynski (Symposium Co-Chair), G. Wollenberg (Symposium Co-Chair), D.

Nitsch (HPEM Co-Chair), M. Bäckström (HPEM, Co-Chair), F. Sabath (UWB Co-Chair), E. Mokole (UWB Co-Chair), H. G. Krauth¨auser (UXO Co-Chair), P. Zwamborn (UXO Co-Chair), K. Ruffing (Exhibition), H. Garbe (Liaison), J.-L. terHaseborg (Int. Coorporation), F. Gronwald (Public Relations), M. Tröger (Social Program), H. Haase (Webpage, Layout, Database), T. Steinmetz (Mail Handling, Layout).

Themes

HPEM / NEM & Related Topics

1. High-Power Microwaves
2. EMP Phenomenology, Propaga-tion, Source Region
3. Electromagnetic Environments
4. Lightning – Characterization & Simulation
5. High-Intensity Radiated Fields
6. Biological Effects and Medical Application
7. Environmental Effects of EM Fields
8. Intentional EMI
9. Coupling to Structures, Cables
10. Vulnerability of Systems & Components
11. Hardening & Protection
12. Hardness Assurance & Maintenance
13. CAD Analysis & Synthesis
14. Simulators & Simulation Techniques
15. Pulsed Power
16. High-Power RF Source Technology
17. Measurements Techniques
18. Electromagnetic Topology
19. Electromagnetic Compati-bility
20. Antennas
21. Signal Processing
22. Electromagnetic Noise
23. Geomagnetic Storms
24. Materials Characterization
25. Numerical & Statistical Methods
26. EM Standards & Specifications
27. Nonlinear Dynamics and Chaos

UWB & Related Topics

1. Electromagnetic Theory
2. Scattering
3. Propagation
4. UWB Polarimetry
5. UWB Radar Systems
6. Underground & Subsurface Propagation
7. UWB Antennas
8. Applications of UWB Antennas
9. Antennas for UWB Communication
10. Wavelets & Multi-Resolution Algorithms
11. Time-Domain Signal Processing
12. Target Detection & Discrimination
13. Time-Domain Computation Techniques
14. Short-Pulse Measurement Techniques
15. Pulsed Power 16. Sus-ceptibility
17. UWB Communication
18. Biological Effects
19. UWB- Interference with Aircraft Systems
20. New Canonical Problems, Benchmark Solutions
21. Special Sessions

UXO & Related Topics

1. Defining UXO – Sites, Problems
2. EM Characterization of Soils
3. UXO – Detection, Sensor Technologies
4. UXO ID, Feature Signatures, Discrimination
5. Signal Processing
6. Sensor Fusion
7. Time-Domain Signal Processing
8. EOD Tools, Robotics
9. Containment
10. Modeling & Simulation
11. Clutter & Discrimination
12. Clutter Rejection Algorithms
13. Landmines – Detection & Sensor Technologies
14. Landmines – ID, Signatures, & Discrimination

For more information please visit our website http://www.euroem.org

URSI CONFERENCE CALENDAR

March 2004

Métrologie et capteurs en électromagnetisme
(Journees scientifiques du CNFRS)
Meudon, France, 29-30 mars 2004
Contact : http://cnfrs.get-telecom.fr

May 2004

International NIR Workshop & Symposium
Seville, Spain, 20-22 May 2004
Contact : Dr. Bernard VEYRET, Labo PIOM/ENSCPB , Université de Bordeaux, BP 108, F-33402 TALENCE CEDEX, FRANCE, Phone : +33 5 56 84 66 29, Fax : +33 5 56 84 66 31, E-mail :b.veyret@piom.u-bordeaux.fr, b.veyret@enscpb.fr , http://www.icnirp.de/NIRProg.htm

EMTS'04 - 2004 International Symposium on Electromagnetic Theory
Pisa, Italy, 23-27 May 2004
cf. announcement in RSB September 2003, p.61-62
Contact persons : Prof. Makoto Ando, Commission B Chair, Dept. of Electrical and Electronic Engineering, Tokyo Institute of Technology, J2-12-1, Ookayama, Meguro, Tokyo 152-8552, Japan, E-mail: mando@antenna.ee.titech.ac.jp and Prof. Lotfollah Shafai, Commission B Vice-Chair, Dept. of Electrical & Computer Eng., University of Manitoba, 15 Gillson Street, Winnipeg, MB R3T 5V6, Canada, E-mail: shafai@ee.umanitoba.ca

June 2004

URSI Commission F Open Symposium
Cairns, Great Barrier Reef, Australia, 1-4 June 2004
Contact: URSI-F 2004 Conference Secretariat, c/-Unit 13, Milton Village 43 Lang Parade, Milton, Qld 4064, Australia, E-mail: registration@ursi-f2004.com (E-mail is the preferred correspondence option), Fax: +61 7 3721 6667, http://www.ursi-f2004.com

EMC'04 Sendai - 2004 International Symposium on Electromagnetic Compatibilty/Sendai
Sendai, Japan, 1-4 June 2004
Contact :Prof. R. Koga, Dept. of Communications Network Engineering, Okayama University, Japan, koga@cne.okayama-u.ac.jp, www.dev.cne.okayama-u.ac.jp

MSMW'04 - 5th International Kharkov Symposium on Physics and Engineering of Microwaves
Kharkov, Ukraine, 21-26 June 2004
cf. announcement in RSB September 2003, p.62-63
Contact : MSMW'04, IRE NASU 12, Ac. Proskura St., Kharkov 61085, Ukraine, Phone/Fax : +380 572-441105, E-mail: msmw04@ire.kharkov.ua, E-mail : www.ire.kharkov.ua/MSMW2004/

July 2004

EUROEM 2004
Magdeburg, Germany, 12-16 July 2004
Contact: website http://www.euroem.org, E-mail: magdeburg@euroem.org

35th COSPAR Scientific Assembly an Associate Events
Paris, France, 18-25 July 2004
cf. announcement in RSB September 2003, p.63-64
Contact :COSPAR Secretariat, 51, bd. de Montmorency, F-75016 Paris, France, Tel: 0033-1-45250679, Fax: 0033-1-40509827, E-mail: COSPAR@COSPARHQ.org , http://www.copernicus.org/COSPAR/paris2004/useful.htm

August 2004

ISSSE'04 - 2004 Int. Symp. on Signals, Systems and Electronics
Linz, Austria, 10-13 August 2004
Contact : Prof. Dr. Andreas Springer, Technical Program Committee Co-Chair, ISSSE'04, c/o ISSSE'04 Secretariat, Institute for Communications and Information Engineering, Johannes Kepler University of Linz, Altenbergerstrasse 69, A-4040 Linz, Austria, E-mail: issse04@icie.jku.at, http://www.icie.jku.at/issse04/

ISAP'04 - 2004 Int. Symp. on Antennas and Propagation
Sendai, Japan, 17-21 August 2004
Contact : ISAP'04, Attn. Dr. Tokio Taga, NTT DoCoMo, Inc., 3-5, Hikarino-oka, Yokosuka, 239-8536 Japan, E-mail : isap-2004@mail.ieice.org , http://www.ieice.org/cs/isap/2004

AP-RASC 2004 - 2nd Asia-Pacific Radio Science Conference
Qing, China, 24-27 August 2004
Contact : Prof. Zong Sha, China Research Institute of Radio Propagation, P.O Box 134-70, 100040 Beijing, China (CIE), Phone: +86 10 6821 2267, Fax: +86 10 6857, E-mail: z.sha@ieee.org, website http://www.cie-china.org/AP-RASC/

September 2004

Bianisotropics 2004
Ghent, Belgium, 22-24 September 2004
Contact: Mrs. Isabelle Van Der Elstraeten, INTEC, Sint-Pietersnieuwstraat 41, B-9000 Gent, Belgium, Tel. +32 (0) 9 2643321, Fax: +32 (0)9 2643593, E-mail: isabelle.vanderelstraeten@intec.ugent.be, website: http://www.intec.ugent.be/bian04/

November 2004

JINA 2004 - 13èmes Journées Internationales de Nice sur les Antennes
Nice, France, 8-10 november 2004
Contact: Secretariat JINA, France Telecom R&D, Fort de la Tête de Chien, F-06320 La Turbie, France, Fax: +33 4 92 10 65 19, E-mail: jina.2004@wanadoo.fr, website http://www.jina2004.com

August 2005

ISMOT 2005 - 10th International Symposium on Microwave and Optical Technology
Fukuoka, Japan, 22-25 August 2005
Contact: Prof. Kiyotoshi Yasumoto, Dept. Comp. Sci. & Comm. Eng., Kyushu University, 6-10-1, Hakozaki, Higashi-ku, Fukuoka 812-8581, Japan, Phone: +81 92 642 4045, Fax: +81 92 632 5204, E-mail: yasumoto@csce.kyushu-u.ac.jp, internet http://ismot2005.fit.ac.jp

October 2005

XXVIIIth URSI General Assembly
New Delhi, India, 23-29 October 2005
Contact: URSI Secretariat, c/o INTEC, Sint-Pietersnieuwstraat 41, B-9000 Gent, Belgium, Phone: +32 (0)9 264 3320, Fax: +32 (0)9 264 4288, E-mail: ursi@intec.rug.ac.be, internet http://www.ursi.org.

An up-to-date version of this Conference Calendar, with links to the various conference web sites can be found at www.ursi.org : Calendar of supported meetings.
If you wish to announce your meeting in this calendar, you will find more information at www.ursi.org.
URSI cannot be held responsible for any errors contained in this list of meetings.

URSI Publications

Modern Radio Science 1999

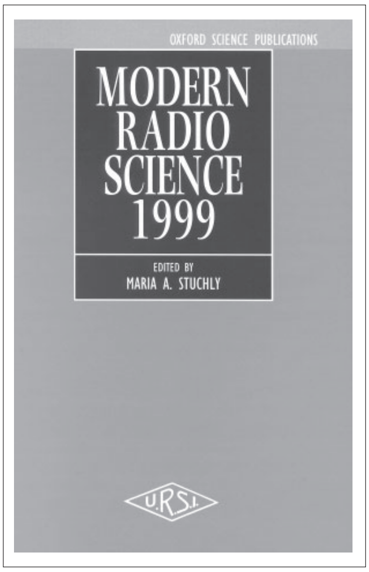

Editor: Maria Stuchly
ISBN 0-7803-6002-8
List Price : USD 49.95 Member Price : USD 45.00
IEEE Product No. PC5837

Published by Oxford University Press
in cooperation with URSI and IEEE Press
Order 24 hours a day, 7 days a week :
1-732-981 0060 (Worldwide)
1-800-678 4333 (USA & Canada)
Fax 1-732 981 9667
E-mail : customer-service@ieee.org

Review of Radio Science 1999-2002

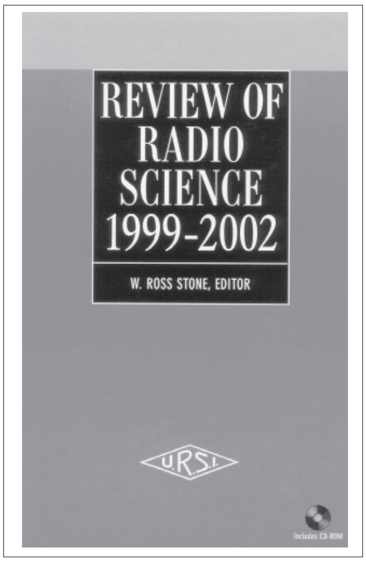

Editor: W. Ross Stone
July 2002/Hardcover/977 pp
ISBN 0-471-26866-6
List Price : USD 125.00 Member Price : USD 106.25
IEEE Product No. #18493

Published by Wiley-Interscience
in cooperation with URSI and IEEE Press
Order can be sent to John Wiley & Sons, Inc.
from 8.30 a.m. to 5.30 p.m. :
1-732-469-4400 (Worldwide)
1-800-225-5945 (USA & Canada)
Fax 1-732 302-2370
E-mail : customer@wiley.com

Handbook on Radiopropagation Related to Satellite Communications in Tropical and Subtropical Countries

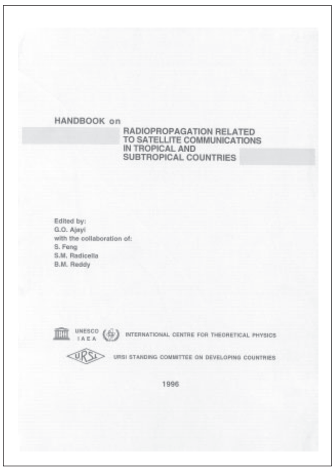

Editor: G.O. Ajayi
with the collaboration of :
S. Feng, S.M. Radicella, B.M. Reddy

Available from the URSI Secretariat
c/o Ghent University (INTEC)
Sint-Pietersnieuwstraat 41
B-9000 Gent, Belgium
tel. +32 9-264-33-20
fax +32 9-264-42-88
e-mail : ursi@intec.rug.ac.be

The Journal of Atmospheric and Solar-Terrestrial Physics

SPECIAL OFFER TO URSI CORRESPONDENTS

AIMS AND SCOPE

The *Journal of Atmospheric and Terrestrial Physics* (JASTP) first appeared in print in 1951, at the very start of what is termed the "Space Age". The first papers grappled with such novel subjects as the Earth's ionosphere and photographic studies of the aurora. Since that early, seminal work, the Journal has continuously evolved and expanded its scope in concert with - and in support of - the exciting evolution of a dynamic, rapidly growing field of scientific endeavour: the Earth and Space Sciences. At its Golden Anniversary, the now re-named *Journal of Atmospheric and Solar-Terrestrial Physics* (JASTP) continues its development as the premier international journal dedicated to the physics of the Earth's atmospheric and space environment, especially the highly varied and highly variable physical phenomena that occur in this natural laboratory and the processes that couple them. The *Journal of Atmospheric and Solar-Terrestrial Physics* is an international journal concerned with the inter-disciplinary science of the Sun-Earth connection, defined very broadly. The journal referees and publishes original research papers, using rigorous standards of review, and focusing on the following: The results of experiments and their interpretations, and results of theoretical or modelling studies; Papers dealing with remote sensing carried out from the ground or space and with in situ studies made from rockets or from satellites orbiting the Earth; and, Plans for future research, often carried out within programs of international scope. The Journal also encourages papers involving: large scale collaborations, especially those with an international perspective; rapid communications; papers dealing with novel techniques or methodologies; commissioned review papers on topical subjects; and, special issues arising from chosen scientific symposia or workshops. The journal covers the physical processes operating in the troposphere, stratosphere, mesosphere, thermosphere, ionosphere, magnetosphere, the Sun, interplanetary medium, and heliosphere. Phenomena occurring in other "spheres", solar influences on climate, and supporting laboratory measurements are also considered. The journal deals especially with the coupling between the different regions. Solar flares, coronal mass ejections, and other energetic events on the Sun create interesting and important perturbations in the near-Earth space environment. The physics of this subject, now termed "space weather", is central to the Journal of Atmospheric and Solar-Terrestrial Physics and the journal welcomes papers that lead in the direction of a predictive understanding of the coupled system. Regarding the upper atmosphere, the subjects of aeronomy, geomagnetism and geoelectricity, auroral phenomena, radio wave propagation, and plasma instabilities, are examples within the broad field of solar-terrestrial physics which emphasise the energy exchange between the solar wind, the magnetospheric and ionosphericplasmas, and the neutral gas. In the lower atmosphere, topics covered range from mesoscale to global scale dynamics, to atmospheric electricity, lightning and its effects, and to anthropogenic changes. Helpful, novel schematic diagrams are encouraged. Short animations and ancillary data sets can also be accommodated. Prospective authors should review the *Instructions to Authors* at the back of each issue.

Complimentary Information about this journal:
http://www.elsevier.com/locate/JASTP?
http://earth.elsevier.com/geophysics

Audience:
Atmospheric physicists, geophysicists and astrophysicists.

Abstracted/indexed in:

- CAM SCI Abstr
- Curr Cont SCISEARCH Data
- Curr Cont Sci Cit Ind
- Curr Cont/Phys Chem & Sci
- INSPEC Data
- Meteoro & Geoastrophys Abstr
- Res Alert

Editor-in-Chief:
T.L. Killeen, National Centre for Atmospheric Research, Boulder, Colorado, 80307 USA

Editorial Office:
P.O. Box 1930, 1000 BX Amsterdam, The Netherlands

Special Rate for URSI Radioscientists 2003:
Euro 149.00 (US$ 149.00)
Subscription Information
2002: Volume 65 (18 issues)
Subscription price: Euro 2659 (US$ 2975)
ISSN: 1364-6826

CONTENTS DIRECT:
The table of contents for this journal is now available pre-publication, via e-mail, as part of the free ContentsDirect service from Elsevier Science. Please send an e-mail message to cdhelp@elsevier.co.uk for further information about this service.

For ordering information please contact Elsevier Regional Sales Offices:

Asia & Australasia/ e-mail: asiainfo@elsevier.com
Europe, Middle East & Africa: e-mail: nlinfo-f@elsevier.com
Japan: Email: info@elsevier.co.jp
Latin America : e-mail: rsola.info@elsevier.com.br
United States & Canada : e-mail: usinfo-f@elsevier.com

APPLICATION FOR AN URSI RADIOSCIENTIST

I have not attended the last URSI General Assembly, and I wish to remain/become an URSI Radioscientist in the 2003-2005 triennium. Subscription to *The Radio Science Bulletin* is included in the fee.
(please type or print in BLOCK LETTERS)

Name: Prof./Dr./Mr./Mrs./Ms. ______________________________________
Family Name *First Name* *Middle Initials*

Present job title: ______________________________________

Years of professional experience: ______________________________________

Professional affiliation: ______________________________________

I request that all information, including the bulletin, be sent to my ☐ home ☐ business address, i.e.:

Company name: ______________________________________

Department: ______________________________________

Street address: ______________________________________

City and postal / zip code: ______________________________________

Province / State: __________________ Country: ______________________

Phone: ______________________ ext: _________ Fax: ______________________

E-mail: ______________________________________

Areas of interest (please tick)

☐ A Electromagnetic Metrology

☐ B Fields and Waves

☐ C Signals and Systems

☐ D Electronics and Photonics

☐ E Electromagnetic Noise & Interference

☐ F Wave Propagation & Remote Sensing

☐ G Ionospheric Radio and Propagation

☐ H Waves in Plasmas

☐ J Radio Astronomy

☐ K Electromagnetics in Biology & Medicine

The fee is 40 Euro.
(The URSI Board of Officers will consider waiving of the fee if the case is made to them in writing)

Method of payment: VISA / MASTERCARD (we do not accept cheques)

Credit Card No ☐☐☐☐ ☐☐☐☐ ☐☐☐☐ ☐☐☐☐ Exp. date: _________

Date: _________________ Signed ______________________________________

Please return this signed form to: